SVERIGES GEOLOGISKA UNDERSÖKNING
BERGGRUNDSGEOLOGISKA OCH GEOFYSISKA KARTBLAD
SKALA 1:50 000
Serie Af · Nr 17–20

FRED WITSCHARD

DESCRIPTION
OF THE GEOLOGICAL MAPS
FJÄLLÅSEN NV, NO, SV, SO

WITH AN APPENDIX ON GEOPHYSICAL ASPECTS
BY HERBERT HENKEL

BESKRIVNING TILL BERGGRUNDSKARTBLADEN
FJÄLLÅSEN NV, NO, SV, SO

STOCKHOLM 1975

SVERIGES GEOLOGISKA UNDERSÖKNING

BERGGRUNDSGEOLOGISKA OCH
GEOFYSISKA KARTBLAD
SKALA 1:50 000
Serie Af · Nr 17—20

FRED WITSCHARD

DESCRIPTION OF THE GEOLOGICAL MAPS FJÄLLÅSEN NV, NO, SV, SO

WITH AN APPENDIX ON GEOPHYSICAL ASPECTS
BY HERBERT HENKEL

BESKRIVNING TILL BERGGRUNDSKARTBLADEN
FJÄLLÅSEN NV, NO, SV, SO

STOCKHOLM 1975

ISBN 91-7158-073-5

C DAVIDSONS BOKTRYCKERI AB, VÄXJÖ 1975

CONTENTS

ABSTRACT

The account presents the results of geological investigations carried out in the years 1968—1970 on the map-sheet 28J Fjällåsen (2 500 km²), Norrbotten county, northern Sweden. It is part of the systematic mapping programme being conducted by the Ore Investigation Department of the Geological Survey of Sweden.

Swedens largest marsh (Sjaunja-ape) is partly situated in the map-sheet area. On account of this and of widespread quarternary glacial deposits, the bedrock is poorly exposed.

The account deals entirely with the Pre-Cambrian bedrock. The oldest group of rocks in the map area is the Porphyry Group consisting of banded volcanic rocks of rhyolitic, andesitic or basaltic composition. Sediments are associated with this group. These rocks are generally strongly folded and have been partly transformed to schists and gneisses. Minor gabbro massives and dolerites were emplaced after the deformation. Granites, which are younger than the former, predominate in the area. The Perthite Granite Series consists of highly perthitic rocks ranging in composition from quartz-monzonites to quartz-free, pyroxene-bearing monzonites. The Lina Granite Series has an average quartz-monzonitic composition. A genetic relationship, apparently existing between the Porphyry Group and the Perthite Granite Series, is discussed to some extent. Field investigation and aeromagnetic interpretation have revealed the presence of a major diabase, the Nabrenjarka gabbro diabase, which is younger than granites. It is accompanied by a large number of minor basic dykes. Its length exceeds 100 km in the Fjällåsen and neighboring map-sheet areas.

The geological interpretation relies on aeromagnetic maps presented together with the geological maps in a separate folder (scale = 1:50 000). The geophysical aspects of the work are presented in an appendix by H. Henkel.

GEOLOGISK ÖVERSIKT

Fjällåsen är namnet på en liten hållplats vid järnvägen Gällivare—Kiruna i norra delen av Norrbottens län. Kartbladet 28 J Fjällåsen som omfattar en yta av 50 × 50 km, är beläget söder om kartbladet 29 J Kiruna. De geologiska och flygmagnetiska kartorna 28 J NV, NO, SV och SO i skala 1:50 000 bifogas i separat folder. De geologiska kartorna är baserade på fältarbeten utförda under åren 1968—70.

Det mest anmärkningsvärda morfologiska draget i området utgör Sjaunja-ape, Sveriges största, sammanhängande myrområde (Fig. 2). Vid sidan av myrland karaktäriseras landskapet av ganska branta skogklädda kullar, vars toppar ofta når över skogsgränsen.

Förutom den geologiska kartan över Norrbottens län, sammanställd av Ödman (1957), är den publicerade litteraturen rörande kartbladet mycket begränsad. En geologisk och geofysisk undersökning har nyligen utförts av SGU på titanjärnmalmen Akkavare (Ambros och Henkel 1973).

De geofysiska resultaten av arbetet presenteras i ett appendix av Herbert Henkel.

A – GEOLOGI

Beskrivningen berör enbart det prekambriska urberget. Kartbladets berggrund domineras mycket starkt av granit, vilka innesluter stora suprakrustala reliker av övervägande porfyrgruppens bergarter. Till stor del har suprakrustalbergarterna omvandlats till skiffrar och gnejser. De saknar "uppåt"-strukturer och ännu återstår många problem rörande de lokala och regionala stratigrafiska förhållandena. En mäktig diabas, Nabrenjarka gabbrodiabas, har upptäckts i samband med undersökningen.

Den petrografiska och petrologiska beskrivningen är baserad på sammanlagt 340 slipprov och 80 nya kemiska analyser (tabell 2). De har visat att de petrografiska och kemiska förhållandena inom pertitgranitserien är mycket likartade med dem inom porfyrgruppen och att dessa två bergartsgrupper troligen är genetiskt besläktade.

Mätning av magnetisk susceptibilitet, remanens och densitet har utförts på alla stuffprov från kartbladet. Mätresultaten har jämförts med resultaten från de petrografiskt-petrologiska undersökningarna i avsikt att underlätta tolkningen av de flygmagnetiska kartorna.

Porfyrgruppen eller den vulkaniska serien antas vara likåldrig med Kirunaporfyren (± 1605 m.y.). Den består huvudsakligen av porfyrer och vulkaniter med sur (ryolitisk) och intermediär (andesitisk) sammansättning. Basaltiska grönstenar och ultrabasiska bergarter är sällsynta. Associerade sediment förekommer undantagsvis i den översta delen av gruppen. En relativt intensiv omkristallisering, som tidsmässigt förmodligen är knuten till tektonisk deformation, har omvandlat en stor del av vulkaniterna och sedimenten till skiffrar och gnejser. Porfyrgruppen är bäst representerad på de östra delbladen (NO och SO), där den bildar ett omfatande, N—S-ligt stråk, vilket tydligt framträder på de flygmagnetiska kartorna. Detta område karaktäriseras av bandade, veckade och ofta kraftigt förskiffrade vulkaniter. Mer eller mindre granitiserade relikter av vulkaniskt ursprung förekommer inom de vidsträckta Lina- och pertitgranitområden, som täcker större delen av delbladen NV och SV. 35 kemiska analyser av bergarter hörande till porfyrgruppen presenteras i tabell 2 (nr 26—60). Nomenklatur, svittyp och svitindex enligt Rittman, återges i tabell 1.

Gabbror och diabaser anses som yngre än porfyrgruppens bergarter, vilket överensstämmer med de uppfattningar som framförts på angränsande kartblad. Åldersförhållandet kan emellertid inte verifieras på kartbladet Fjällåsen, eftersom kontakten mellan bergartstyperna inte har påträffats. Gabbrorna bildar i regel endast smärre massiv. De är ofta delvis granitiserade och deras yttre begränsningar på de flygmagnetiska kartorna är något diffusa. Den vanligaste typen utgöres av en uralitiserad augitgabbro, med eller utan hypersten. Den magnetit- och titanrika gabbron vid Akkavare (SV) är ibland olivinförande och har den utmärkande egenskapen att dess apatit uppträder interstitialt. Akkavaregabbrons kontakter mot omgivande berggrund är väl markerad på den flygmagnetiska kartan. Enligt den geofysiska tolkningen är den endast ett par hundra meter mäktig och har en relativt flack bottenyta. Diabaser förekommer och kan ibland enbart vara bevarade som starkt assimilerade relikter i granit.

Pertitgranitserien består av starkt pertitiska bergarter, som varierar i sammansättning från kvartsmonzoniter till kvartsfria, ibland pyroxenförande monzoniter. Serien är övervägande blottad på Fjällåsen NV och SV. Porfyriska och sub-kataklastiska typer är vanliga. Hybridformer uppkomna genom partiell assimilation av olika vulkaniter förekommer. 25

kemiska analyser av pertitgranitseriens bergarter återfinns i tabell 2 (nr 1—25).

Linagranitserien är rikligt representerad i området öster om vulkaniterna (delbladen NO och SO), där den ofta bildar migmatiter, som ger upphov till komplexa anomalier på de flygmagnetiska kartorna. Låganomala granitområden representerande mer homogena bergartstyper förekommer väster om vulkaniterna (SO) och söder om det område, som intas av pertitgranitserien (SV). Vid sidan av de migmatitiska formerna är Linagraniten vanligen skär och massformig eller svagt parallellstruerad. Till sammansättningen är den kvartsmonzonitisk med ungefär lika halter kvarts, plagioklas och mikroklin.

Nabrenjarka gabbrodiabas är blottad på Fjällåsen SV och NV. Den kan följas på de flygmagnetiska kartorna in på närliggande kartblad och den är, trots vissa förkastningar, uppenbarligen sammanhängande. Bredden varierar från några hundra meter till omkring en kilometer och stupningen är på Fjällåsenbladen mot väster. Området väster om diabasen kännetecknas av ett stort antal basiska gångar, som genomsätter olika graniter. Basitgångarna anses som samhöriga med Nabrenjarka gabbrodiabas. Dessa bergarter är de yngsta kända inom kartbladen. Vanligen uppträder en starkt uralitiserad augit-gabbro, som ibland är hypersten-förande. De kemiska analyserna indikerar att Nabrenjarka gabbrodiabas innehåller relativt höga halter av Fe, Ti och V och att den är ganska SiO_2-fattig.

B – TEKTONIK

Den tektoniska tolkningen är övervägande grundad på de flygmagnetiska kartorna. Veckstrukturer med stora amplituder framträder bäst i de vulkaniska bergarterna på Fjällåsen NO och SO, där växellagrande vulkaniter med varierande sammansättning och magnetisk susceptibilitet mycket tydligt kan urskiljas på de flygmagnetiska kartorna. En schematisk bild över huvudveckaxlarna återges i fig. 9. Dessa veckaxlar stryker övervägande i N—S-lig riktning. Det förekmmer även en svagare veckning efter O—V-liga veckaxlar. Kombinationen av veckningsriktningarna ger upphov till en följd av nord-sydligt utdragna domer och bassänger.

Förskiffringen i de vulkaniska bergarterna är vanligen parallell med litologiska gränser och indikerar därmed att den förmodligen är samtidig

med deformationens huvudfas. En postgranitisk deformationsfas, karaktäriserad av intensiva förkastningsrörelser och uppkrossning, har påverkat alla anstående bergarter. Förkastningarnas huvudriktningar är NV—SO och NNO—SSV.

INTRODUCTION

Fjällåsen is the name of a small station along the railway Gällivare—Kiruna, in the northern part of Norrbotten county. The map-sheet 28 J Fjällåsen (Fig. 1), with an area of 2 500 square kilometres, is surrounded by the following map-sheets: to the north 29 J Kiruna, to the east 28 K Gällivare, to the south 27 J Porjus and to the west 28 I Stora Sjöfallet. The geological and aeromagnetic maps, on the scale of 1:50 000, are presented together in a separate folder as four distinct sheets: north-west (NV), north-east (NO), south-west (SV) and south-east (SO).

The area investigated is very sparsely inhabited and the only settlements worthy of note are: Killinge, situated on the banks of Kaitumälven (NO) and Ålloluokta, on the shores of Stora Lulevatten (SO). Besides the Gällivare—Kiruna and Gällivare—Porjus railways, in the eastern part of the area, there exist only two main ways of access: the Killinge—Fjällåsen road branching from the Gällivare—Svappavaara road and the Porjus—Vietas road running along the northern shore of Stora Lule-

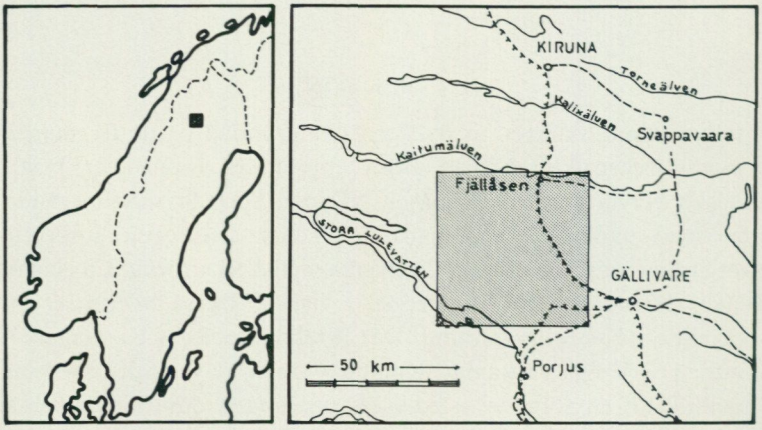

Fig. 1. Situation of the area investigated.
Kartbladets läge.

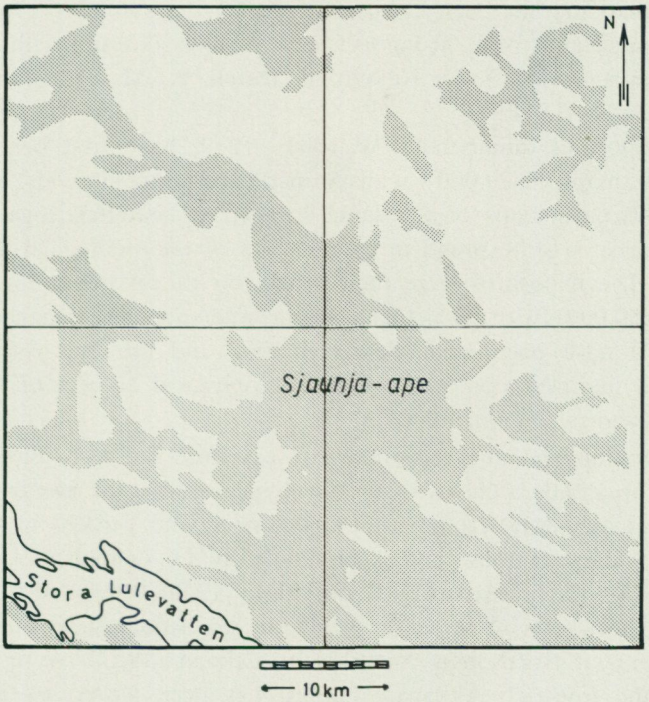

Fig. 2. Extent of the Sjaunja marsh (Sjaunja-ape) and other major marshes in the map area.
Sjaunja-ape och andra större myrområden inom kartbladet.

vatten. The minor ways of access, all situated in the eastern part of the map area, are: the Porjus—Ålloluokta road, the Gällivare—Linajoki forest road and the Malmberget—Allavaara road. Because of the difficult access in the western part of the area, the geological mapping has often been carried out there with the help of a helicopter.

One of Swedens largest marsh areas, Sjaunja-ape, is an important feature in the landscape. The extent of marsh in the map area exceeds 1 000 square kilometres (Fig. 2), their access being always difficult. Outside the marsh areas, the landscape is characterized by rather steep hills, the summits of which are often situated above the forest limit. As a result of quaternary glacial erosion, these hills often display steep eastern or south-eastern flanks, while those situated to the north and to the west are more gently sloping.

Field mapping has been carried out during the summers 1968—1970 with the assistance of L. Rönnbäck and H. Sjöström and with the temporary assistance of B. O. Nilsson, P. Darell, K. M. Ehrenberg, S. Å. Larsson and S. Liedberg.

The exposures, numbered FW 1001—1649, have first been plotted on photo maps (1:20 000) with 5 metre contour intervals and then transferred onto maps of the same scale. This material, together with field reports, is to be found in the archives of the Geological Survey of Sweden. The exposures were then drawn on the excellent topographic maps (1:50 000) with 5 metres contour intervals. Aeromagnetic maps (1:50 000) have been available since 1967 and are the base for the geological interpretation. Some of the geophysical aspects of the work are discussed in the appendix.

Prior to this account, there existed very little literature dealing with the map area. The archives of the Geological Survey of Sweden contain the diaries and notes from various geologists who worked in the area. The main contributions have been made by O. Ödman (1939, 1942, 1943, 1948—1950) assisted by E. Viluksela (1948, 1949) and O. Brotzen (1949). The results of these investigations are summarized on the geological map of Norrbotten compiled by Ödman (1957). A report concerning the iron-rich Akkavare gabbro has been writen by P. Geijer (1930). The results of investigations by drilling of the iron ores Akkavare (Melko) and Peltovaara, carried out by Stora Koparbergs Bergslags AB (1958—1962), are now the propriety of the Swedish State and have been consulted. A recent geological and geophysical investigation has been carried out by SGU on the titanium iron ore at Akkavare by M. Ambros and H. Henkel (1973).

By analogy with other areas of Norrbotten for which there exist radiometric age determinations, the rocks (and structures) of the Fjällåsen map area are thought to be of Pre-Cambrian age. Rocks of volcanic or volcano-sedimentary origin and somewhat younger granites predominate. Primary "way-up" structures have not been encountered in the supracrustal rocks of the area. Detailed stratigraphy is therefore impossible. The stratigraphic succession can nevertheless often be deduced from the nature, the distribution, the type of deformation and the relationships existing between the different types of rocks. An extensive basic dyke, the Nabrenjarka gabbro diabase, partly exposed in the map areas SV and NV, has been discovered during the present investigation. Its total

length exceeds 100 km. It extends to the south-west into the Porjus and Tjåmotis map areas and, to the north-West, into the Stora Sjöfallet map area. (See Fig. 15.)

To all persons having contributed directly or indirectly to the results presented in this publication, the author wishes to offer here his sincere thanks.

TERMINOLOGY AND METHODS OF INVESTIGATION

The terminology adopted for the plutonic and metamorphic rocks is mainly based on petrographic criteria. It is described, to some extent in a previous publication (Witschard 1970).

The classification of the volcanic rocks is based on petrography when dealing with weakly metamorphosed porphyries and on chemical analyses in the case of strongly metamorphosed or fine-grained types. The classification of volcanic rocks according to Rittmann (nomenclature, suite-type and suite-index) is given in Table 1.

The petrographic investigation relies on a total of 340 thin sections. Table 3 gives modal estimates of 80 samples for which chemical analyses exist. The drawings of thin sections presented in this account have been made by the author. They are often the result of a juxtaposition of observations made both under normal and polarized light.

The petrological investigation is based on 80 (new) chemical analyses presented in Table 2. It comprises analyses by the wet-method (25 samples) and spectrographic analyses (smältisoformering B). In the latter, FeO, H_2O, P_2O_5, CO_2, F and S are not analysed and the total iron content is given as Fe_2O_3. References as to the precision of the method are given in Witschard 1970. Trace-elements have been analysed by spectrographic methods. The analyses are presented, for each rock group, with decreasing silica content from the first to the last.

The results of chemical analyses have been treated by a computer program (BENORM 2) in order to obtain the cation percentage, the anion content (for 100 cations), the Niggli values, the CIPW norms and many other parameters permitting the drawing of various triangular diagrams.

Measurements of the magnetic susceptibility, magnetic remanence and specific weight have been made on all samples from the map area. The results of this investigation have been compared with the results of petrography-petrology in order to obtain a better interpretation of the aeromagnetic maps. This study has also contributed to the discovery of many

interesting new facts, particularly in the case of volcanic rocks and perthite monzonites. Parameter measurements are also discussed in the appendix.

THE PORPHYRY GROUP

The Porphyry Group, also refered to as the *Volcanic Series,* is supposed to be of the same age as the Kiruna Porphyries (1605 ± 65 m.y., Welin 1970). It mainly comprises volcanic effusives of acid (rhyolitic) and intermediate (andesitic) composition. Rocks of basic (basaltic greenstones) and ultrabasic composition are rare. Meta-sediments, of probable volcano-sedimentary origin, are associated with this group of rocks as accessories.

Under the combined effects of stress and metamorphism, rocks of the Porphyry Group have, to a large extent, been transformed to schists and gneisses. It is often only due to the occurrence of more or less preserved relics that their origin can be determined.

The Porphyrite Group, defined by J. Offerberg (1967) for the Kiruna map-sheet and indicated on it by the initials PG, apparently lies higher in the stratigraphy than thought by this author and belongs, at least partly, to the Porphyry Group. This interpretation is based on aeromagnetic interpretation and on geological observations along the border of the two map areas Kiruna and Fjällåsen. For the Vittangi map-sheet (B. Eriksson and U. Hallgren 1972), situated to the east of the Kiruna map-sheet, the authors have come to the same conclusion and have moved the porphyrites higher up in the stratigraphy to the Porphyry Group. As described below, porphyrites often occur as concordant horizons in acid volcanic rocks.

The aeromagnetic maps have been of great help for the structural interpretation of areas where volcanic rocks are widespread. This is mainly due to the relatively high magnetite content of the intermediate and basic volcanic rocks, frequently occurring as somewhat thin horizons, interbanded with poorly magnetic acid volcanic rocks. This is mainly visible in Fjällåsen NO and SO.

The Porphyhy Group is best represented in a long, north-south band, well marked on the aeromagnetic maps (NO and SO) and extending to the north on 29 J Kiruna (SO) and to the south on 27 J Porjus (NO). It is characterized there by more or less banded and often schistose volcanic rocks. In the case of finely banded types, the geological map only indicates the predominant type.

Fig. 3. Well-banded, sub-vertical acid volcanic rocks at Nietsakistjåkkå (0h). *Bandade sura vulkaniter, Nietsakistjåkkå (0h).*

The volcanic rocks, partly surrounding a gabbro at Siekavare (1j, 2j), are very poorly exposed in the area and their limit has been set after consultation of a preliminary Gällivare map-sheet established by K. A. Sandahl.

Well-preserved acid volcanic rocks and porphyries are exposed in the region of Ålloluokta (Ob, Oc). They are generally pink, rather massive and sometimes display a diffuse banding.

On the southern slopes of Lulep Nabretjåkkå (1c), banded light and dark rocks display beautifully preserved complex volcanic structures. They belong to a large relic surrounded by Lina granite. Granite dykes and pegmatites, intersecting the volcanic rocks, are common.

Porphyries and acid volcanic rocks are frequently associated to perthite granites and perthite monzonites widespread in the western areas. Andesites and greenstones occur less frequently there. In some cases, these volcanic rocks are rather well preserved and exhibit textures and structures of extrusive character. In most cases however, they are so strongly recrystallized that their origin cannot be determined with any certainty. A genetic relationship, apparently existing between the Porphyry Group and the Perthite Granite Series, is discussed below (pp. 39—43).

The petrographic and petrological investigation of the Porphyry Group is based on about 200 thin sections and 35 chemical analyses (Table 2, Nr 26—60). The chemical analyses have been particularly valuable for classifying fine-grained and strongly recrystallized volcanic rocks which are difficult to study under the microscope. The nomenclature, suite-type and suite-index, according to Rittmann (1952, 1962) is given in Table 1. Diagrams dealing with the chemical and physical parametres are presented in Figs. 16—27.

A – PORPHYRIES

A wide variety of porphyries exsist in the area and their stage of preservation is very variable from one place to another. They are mainly feldspar-porphyritic with plagioclase or microcline phenocrysts (or both). *Perthite porphyries,* with complex perthite phenocrysts of the type occurring in perthite granite, are rather common in the western map areas.

The presence of feldspar phenocrysts in a fine-grained matrix is best observed on slightly weathered exposures. Microscope investigation shows that the phenocrysts have often recrystallized to granular feldspar-aggregates under the effects of metamorphism.

Further recrystallization and the widespread development of sutured boundaries obscures the porphyritic texture to such an extent that the porphyries can hardly be distinguished from fine-grained acid volcanic rocks. A granophyric "patch" texture (See Fig. 8.), apparently of secondary origin, is sometimes well-developed. This problem is again discussed below (p. 42).

To the north and to the west of Allavaara (3h, 4h), the porphyries have been partly transformed to gneisses and display strongly cataclastic characteristics (Fig. 12). Mortar texture is common, with chlorite, saussurite and sericite generally occurring in the crush-zones and along the fracture planes. The aeromagnetic map (SO) indicates that the mylonitization is possibly related to the emplacement of a rather homogeneous Lina granite massif situated to the west.

The following results are obtained from 46 thin sections of the porphyries. Quartz is abundant and interstitial in the matrix. Somewhat rounded quartz phenocrysts, with embayed gulfs, are rare. In cataclastic and schistose rocks, quartz has often recrystallized as elongated cores or sub-veinlets outlining the schistosity. Plagioclase is always present in

the matrix. Plagioclase phenocrysts are present in about half of the samples examined. Their anorthite content varies between 10 and 35 % and albite is sometimes present in the matrix. Medium-grade sericitization is common. Microcline is present in all but two samples. It occurs interstitially in the matrix and also forms subhedral phenocrysts. Perthite porphyries, with perthites as the only phenocrysts, represent more than one third of the samples examined. They have been marked with a special overprint on the map. Biotite is generally present as an essential mineral. In one case, it outlines a well-preserved micro-flow structure. Biotite is generally strongly replaced by chlorite in the cataclastic types. Amphibole (green hornblende) is present, as an essential mineral, in about 30 % of the samples. It sometimes forms large poikilitic crystals of a late generation. Magnetite and sphene are the two most common accessories. The others are, in order of importance, apatite, epidote, rutile and zircon. Green tourmaline, calcite and scapolite have exceptionally been encountered.

Seventeen chemical analyses have been made on the porphyries and meta-porphyries. The triangular diagrams (Figs. 18—21) indicate well-marked differentiation trends in these rocks. With increasing quartz, the main trend is from a soda-rhyolite to an alkali-rhyolite and the factor Q/Or remains rather constant (Fig. 18). The Q-L-M diagram (Fig. 19) outlines the strongly acidic tendency of these rocks.

B – ACID VOLCANIC ROCKS

Acid volcanic rocks are pink or grey, somewhat fine-grained rocks which are often refered to as leptites in swedish literature. They are generally massive but occasionally display a beautiful banding detween differently coloured horizons (Fig. 3). The occurrence of strongly recrystallized, anhedral to subhedral feldspar of large size, often observed in these rocks, indicates that some of them are probably metamorphic porphyries. Banded types are rather rare and can best be observed at Nietsakistjåkkå (0h) and on the southern slopes of Lulep Nabretjåkkå (1c). An irregular banding between acid- and intermediate-composition volcanic rocks is common to the north of Allavaara (Fig. 10b) where gneissification has strongly obscured the structures. A volcanic breccia with fine-grained dark and magnetite-rich fragments enclosed in a lighter, fine-grained groundmass, is exposed at Apponjarka (1b).

Due to their composition, acid volcanics rocks are easily granitized and, at a certain stage of transformation, it becomes impossible to differentiate them from medium-to-fine-grained granites. Many uncertainties therefore remain in the delimitation of acid volcanic rocks in granite areas. This is particularly true for the map-sheets NV and SV. A granophyric tendency of the matrix has sometimes been observed in strongly recrystallized types (see p. 42).

The following observations have been obtained from 55 thin sections of the acid volcanics. The texture is mainly fine-grained granular or sutured and many samples display a weak-to-medium foliation. Quartz is always present and generally strongly sutured. Plagioclase, not always present, has an anorthite content situated between 0 and 35 % (average 28 %). Microcline is always abundant and complex perthites are common in areas where perthite granite predominates. In strongly recrystallized rocks, microcline (or perthite) presents a poikiloblastic tendency. Magnetite is generally subordinate and is mainly found as minute disseminated crystals. Biotite and chlorite are subordinate and outline the schistosity in foliated types. Amphibole (green hornblende) is present in about one third of the samples and is subordinate. In order of importance, the accessories are: sphene, epidote, apatite, zircon and rutile. Green tourmaline, augite, calcite and allanite are exceptional. Three drillings, a few kilometres to the south of Fjällåsen (9g), have encountered garnet-bearing rocks of probable volcanic origin. The garnets form large poikiloblasts.

Eight chemical analyses have been made on the acid volcanic rocks. They indicate that the rocks have approximately the same chemical composition (mainly rhyolitic) as the porphyrie. The areas corresponding to these rocks on various triangular diagrams (Figs. 18—21) are generally slightly more restricted than the areas corresponding to porphyries but, nevertheless, show the same trends.

The magnetic susceptibility-specific weight diagram (Fig. 25) clearly shows the same general distribution for acid volcanic rocks as for porphyries with, however, a slight deplacement towards lighter rocks for the former. This confirms the volcanic origin of these fine-grained rocks (sediments show a rather dispersive trend towards lower magnetic susceptibilities).

In conclusion it can be said that the acid volcanic rocks and the porphyries present approximately the same petropraphic, chemical and physical characteristics.

C – ANDESITES AND PORPHYRITES

According to the terminology commonly used in Scandinavia, Porphyrites are andesites with a particular (ophitic) texture consisting of elongated plagioclase laths (a few mm to a few cm) enclosed in a dark, fine-grained matrix (see Fig. 10 a, c—f). Well preserved andesites are rather rare and, with increasing metamorphism, they grade imperceptibly into fine-grained greenstones.

From the aeromagnetic interpretation and field evidence, the andesites and porphyrites mainly occur as concordant horizons within the Porhyry Group and, in the area, are devoid of intrusive characteristics.

In porphyrite, the phenocrysts are generally randomly orientated. Along the banks of Kaitumälven (9i, 9j) and in expossures situated along the Fjällåsen road (9i), however, the phenocrysts display a good preferred orientation which is in general parallel to the lithological boundaries. The surrounding rocks are strongly gneissified and migmatized. A peculiar flow (?) texture is outlined by plagioclase laths in a porphyrite at Nietsakistjåkkå (0h, Fig. 10 d—f).

The following observations are based on 17 thin sections. The groundmass is either microgranular or slightly ophitic. It is granolepidoblastic in the foliated types. In the less altered types, the plagioclase laths are poorly zoned. The anorthite content lies between 32 and 50 %, with an average of 42 %. It is somewhat lower in the more altered types (15—50 %, average = 35 %). Sericitization and saussuritization are the principal forms of alteration. Amphibole is generally abundant. It is mainly interstitial in the case of green hornblende, but not in the case of actinolite-tremolite which displays blastic development. Somewhat uralitized augite is present in three thin sections. Biotite is an essential mineral in the andesites and a subordinate one in the meta-andesites, where it is partly replaced by chlorite. Magnetite, mainly found as disseminated minute crystals, is essential or subordinate, thereby accounting for the relatively high magnetic anomalies corresponding to these rocks. Sphene and apatite are subordinate or accessories. Scapolitization is rare.

Five chemical analyses indicate that we are dealing with a differentiated series of rocks, with compositions ranging from normal andesite to olivine-basalt according to the nomenclature of Rittmann (1952). The triangular diagrams, where andesites, meta-andesites and greenstones have been plotted (Figs. 18—21), show very neat diffetentiation trends.

These trends are generally a direct extension of the trends observed in the porphyries and acid volcanic rocks with, however, a greater dispresion of values for the andesites and greenstones. The magnetic susceptibility-specific weight diagram (Fig. 25) also shows a continuous trend from acid to basic volcanic rocks. What is more, the distribution of trace elements (as a function of SiO_2) in the Porphyry Group points to a well differentiated series of rocks (Figs. 22 and 23).

The observations above indicate that the Prophyry Group consists of a continuous, differentiated series of rocks, predominantly rhyolitic and andesitic.

D – GREENSTONES

In the map area, greenstones have always been found associated to other volcanic rocks of the Porphyry Group. They are somewhat fine-grained, massive or schistose and mainly made-up of plagioclase, amphibole and epidote-saussurite. The presence of strongly altered plagioclase phenocrysts and the rare occurrence of a relic ophitic texture indicate that they derive, at least partly, from andesites or more basic volcanic rocks. Under the effects of stress and metamorphism, greenstones have often been transformed to the amphibole schists and gneisses described below (p. 20). In several places, it has been possible to identify clastic textures and structures in these rocks.

A volcanic breccia, consisting of more or less deformed porphyry fragments enclosed in a schistose, tuffitic groundmass, is exposed about one kilometre to the south-west of Kassakåbbå (5f) and further to the south (5g). The fragments are often lens-shaped and surrounded by a bleached margin (Fig. 11a, b). Some irregular-shaped fragments are probably volcanic bombs (Fig 11c, d).

A total of 19 thin sections of the greenstones permit the following observations. The texture is either fine-grained granular, decussate or granolepidoblastic (foliated types). The plagioclase (0—45 % anorthite, average = 30 %) has a lower average anorthite content than the andesites. This confirms the trend (decreasing anorthite content with increasing alteration already observed from the andesites to the meta-andesites. Greenstones always contain plagioclase and amphibole (green hornblende or actinolite-tremolite). The other minerals, occurring in variable amounts,

are: epidote-saussurite, sericite, chlorite, magnetite, sphene and apatite. Quartz is essential and microcline subordinate in about one third of the samples examined.

Five chemical analyses made of the greenstones indicate a differentiation of the same type as the one observed in the andesites and porphyrites. This is a further argument in favour of a predominantly volcanic origin for these rocks.

E – SKARN AND ULTRABASIC ROCKS

Skarn and ultrabasic rocks apparently form somewhat thin and concordant horizons in porphyrite and greenstone milieu. They are rather difficult to follow in the field because the skarn-like or ultrabasic characteristics of these rocks are often only apparent under the microscope.

The only skarn horizon worthy of note lies concordantly in the porphyrites partly surrounding the Pikku Svierkku perthite monzonite massif (1i—3i). The rock is equigranular and consists mainly of strongly uralitized augite. Magnetite and sericite are subordinate. Chemical analysis Nr 72 (Table 2h) corresponds to this rock.

A diopside-rich and banded feldspathite (skarn-altered meta-sediment) is exposed to the north of Peltovaara (0h). A gradual transition to feldspathic quartzite occurs towards the west. A chemical analysis (Nr 71) is given in Table 2h.

Along Kaitumälven (9j), a magnetite-rich skarn occurs at the contact between porphyrites and acid volcanic rocks. The rock displays in places large epidote or amphibole crystal-aggregates.

Ultrabasic rocks are only known to occur at the very border of Sjaunjaape (5f), where they are interbanded with various volcanic rocks of intermediate composition. A light-green variety is mainly made-up of decussate serpentine and tremolite, with subordinate calcite and magnetite. Another variety consists of actinolite, tremolite and talc. Chemical analyses of these two rock-types are presented in Table 2h (respectively: Nr 74 and Nr 73). The ultrabasic character of these rocks is outlined by the relatively high nickel contents (above 1 500 ppm) which are the highest values obtained for the map area.

F – META-SEDIMENTS

Rocks displaying preserved primary sedimentary structures have not been discovered during the present investigation. Besides the clastic greenstone described above (p. 18), a wide range of rocks exist with petrographic or chemical characteristics pointing to a probable sedimentary (or volcano-sedimentary) origin.

Meta-sediments, found in regions where acid volcanic rocks and porphyries predominate, are quartz-rich and generally contain notably less potassic feldspar than the latter (see analyses Nr 61 and 62, Table 2g). The most common rock-type is a somewhat fine-grained, equigranular and often slightly schistose quartz-feldspathite. Feldspathic quartzite is less common. The equigranular texture, characteristic of some of these rocks, can only be observed when recrystallization is weak. Magnetite, muscovite and, to a lesser extent tourmaline, are more abundant in meta-sediments than in acid volcanic rocks.

G – SCHISTS AND GNEISSES IN VOLCANIC MILIEU

Under the combined effects of stress and metamorphism and possibly during the main phase of tectonic deformation (see p. 44), rocks of the Porphyry Group have often recrystallized to coarser-grained schists and gneisses. As the magnetic proprieties do not seem to be notably modified during the process, the aeromagnetic maps have been of valuable help for the geological interpretation of areas where schists and gneisses predominate. For example, the aeromagnetic maps indicate that gneisses occurring in Fjällåsen NO are situated in the direct extension of well-preserved volcanic rocks exposed in Fjällåsen SO.

Sediments, acid volcanic rocks and porphyries often grade imperceptibly to acid-composition schists and gneisses with granolepidoblastic or, more seldom, augen textures. Porphyries occurring to the north of Allavaara (3h, 4h) have been partly transformed to gneisses under the effects of cataclastic deformation and recrystallization (see Fig. 12). A biotite schist, containing large garnet poikiloblasts, quartz and plagioclase (35 % anorthite), is exposed along the Fjällåsen road (8j).

Amphibole schists and gneisses mainly originate from andesites and greenstones. Porphyrites, exposed in the Kaitumälven region and along the Fjällåsen road (9j), display a rather good foliation resulting from

the preferred orientation of plagioclase laths and giving to the rock the aspect of an augen gneiss (Fig. 10a). In these intermediate-composition gneisses, plagioclase is generally the predominant mineral, with an average anorthite content of 30 %. The highest metamorphic type encountered is a dark, sillimanite-biotite gneiss, exposed in the vicinity of the Gällivare—Kiruna railroad (8g).

The low quartz and microcline contents of most of the schists and gneisses (dioritic tendency) indicate that Si and K metasomatism, related to granite emplacement, is often negligible.

GABBROS AND DIABASES

This chapter deals with gabbros and diabases which, by analogy with adjacent map areas, are thought to be younger than the Porphyry Group. For the Fjällåsen map area, however, this cannot be verified in the field because of the lack of gabbro-porphyry contacts. The gabbros and diabases are older than the Lina and perthite granites and are often strongly granitized. The iron-rich Akkavare gabbro is described in a distinct subchapter.

A – MINOR GABBRO MASSIFS AND DIABASES

In the map area, gabbros generally form relatively small massifs. On the aeromagnetic maps, they often give rise to rather high anomalies with somewhat diffuse contours resulting from granitization. A brief discription of the main gabbros occurring in the map area is given below.

The Siekavare gabbro (1j, 2j) is rather well exposed on the north-eastern slopes of the hill Siekavare. In places, it is cut by granite veins and pegmatites belonging to the Lina granite. On the aeromagnetic maps, this gabbro corresponds to a rather high and complex anomaly, with diffuse margins towards the south-west. The limits of the gabbro, towards the east, have been set according to a preliminary Gällivare map-sheet established by K. A. Sandahl. One thin section from this gabbro shows that metamorphism is at an advanced stage, with the development of uralite, actinolite and tremolite crystal-aggregates, strongly obscuring the original (ophitic) texture. The plagioclase is strongly sericitized and has an anorthite content as low as 40 % giving to the rock a dioritic composition (epidiorite). The rock contains about 10 % biotite.

The Pikku Svierkku gabbro (2h, 2i) gives rise to small, diffuse magnetic anomalies and its contours on the geological map are therefore imprecise. We are apparently dealing with strongly assimilated gabbro relics enclosed in perthite monzonite. One thin section cut in granitized gabbro shows the presence of complex perthites, often corroding the plagioclase. Strong recrystallization has obscured, to a large extent, the ophitic texture. The anorthite content of the plagioclase is only 40 % (epidiorite). Somewhat uralitized augite is abundant and biotite amounts to about 10 %. Magnetite is rare, thereby explaining the absence of high magnetic anomalies.

The Sjaunjajaure gabbro (4e) is known from only a few small exposures occurring a few hundred metres north of Sjaunjajaure. The grain-size varies considerably from one place to another (medium-grained ophitic to fine-grained doleritic). One thin section cut in the finer grained type shows a well preserved doleritic texture with interstitial diopside. Olivine is abundant and is generally surrounded by two concentric alteration rims: a weakly coloured amphibole rim (inwards) and a greenish-brown chlorite rim (outwards). The plagioclase is a labrador-bytownite. This rock is possibly a gabbro diabase.

The Sabrojaure gabbro (6b, 6c, 7b, 7c) is a small massif giving rise to very diffuse magnetic anomalies. It lies about 1.5 km to the south-west of Sabrojaure. The rock is dark, massive and varies in grain-size from medium-grain to fine-grain, indicating that we are possibly dealing with a diabase. Granite veins cut the fine-grained type in a few places. Metamorphism is quite variable from one place to another. The least metamorphic type displays a well preserved, somewhat fine-grained, ophitic texture and consists of uralitized augite and hypersthene, plagioclase (73 % anorthite), biotite, abundant apatite and subordinate interstitial quartz. A thin section cut in a coarser-grained, more metamorphic type is mainly made-up of a strongly uralitized pyroxene and a plagioclase with low anorthite content (40 %). One chemical analysis of the finer-grained type is presented in Table 2h (Nr 75).

The Råvvokåppasj gabbro (8d) is known from only one exposure and its contours have been drawn with the help of the aeromagnetic map. It is an olivine-hypersthene-diopside gabbro with a labrador-bytownite as the plagioclase. Biotite is an essential mineral. Magnetite is abundant and sometimes occurs as complex exsolutions in olivine. Slightly coloured apatite is present. A chemical analysis is given in Table 2h (Nr 76).

Besides the gabbro massifs described above, a few diabases (marked 1 on the geological maps) have been encountered in Fjällåsen NV and SV. They are generally granitized and sometimes only subsist as strongly assimilated selics in granite. Fig. 13a, b and c shows the granitization of such a diabase by the perthite granite.

B – THE AKKAVARE GABBRO

Akkavare is the name of a hill and of a small settlement, both situated in Fjällåsen SV, on the western margin of the extensive Sjaunja marsh (2e, 3e). The Akkavare gabbro is an isolated massif, surrounded by granite. It gives rise to a well-defined high anomaly on the aeromagnetic map. This has permitted its contours to be drawn quite precisely. On account of its relatively high iron and titanium percentage, it has been prospected on different occasions. The economic aspects are discussed in a chapter reserved for this purpose (p. 47). The results of geophysical investigations on the gabbro are presented in the appendix. Intersecting pegmatites occurring in trenches (Geijer, 1930) and in drill holes indicate that the Akkavare Gabbro is older than the surrounding Lina Granite.

The most striking feature, visible on the aeromagnetic map, is a well-marked fault, striking approximately north-south and subdividing the gabbro massif into two distinct parts: a somewhat rounded north-east part and a 3.5 km long and 750 m wide part, striking NE—SW. According to geophysical investigation, the fault dips about 60° to the east. The horizontal deplacement is estimated at about 750 m, the north-east part having been deplaced towards the north. The average depth of the gabbro is 450 metres for the north-east part and 200 metres for the south-west part, thereby indicating a probable sinking of the former.

The gabbro is dark, medium-grained, somewhat massive and displays strongly weathered or "rusty" surfaces reflecting its high iron content. The petrographic investigation is based on a total of 13 thin sections, 9 of which originate from drill-cores collected by M. Ambros. The texture, as seen under the microscope, is hypidiomorphic with a weak ophitic tendency. It is characterized by rather short plagioclase laths and by pyroxene which often does not respect the plagioclase grain-boundary. This texture is untypical of gabbros occurring in Norrbotten which are generally ophitic when not, or weakly altered. Many samples are some-

what cataclastic with abundant micro-fractures, bent plagioclases and irregular extinctions under polarized light. The plagioclase is a labrador-bytownite with an estimated 75 % anorthite content. It is generally fresh, irregularly pigmented (light grey) and often contains a large amount of minute rutile (?) needles which are preferentially orientated. The pyroxene is mainly represented by augite and diallage displaying an irregular pigmentation (light brown) and sometimes presenting lamellar twinning. Hypersthene is also present in lesser amounts and pigeonite ($2V<10°$) has also been observed in a few thin sections. Uralitization is rare and mainly proceeds along the border of pyroxenes. Geijer (1930), however, describes specimens consisting mainly of uralitized augite and plagioclase of low anorthite content (48 %). Strongly fractured and only sligthly altered olivine has been observed in three thin sections. It makes-up 10 to 20 vol.% of the rock and is sometimes surrounded by amphibole containing complex opaque mineral exsolutions (Fig. 4c). The average content of opaque minerals in the 8 gabbro samples investigated by Ambros (1973) is the following: magnetite = 13.0 vol.%, ilmenite = 3.5 vol.% and the mixed (lamellar) magnetite-ilmenite = 1.5 vol.%. The sulphides represent less than 1 vol.%. In some rare cases, the content of opaques exceeds 40 vol.%. The opaques mainly present late-crystallization (interstitial) habits and, along their borders, plagioclase generally displays a thin, clear amphibole rim (Fig. 4a). Small grass-green spinel inclusions rarely occur in magnetite. Biotite is a common accessory and is often found in alteration rims surrounding magnetite and ilmenite. It also occurs as large, poikiloblastic crystals belonging to a very-late pegmatoidal crystallization phase. Apatite is often slightly coloured (ε light grey-blue, ω brownish). It is relatively abundant in some samples and presents the particularity of being generally interstitial (Fig. 4a, b). Geijer (1930), however, describes a sample with 9.7 vol.% of six-sided prism apatite belonging to an early generation. In a few cases, apatite contains opaque, needle-type inclusions which are possibly ilmenite (Geijer 1930).

One chemical analysis (Nr 77) is given in Table 2h. Besides this, the results of partial analyses, carried out on the Akkavare gabbro in connexion with ore investigation, are presented below. The following results concern 10 gabbro samples collected from drill-cores (Ambros 1973). The first number corresponds to the average content, followed by the extreme values in brackets (results given in weight %): Fe_2O_3 = 20.8

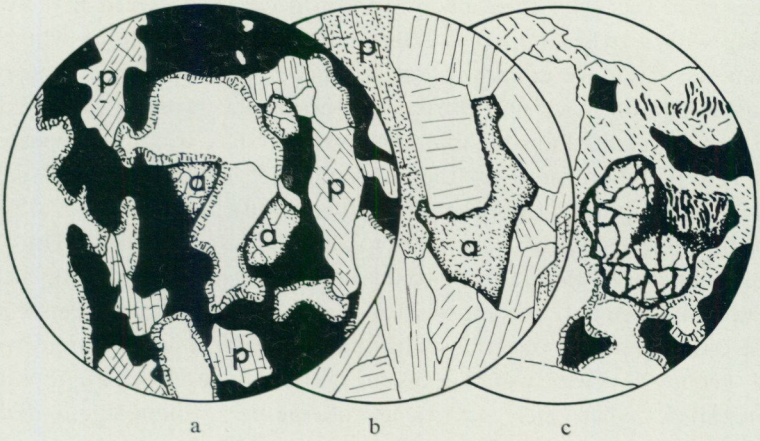

Fig. 4. Akkavare gabbro (normal light × 10). Samples M. Ambros (1972) nr 50 (a), 43 (b), 45 (c).
a — Magnetite (black) is interstitial and poikiloblastic. The plagioclase (clear) is often surrounded by a thin amphibole rim. p = pyroxene, a = apatite.
b — Apatite (a) is interstitial with respect to the plagioclase.
c — A fractured olivine is enclosed in uralite-diopside displaying magnetite exsolution phenomena.
Akkavaregabbro.

(8.0—32.3), TiO_2 = 4.4 (1.5—8.3), MgO = 4.3 (2.8—6.7), CaO = 7.5 (5.2—11.0), BaO = 0.16 (0.02—0.70), MnO = 0.25 (0.12—0.41), S = 0.26 (0.02—0.94). Analyses of ore samples, collected by S. Hammarbäck (LKAB) and containing an average Fe_2O_3 of 37 weight %, give an average S content ten times higher (2.1 %) than for the normal type of gabbro. The average P_2O_5 content of these ore samples is only 0.28 w.%, which certainly corresponds to apatite-poor specimens. The average contents of trace-elements in the gabbro are the following (in ppm): V = 636, Co = 100, Cu = 162, Pb = 39, Zn = 141, Cr = 203, Ni = 43, Sr = 315.

The present investigation has shown that, besides the *noritic types* which were known from long ago, there also exists an *olivine gabbro,* marking a more basic development of the magma than was previously supposed. Chemically, the Akkavare gabbro is characterized by relatively high average contents of iron (20.8 w.% Fe_2O_3), titanium (4.4 w.% TiO_2) and vanadium (> 600ppm).

When considering the very peculiar form of the Akkavare Gabbro

(rather thin, flat-lying sheet or "tongue"), it can be inferred that we are dealing with a dyke of limited extension. The channels along which the magma has risen are unknown and no minor basic dykes are exposed in the area. The presence of a diffuse, sub-horizontal layering in the Akkavare gabbro could indicate that the intrusion has occurred repeatedly. This interpretation presents the advantage of explaining in a simple manner many puzzling petrographic particularities such as the different crystallization habits of apatite, pyroxene and the opaques. Thus, the differentitation of the gabbro would not have occurred in-situ, after a unique emplacement, as supposed by Geijer (1930), but in deeper parts of the crust. Repeated injections with slightly different compositions would have occurred. They would explain the presence of petrographically incompatible types such as: 1) an olivine-hypersthene-augite-diallage gabbro with an ophitic texture, 2) an augite-diallage-hypersthene norite with interstitial appatite and a hypidiomorphic texture and 3) a norite with subbhedral to euhedral apatite.

The petrographic and chemical similarities existing between the Akkavare gabbro and the Nabrenjarka gabbro diabase (pp. 34—39) are striking and point to the fact that, although of different ages, these two gabbros possibly originate from the same level of the crust (parent magmas).

THE PERTHITE GRANITE SERIES

The Perthite Granite Series consists of a wide variety of rocks of the granite family (sensu lato) which, according to the petrographic terminology adopted here, range in composition from quartz-monzonites to quartz-free monzonites. Rocks of this series cover almost entirely the map area NV where they form a somewhat rounded massif extending into the map areas NO, SV and, to the west, into the Stora Sjöfallet map area. The other massifs worthy of note are: the *Stuor-Maksjojaure massif* situated in the south-west corner of the map area, the *Sjaunjaätnö massif* extending from Stora Lulevatten (0e) to Killamjaure (2g) and the north-south elongated *Pikku-Svierkku massif* (0i, 1i) surrounded by volcanic rocks and extending to the south into 27 J Porjus.

The Perthite Granite Series is generally marked on the aeromagnetic maps by somewhat anomalous areas, the anomalies being generally situated between 500 and 200 gamma above the normal value set at

51 400 gamma. This often gives a good contrast with the Lina granite corresponding to a lower range of anomalies. The Stuor-Maksjojaure and Pikku-Svierkku massifs are, however, less magnetic than the average rocks of this series. Somewhat diffuse, linear patterns are sometimes visible on the aeromagnetic maps, in perthite granite regions. They sometimes extend into areas occupied by the Lina granite and apparently represent strongly assimilated relics.

The rocks of this series are generally massive, pink (quartz-monzonite), purplish (monzonite) or rather dark (amphibole- and pyroxene-rich varieties). The grain size is very variable, monzonites being generally coarser-grained than quartz-monzonites. Coarse-grained monzonite are locally strongly weathered and produce a characteristic gravel consisting mainly of perthite crystals. Irregular and often sharp transitions to fine-grained types are common (Fig. 13d). Granitization of volcanic rocks and gabbros by perthite granites and monzonites results in widespread hybrid facies (See Fig. 13). Contrary to the Lina granite, granitization mainly proceeds "at random" giving rise to agmatites instead of foliated types. All the rocks of the Perthite Granite Series contain characteristic complex perthites, often zoned (in the quartz-free types) and sometimes forming large subhedral crystals (porphyroidal types).

The problem of genetic relationships, apparently existing between the Perthite Granite Series and the Porphyry Group, is discussed in a special chapter (pp. 39—43).

A – PETROLOGY

On the geological map, the Perthite Granite Series has been subdivided into three main rock types which are, with decreasing quartz content: the perthite granite, the perthite monzonite and the pyroxene-bearing perthite monzonite. In the field, transitions between these three rock-types are gradual and somewhat diffuse. The geological boundaries are therefore difficult to draw and must be considered as approximate. A slight difference in magnetic susceptibility, between the quartz-rich and the quartz-poor types makes it sometimes possible to delimit these rocks on the aeromagnetic maps. This has also revealed somewhat diffuse, concentric structures in the extensive perthite granite and monzonite massifs in Fjällåsen NV.

Perthite monzonites occurring in the Lainio map area are described to some extent (Witschard 1970) and a thorough investigation on perthitic

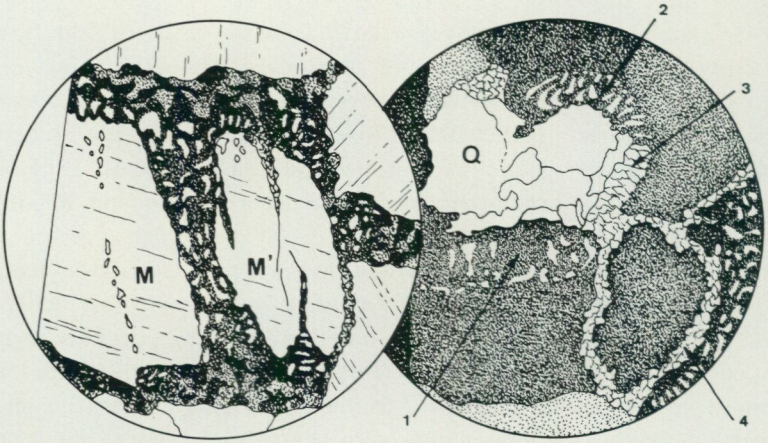

Fig. 5. Perthite granite (normal and polarized light × 11). Sample 1496 B (4a).
a — Cataclastic "compartimented" texture. Myrmekites are abundant in the fine-grained, cataclastic and recrystallized areas surrounding broken and deformed microcline. M and M' are fragments of the same microcline crystal.
b — Incipent "compartimented" texture. 1 and 2 show the development of a myrmekite rim around a quartz core (Q) which is recrystallized in 3. A complete recrystallized rim occurs in 4. Microcline is shaded.
Pertitgranit (4a).

and antiperthitic intergrowths, characteristic of the Perthite Granite Series, is given by Geijer (1931). Only some new aspects of the problem are therefore discussed here.

A total of 65 thin sections have been cut in rocks of the Perthite Granite Series. They include granite, perthite monzonite, pyroxene-bearing monzonites and hybrid types resulting from the granitization of various intermediate and basic rocks.

The texture is generally heterogranular, highly irregular, with sutured crystal boundaries, embayed crystals, replacement intergrowths and zonal replacements often resulting in a porphyroidal development of the perthite crystals. Small crystals sometimes merge together to give large perthite superindividuals which often present irregular concentric zones (coalescence texture). The dark minerals have a strong tendency to concentrate in crystal aggregates. Quartz is interstitial, highly sutured and always presents very irregular extinctions under polarized light. Stress, having affected to various degrees most of the rocks of this series, resulted in the development of a wide variety of sub-cataclastic to cataclastic textures

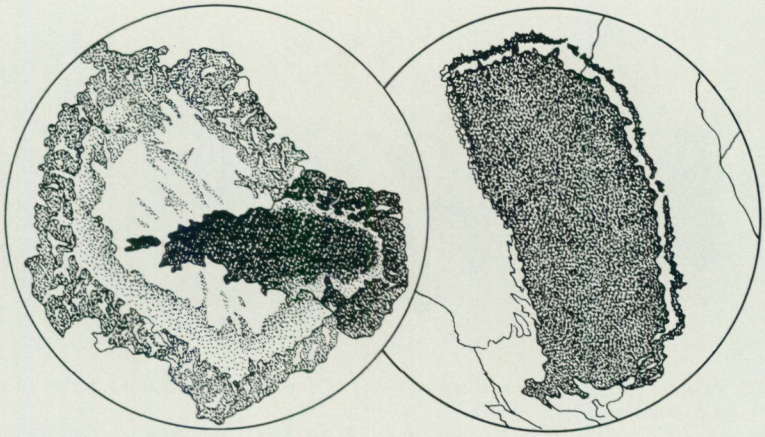

Fig. 6. Perthite monzonite (normal and polarized light × 11).
a — Interpenetration of two complex-zoned perthite crystals. Sample 1494 C (5a).
b — Growth-rim around a perthite crystal. The rim has the same crystallographic orientation as the perthite crystal. Sample 1478 F (4a).
Pertitmonzonit (5a, 4a).

including slip, kinking, bending, fracturing and polygonization, often leading to a "compartimented texture" of the type shown in Fig. 5.

Besides the normal types of perthite and antiperthite intergrowths described by Geijer (1931), the author has observed a wide variety of *strain perthites,* occurring in cataclastic rocks. The most widespread type consists of albite veinlets making up a dense network of microfractures, giving to the perthite crystal the aspect of a microbreccia (Fig. 14a, b, c). In other cases, the perthite crystal is bent along linear, parallel stress planes (strain slip) giving rise to a microschistosity (Fig. 14d). Kinking of perthite crystals, along a plane (Fig. 14e) or an irregular surface (Fig. 14f), is common. Fig. 14e, which shows that some strain perthites are affected by kinking while others are not, indicates that more than one generation of strain perthites exists. Although cataclastic textures, widespread in the Perthite Granite Series, indicate that stress has strongly affected most of the rocks of this series, foliated types are very rare. This problem is again discussed below (p. 32).

Microcline often displays late-crystallization habits (see Witschard 1970, pp. 49—50). All stages of corrosion of the plagioclase by micro-

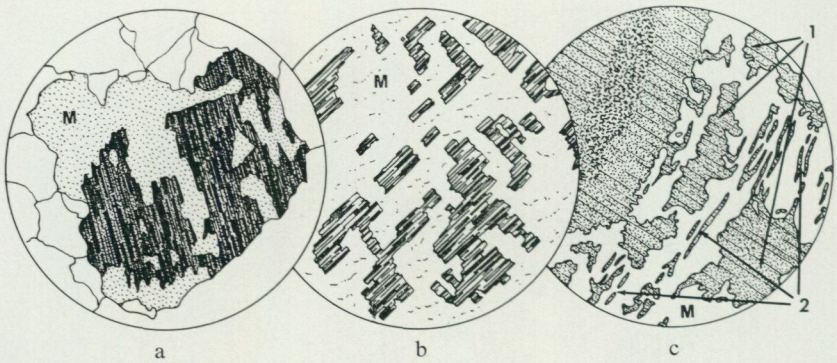

Fig. 7. Various habits of microcline in rocks of the Perthite Granite Series (normal and polarized light × 30).
a — Corrosion of a plagioclase by microcline (M). Sample 1263 (4c).
b — Patch perthite with angular plagioclase relics in microcline. Sample 1395 (2g).
c — Transition from patch perthite (1) to finer, linear perthite (2). All of the plagioclase present in the picture has the same crystallographic orientation. Sample 1313 A (1e).
Olika utbildningsformer av mikroklin i pertitgranitserien (4c, 2g, 1e).

cline can be followed under the microscope. The first stage is represented by border corrosion (Fig. 7a). A more advanced stage consists of patch perthites (Fig. 7b) in which the plagioclase relics are often twinned and their anorthite content can be as high as 25 percent. The last stage which can be observed is the development of linear, string or rod perthites (Fig. 7c) which are very similar to normal (exsolution) types.

The modal estimates of 25 samples, of which there exist chemical analyses, are presented in Table 3 (Nr 1—25). As point-counting measurements are always difficult to make in strongly perthitic rocks, the percentage of quartz, plagioclase and K-feldspar indicated in the triangular diagram Q-Pl-Or (Fig. 18), is taken from the CIPW norms. In this manner, a relatively accurate classification of the rocks making-up the Perthite Granite Series is possible.

The *perthite granite* has been defined and thoroughly described by Geijer (1931). According to the terminology adopted here (see p. 11), it mainly comprises quartz-monzonites (10—35 % quartz) with a trend towards granodiorite (See Fig. 18, diagram 1.). Amphibole is subordinate in about half of the samples. Magnetite, sphene and biotite are subordinate or accessory.

The *perthite monzonite* is represented by quartz-poor to quartz-free types and is essentially made up of rocks of "dioritic monzonite" composition and only a few samples are real monzonites (See Fig. 18, diagram 1.). Green hornblende is essential or subordinate. Biotite and magnetite are subordinate. Sphene is subordinate or accessory. The main accessories are, in order of importance, apatite, sericite, chlorite, rutile, epidote and zircon.

The *pyroxene-bearing perthite monzonite* contains more or less uralitized, essential or subordinate augite or, less frequently, diopside. One sample contains uralitized hypersthene.

Transitional or hybrid types result from the granitization of various rocks, mainly of intermediate or basic composition. Their study has brought many interesting facts as to the mode of emplacement of the Perthite Granite Series. Some examples of hybrid types, with porphyrite and greenstone xenoliths enclosed in perthite granite, are shown in Fig. 13e—f. Exposures and large local boulders of this type are common along the shores of Stora Lulevatten, near the Lapp settlement of Renhagen (0d). Although intermediate- and basic-composition xenoliths are often somewhat recrystallized, they generally display recognizable textures. The more acid xenoliths are, however, strongly assimilated and often present diffuse borders. Fig. 13a—c shows the granitization of a gabbro diabase, proceeding mainly along a network of small fractures. Four thin sections have been cut in granitized gabbro. In one of these, the ophitic texture is well preserved and complex perthites partly surround the plagioclase (labrador). The other thin sections show a strongly obscured ophitic texture characterized by sutured crystal boundaries, fractured plagioclase, strong sericitization and myrmekites. The plagioclase has a relatively low anorthite content (40 %), is often blurred by antiperthite intergrowths and displays border corrosion by microcline.

25 chemical analyses of rocks from the Perthite Granite Series are presented in Table 2 (Nr 1—25). The silica content varies from 75.6 to 63.1 weight % in quartz monzonites and reaches as low as 56.0 % in monzonites. Various diagrams and graphics dealing with chemical parametres are presented at the end of this description (Figs. 16—23). They are discussed at some length in the chapter dealing with genetic relationships existing between the Perthite Granite Series and the Porphyry

Group. A well marked "dioritic trend" of the Perthite Granite Series is outlined in Fig. 18, diagram 1.

The Perthite Granite Series corresponds to a well defined area on the diagram (Fig. 26) dealing with magnetic susceptibility and specific weight. Contrary to the Lina granite, these rocks show a normal increase of specific weight with increasing magnetic susceptibility.

B – MODE OF EMPLACEMENT

Contacts of the type described in the paragraph "transitional or hybrid types" (p. 31) indicate intrusive habits characterized by the local development of xenolith-rich types and of agmatites. Granitization of the acid volcanic rocks is generally of a different sort. It consists mainly of a progressive recrystallization of fine-grained types into coarser-grained, granitoidal rocks. The contact granite-volcanic rocks is often sharp (Fig. 13d). It is however very capricious when observed on large exposures. Gradual transitions between volcanic rocks and granites are best observed under the microscope and, at a certain stage of the transformation, it becomes impossible to determine the origin of the rock.

It is possible that some of the porphyries associated with the Perthite Granite Series are intrusive and have been emplaced at approximately the same time. This is probably the case for the perthite porphyries occurring at the margin of the Pikku-Svierkku perthite monzonite massif (See p. 26). When porphyries, occurring in granite areas, are not directly associated with preserved volcanic effusives (mainly banded types), it is impossible to determine their origin with any certainty.

On account of its wide range of (chemical and petrographic) compositions, the Perthite Granite Series has the possibility to assimilate a large variety of rocks. This results in more or less hybrid types and gives a strongly obscured picture on the aeromagnetic maps.

As indicated above (p. 29), sub-cataclastic to cataclastic textures are common in rocks of this series. Foliated types are, however, very rare and the phyllosilicates (mainly biotite), which are present in most of these rocks, are generally randomly orientated. This indicates that no important directional stress has affected these rocks during or after their emplacement.

THE LINA GRANITE SERIES

The Lina Granite Series is well represented to the east of the area occupied by the volcanic rocks (NO, SO). It is often migmatitic and gives rise, on the aeromagnetic maps, to rather complex anomalies. It is also widespread to the west of the volcanic rocks (SO) and to the south of the extensive perthite granite area (SV) and there, it is generally massive and almost devoid of anomalies on the aeromagnetic maps.

In a general way, the Lina Granite Series is of the same type as described for 29 L Lainio (Witschard 1970, pp. 57—69). Pegmatites and pegmatoidal granites are, however, less widespread than for the Lainio map area.

A – PETROLOGY

The Lina granite is medium-grained and its composition is quartz-monzonitic, with approximately equal amounts of quartz, plagioclase and microcline. In places, it is strongly sheared. Weak to medium foliation is common and is outlined by the preferential orientation of biotite.

29 thin sections of the Lina granite (migmatitic types not included), permit the following remarks. Quartz (25—35 vol.%) is interstitial. In the foliated types, it has often recrystallized as elongated crystal aggregates or as sub-veinlets. Extinctions are always very irregular under polarized light. Myrmekites occur in about one third of the samples. The plagioclase is mainly represented by oligoclase with an average anorthite content of 25 %. Albite occurs in perthites and, sometimes, as small, distinct crystals. Sericitization is weak. Microcline presents late-crystallization habits and has a tendency to form large poikilitic crystals. Biotite is generally subordinate. It is often represented by a green-brown variety with transitions to chlorite. In order of importance, the accessories are: magnetite, sphene, apatite, chlorite, sericite, zircon, rutile, epidote, muscovite, tourmaline.

The *amphibole granite at Apovare* (0a, 1a, 2a) has a quartz-monzonite composition and the plagioclase is an andesine (40 % anorthite). The amphibole is a green-blue variety of hornblende. It is often concentrated in larger crystal aggregates, together with the accessories. The presence of a slightly coloured apatite has been observed. Towards the west, the amphibole granite gently grades to amphibole-free Lina granite.

Migmatites, resulting from partial assimilation of pre-existing rocks by the Lina granite, are widespread to the east of the volcanic rocks (Fjällåsen NO, SO). Gneisses predominate. Their composition is often dioritic thereby indicating that no notable potassium and silica metasomatism has occurred.

Two chemical analyses of the Lina granite are given in Table 2g (Nr 63 and 64). In order to determine with more precision the areas corresponding to the Lina granite on various triangular diagrams (Figs. 18—21), seven chemical analyses of Lina granite have been borrowed from the Lainio map-sheet (Witschard 1970, p. 95).

B – MODE OF EMPLACEMENT

The mode of emplacement of the Lina granite is discussed at some length in the Lainio map description (Witschard 1970, pp. 64—69). Most of the results obtained there have been confirmed in the Fjällåsen map area. The main difference lies in the fact that the host rocks to granitization are mainly meta-sediments of the Pahakurkio Group in the Lainio map area while they are mainly represented by volcanic rocks and meta-sediments of the Porphyry Group in the Fjällåsen map area.

The Lina granite, situated to the east of the volcanic rocks (NO, SO), gives rise to somewhat complex and often distinct anomalies on the aeromagnetic maps. Gneissic relics in granite are common in this area and the plane of foliation is generally parallel to the strike of corresponding magnetic naomalies. Some structures are rather well preserved and indicate that we are dealing with strongly folded relics (Fig. 9, A_2).

The area corresponding to the Lina granite (migmatites not included) on the Q-Pl-Or diagram (Fig. 18) is rather limited and corresponds to what can be called an "ideal granite field" when compared with results from experimental crystallization of silica melts. The area corresponding to the Lina granite on the Q-L-M diagram (Fig. 19) is also very restricted. This problem is further discussed in Witschard 1970 (pp. 61—62, 64—69).

THE NABRENJARKA GABBRO DIABASE

Nabrenjarka is the name of a small peninsula projecting into Stora Lulevatten (1b). Although gabbro exposures were discovered long ago in the map areas NV and SV, they figure as small isolated massifs on the

geological map of Norrbotten (Ödman 1957). The present investigation has shown, however, that we are dealing with an extensive, somewhat circular and continuous dyke (See Fig. 15.) named here the Nabrenjarka gabbro diabase. It i best exposed in the Fjällåsen and Stora Sjöfallet map areas where it has been followed, more or less continuously, for more than 70 km. Its width ranges from about a hundred metres to more than one kilometre (Vuolep Appojaure, 2a) and, according to geophysical investigation, it dips towards its western (or concave) part. It is generally well marked on the aeromagnetic maps (high anomalies) which has permitted it to be traced into the Porjus and Tjåmotis map areas where no systematic mapping has, as yet, been carried out.

The region situated to the west of the diabase is characterized by the presence of a multitude of basic dykes intersecting granites, porphyries and various sediments. These dykes can best be observed in the Stora Sjöfallet map area. It is the authors opinion that they are associated with the Nabrenjarka gabbro diabase.

The Nabrenjarka gabbro diabase and associated basic dykes are the youngest rocks known to exist in the map area. Their age is not precisely known although it can be said that their emplacement occurred after the emplacements of the perthite and Lina granites and probably before the deposition of schist and siltstones underlying the Caledonian nappes and representing the base of the autochthonous (according to observations carried out by the author in the Stora Sjöfallet map area).

A – PETROLOGY

The average gabbro is medium-to-coarse-grained, massive and very dark. In places, intense weathering gives rise to a characteristic coarse-grained, dark and biotite-rich gravel. The minor basic dykes exhibit very variable textures ranging from fine-grained doleritic to coarser-grained "porphyrite" types consisting of large plagioclase laths randomly distributed in a dark green, fine-grained matrix.

Although these basic rocks are the youngest known to exist in the map area, they are often strongly metamorphosed and only a few gabbro samples present well preserved pyroxenes. This problem is discussed below.

The following petrographic description is based in a total of twelve thin sections, six cut in gabbro and six in minor basic dykes. The

plagioclase is often irregularly coloured light brown or grey. It is generally rather fresh although a few slides show partial sericitization. The anorthite content varies between 55 and 75 % in normal gabbro. One Strongly metamorphosed type contains andesine with only 40 % anorthite. Zoned extinctions are common. The ophitic texture is generally preserved in the gabbros. In the minor basic dykes, however, it often only subsists as a relic-texture, strongly obscured by the late crystallization of amphibole. The amphibole is mainly a secondary hornblende (uralite) and, less frequently, actinolite-tremolite. Sieve texture and a very irregular colour distribution (light green to dark grass-green) are common. Augite is abundant in all but one gabbro samples. It is irregularly coloured (light brown) and generally surrounded by an uralite rim. Pigeonite ($2V = 15°$) has been observed in one thin section. Two thin sections contain irregularly coloured hypersthene (light to dark brown). Biotite is an essential mineral of both gabbros and minor basic dykes. It is often reddish-brown. Magnetite is generally abundant (up to 10 vol.%). This is reflected by chemical analyses of gabbros indicating an average Fe_2O_3 content of 13.1 W.% (37 analyses). The habits of magnetite are very variable: sub-graphic (schiller) relics in biotite or amphibole, minute well-formed crystals or large and somewhat poikilitic crystals. The gabbro is almost devoid of such Ti-minerals as sphene and rutile. As the average titanium content is relatively high (average = 2.7 w.%), it is probable that the opaque mineral is, at least partly, titanomagnetite or magnetite with ilmenite inclusions. The opaques are often surrounded by a variety of simple or complex rims (epidote, biotite-uralite, biotite-chlorite etc.). Apatite, generally found as more or less broken needles, is an important accessory of the gabbros and dolerites. Two minor basic dykes contain an estimated 5—10 % apatite concentrated in amphibole. The other accessories worthy of mention are: sphene which is an accessory of the minor basic dykes, rutile, found in small amounts in gabbro and epidote-saussurite occurring in the more altered types.

Two chemical analyses of gabbro (Nr 79 and 80) and one of a minor basic dyke (Nr 78) are presented in Table 2. Besides these, 35 additional chemical analyses of gabbro have been consulted. They originate from a geochemical and geophysical investigation of the Nabrenjarka gabbro diabase by means of systematic sampling of well exposed cross-sections of the diabase. Some of the geophysical aspects of the problem are presented in the appendix. The average chemical composition and extreme

values are presented in Table 4 where a comparison is made with older gabbros from 28 J Fjällåsen, 29 L Lainio, 28 L Tärendö and 29 J Kiruna. This gives the following results: the Nabrenjarka gabbro diabase is richer in Fe_2O_3 (+6.5 to 9.0 %), in TiO_2 (+1.4 to 1.9 %) and in MnO (+0.05 to 0.07 %) than the older gabbros. It is, however, poorer in SiO_2 (— 4.1 to 5.3 %) and Al_2O_3 (— 2.0 to 3.9 %) than the latter. The average content of trace elements is the following (in ppm): Cu 88, Pb 30, Zn 122, Ni 64, V 632 and Cr 93. P_2O_5 has not been analysed but it must give relatively high values when dealing with the apatite-rich minor basic dykes.

As a conclusion to the geochemical investigation, it can be said that the Nabrenjarka gabbro diabase is characterized by relatively high percentages of Fe, Ti and V and a rather low silica content. The Akkavare gabbro (See pp. 23—26.) is, to the authors knowledge, the only gabbro of Norrbotten having approximately the same composition as the Nabrenjarka gabbro diabase. The study of post-granite diabases has, however, just begun in this northern part of Sweden.

B – MODE OF EMPLACEMENT

According to the geophysical interpretation, the Nabrenjarka gabbro diabase dips towards the west at a rather low angle (See appendix.). In the field, contacts of the diabase with the host-granite are rather scarce and mainly occur on the eastern flanks of Jårpåtjåkkå (4a). Two exposures there show that the contact dips steeply towards the west. It is probable that the diabase flattens out rather rapidly with depth, thereby accounting for the results obtained by the geophysical investigation. The diabase apparently lies rather flat in its northern part (5a) where it follows the northern flanks of Råvemåske.

The contact between granite and gabbro is generally very sharp. The granite often displays a shear-zone running parallel with it. At, and near the contacts, the diabase is often fine-grained and locally contains concentrations of plagioclase. In one exposure (5a), the diabase contains angular, somewhat fine-grained granite fragments and is intersected by a few quartz veins. One gabbro sample contains a few complex perthites and quartz thereby indicating that a small contact aureole can locally be present (local remobilization of granitic material).

Detailed photo-maps (1:10 000), covering the boundary between the

two map-sheets 28 J Fjällåsen and 28 I Stora Sjöfallet, clearly show that the minor basic dykes are mainly parallel to a fault-system which is well marked in the granite. The contact between these dykes and the host granite, is very sharp and the basic rock is often strongly sheared along the contact. Unaltered, angular granite fragments have been observed by the author in minor basic dykes occurring along the shores of Satisjaure (28 I Stora Sjöfallet).

The rather strong metamorphism affecting the Nabrenjarka gabbro diabase and the minor basic dykes is characterized by intense uralitization of the pyroxene and by the development of blastic biotite-amphibole crystal aggregates, often obscuring the original texture. This metamorphism is difficult to explain when considering the fact that no regional metamorphism is known to have occurred in the area after the emplacement of the perthite and Lina granite. What is more, gabbros which are older than the Nabrenjarka gabbro diabase, are often less metamorphic than the former. A logical interpretation of these facts is that the metamorphism affecting the Nabrenjarka gabbro diabase and the minor basic dykes is contemporaneous with the emplacement of these rocks. In other words, we are apparently dealing with a particular type of *retrograde metamorphism*. The succession of events, leading to the emplacement of the diabases, can be interpreted in the following manner. At a time when granite was already rigid (low temperature conditions), basic magma was injected in an extensive fault system, more or less controlled by a major, somewhat circular *Nabrenjarka fault*, giving rise to the Nabrenjarka gabbro diabase. The cooling of the magma, of probable original noritic composition, was probably rapid on account of the low temperature of the host rocks and also on account of the diminishing pressure. This resulted in constant readjustments of the solidifying magma to the varying pressure-temperature conditions. This, in turn, resulted in constant modifications of the mineralogical composition of the rock. Pyroxene was most affected by the process and was totally replaced by uralite in the minor basic dykes. It only subsisted locally in the wider Nabrenjarka dyke where it is, nevertheless, strongly uralitized.

In agreement with the interpretation above, the texture of the minor basic dykes is controlled, to a large extent, by the width of the dykes. For example, the texture is coarse-grained ophitic in the larger dykes (down to about 100 m wide), porphyritic-ophitic (porphyrites) in smaller dykes (down to about 10 m wide) and fine-grained ophitic in the small dykes.

Zoned dykes, with fine-grained margins and porphyritic or gabbroic centres have often been encountered by the author in 28 I Stora Sjöfallet.

It is probable that some of the larger dykes have been injected repeatedly, in relation to successive widening of the fractures along which the basic magma progressed. This would explain the fact that, according to geophysical investigations, the Nabrenjarka gabbro diabase shows a certain layering. Apatite-rich diabases, occurring mainly in 28 I Stora Sjöfallet, indicate that differentiation of the magma has probably taken place in deeper parts of the crust.

DISCUSSION OF THE GENETIC RELATIONSHIPS EXISTING BETWEEN THE PORPHYRY GROUP AND THE PERTHITE GRANITE SERIES

The fact that rocks of the Porphyry Group occur preferentially in association with rocks of the Perthite Granite Series is striking and can be observed in the map areas 28 J Fjällåsen, 29 J Kiruna and 29 L Lainio. This has been the basis for a comparative study of these two series of rocks in order to find out if there exists a genetic relationship between them and, if so, of what type.

Fine-grained volcanic rocks and highly perthitic granites are difficult to study under the microscope. Thirty-five chemical analyses have therefore been made on rocks of the Porphyry Group and twenty-five on rocks of the Perthite Granite Series (Table 2, respectively: Nr 26—60 and Nr 1—25). The comparison between these two series of rocks is mainly based on these chemical analyses which are described to some extent on p. 11.

The (average) variations of the Niggli values *al, fm, c* and *alk,* as a function of *si,* have been separately plotted on a diagram (Fig. 16). The variation-curves for *al, c* and *alk,* for both series of rocks, coincide extremely well. The relatively high *fm* value for the volcanic rocks, at about 300 *si,* is due to rather exceptional rock-types: a dark rhyolite and a dacite.

The variations of the Niggli values *k, mg* and *fm,* as a function of *si,* have been plotted in Fig. 17. They show a larger dispersion of values for the volcanic rocks than for the granites although the average values are about the same for both series.

Triangular variation diagrams, dealing with various chemical parameters, are presented in Figs. 18—21. In general, they all show that the Perthite Granite Series exhibits the same trends as the Volcanic Series. The main trend, from diorite to quartz-monzonite, is well marked on the Q-Pl-Or diagram (Fig. 18). The trend towards basic types or "basic trend" is more developed in the Volcanic Series than in the Perthite Granite Series. In the field, this is reflected by the difficulty of the Perthite Granite Series to assimilate the more basic types.

Figs. 22 and 23 show the (average) variations of some major and trace elements, as a function of the silica content. A good coincidence of the curves corresponding to the Volcanic Series and to the Perthite Granite Series is obtained for MnO, Sr, Zn and V. Slight differences occur for TiO_2, Ni and Cu although the trends are of the same sort.

Specific weight and magnetic susceptibility measurements, carried out on every sample from the map area, have proved to be of valuable help for the comparative study of volcanic rocks and granites. In order to avoid misinterpretation, only the samples for which there exist thin sections, are taken into consideration in the diagrams presented below (Figs. 24—27).

Fig. 24 shows that most of the specific weight/magnetic susceptibility values, for 135 samples belonging to the Volcanic Series and to the Perthite Granite Series, fall within a characteristic, well-defined area.

The areas corresponding to various volcanic rock-types (Fig. 25) are generally well-delimited and show that we are dealing with a differentiated and continuous series of rocks. The acid volcanics area is almost totally enclosed in the area corresponding to porphyries, pointing to the close relationships existing between these two rock-types. The acid volcanic rocks have a slightly lower average specific weight than the porphyries while their susceptibilities cover about the same range.

Fig. 26, in which the area of the Lina Granite has been indicated for comparison, shows that the area of the Perthite Granite Series coincides rather well with most of the area corresponding to the Volcanic Series. This is however not true for areas of higher specific weights (> 2.8) corresponding mainly to andesites and greenstones (See Fig. 25.).

It is of interest to note here that diagrams dealing with geophysical parameters give precisely the same picture as diagrams dealing with chemical parameters: the Perthite Granite Series and the Volcanic Series show the same variations, exception being made for some andesites and

greenstones. In both types of diagrams, the Lina granite corresponds to distinct and generally rather limited areas.

When considering average values, the Perthite Granite Series and the Volcanic Series display approximately the same susceptibility/specific weight variations (Fig. 27, upper diagram). The diagram dealing with variations of specific weight, as a function of the silica content (Fig. 27, lower-right), shows the very interesting phenomenon that, for a given SiO_2 value below 70 weight %, rocks of the Volcanic Series are denser (or have a smaller volume) than rocks of the Perthite Granite Series. The difference in specific weight is rather constant below 68 weight % SiO_2 and is estimated at about 0.04 specific weight units.

The observations above indicate that, besides the strong geographic affinities mentioned before, there exists many chemical and physical similarities between the rocks of the Porphyry Group and those of the Perthite Granite Series.

No radiometric age determinations have been carried out in the map area on rocks of the Prophyry Group. Structural considerations in the northern part of 28 J Fjällåsen and in the southern part of 29 J Kiruna allow the supposition that the Porphyry Group is of the same age as the Kiruna porphyries. This is still hypothetical. Radiometric age determinations give, for the Kiruna porphyries, an age of ± 1605 m. y. (Welin 1970). Another age determination of volcanic rocks apparently related to the Kiruna porphyries, the Kaska Tjaurek volcanic rocks, gives an age of 1635 m. y. (Welin et al. 1971) with, however, a rather large margin of error (± 90 m. y.). The age of the perthite granite occurring at Masugnsbyn, on the Lainio map-sheet, has been determined at ± 1535 m. y. (Gulson 1972). Furthermore, the age determination carried out on a perthite monzonite and perthite granite massif situated in 28 J Fjällåsen (SV), give the result of ± 1565 m. y. (Gulson 1972). Provided these average ages are accurate and, with many uncertainties still remaining as to the age of the volcanic rocks of the Fjällåsen map area, it can be said that a time-gap of about 40 million years exists between the intrusion and deposition of the Porphyry Group and the emplacement of the Perthite Granite Series.

The rocks of the Porphyry Group are intensively folded and have been, to a large extent, transformed to schists and gneisses (see p. 20). Although rocks of the Perthite Granite Series are often sub-cataclastic, foliated types are extremely rare (see p. 32). Phyllosilicates (mainly

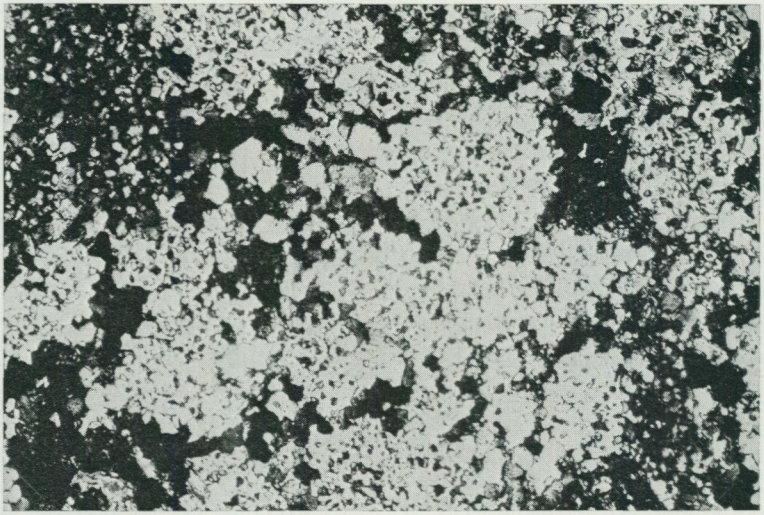

Fig. 8. Granophyric "patch" texture in a metamorphic porphyry. Sample 1256 (3d), polarized light × 20.
Granofyrisk metaporfyr (3d).

biotite) are abundant in perthite granites and monzonites and a directional stress, of the type which has affected the Porphyry Group, would certainly have resulted in the widespread development of foliated types. The absence of foliation in these rocks strongly suggests that an important time-gap (with folding and metamorphism) existed between the intrusion and deposition of the Porphyry Group and the emplacement of the Perthite Granite Series. This is in agreement with results obtained from radiometric age determinations.

The observations above indicate that we are apparently not dealing with a *subvolcanic* type of intrusion (subcontemporaneous volcanic rocks and granites) but, on the contrary, the perthite granites and monzonites probably originate from a slow process of recrystallization (of isochemical type) occurring in the volcanic rocks. This permits a simple explanation of the many similarities existing between the Porphyry Group and the Perthite Granite Series.

A few thin sections of strongly recrystallized volcanic rocks show that one of the stages of transformation (to coarser-grained types) is sometimes represented by the development of a type of granophyric "patch" texture (Fig. 8). In some cases, it is possible to observe the "blastic" character of

these granophyr patches which have developed across phenocrysts and partly obscur the original texture in the porphyries (superimposed metamorphic texture).

Although the transformation from volcanic rocks to granite is, on a large scale, mainly isochemical, small-scale remobilizations have certainly taken place during the granitization process. They would account for the rather "homogeneous" aspect of the perthite granite and monzonite. The neat intrusive characteristics sometimes displayed by the perthite granite, as for example the xenolith-rich types and the agmatites exposed on the shores of Stora Lulevatten (See p. 31.), indicate that a rather "fluid" or magmatic stage has locally been reached during its emplacement.

The diagram dealing with the specific weight and the silica content of the volcanic rocks and granites (Fig. 27) shows that, for an equal silica content, rocks of the Perthite Granite Series are more voluminous (or less dense) than rocks of the Volcanic Series (See p. 41.). The diagram dealing with the specific weight and the magnetic susceptibility (Fig. 27) shows nevertheless that the variations, for both series of rocks, coincide rather well. This permits to say that, provided this difference in in volume can be considered as correct over large areas, an isochemical transformation from volcanic rocks to granite would certainly be accompanied by rather important "stress-building" phenomena. It can be inferred that stress originating in this manner would be rather evenly (or randomly) distributed in rocks undergoing recrystallization (hydrostatic-type distribution) and it is unlikely that it would give rise to widespread foliated types. It could, however, be the cause of the important cataclastic phenomena generally observed in rocks of the Perthite Granite Series. This interpretation presents the avantage of explaining the important deformation to which these rocks have been subjected, without the development of a preferred orientation or foliation.

TECTONIC INTERPRETATION

The tectonic interpretation of such an area, where plutonic rocks predominate and where supracrustal rocks, often transformed to schists and gneisses, are devoid of primary or "way-up" structures, can only be hypothetical. The interpretation is mainly based on aeromagnetic maps. The strike and dips, according to geophysical investigations, have been of valuable help for identifying structures in regions devoid of exposures.

A – STRUCTURES IN THE VOLCANIC ROCKS

Large-amplitude folds occurring in the volcanic rocks are well marked on the aeromagnetic maps NO and SO. A schematic picture of the major fold axes is given in Fig. 9. The strongest folding has occurred along a north-south to north-west — south-east direction (A_1 and S_1 in Fig. 9). Minor folding has also occurred in an average east-west direction. It is the combination of these two fold-axis directions which gives rise to domes and basin structures, often well-marked on the aeromagnetic maps. The symbole referred-to below, are to be found in Fig. 9.

A major antiform (A_1), generally with granite at its centre, can be traced from the south to the north of the map-sheet. A few kilometres to the west of A_1, and running parallel to it, occurs a major and probably deep-going synform (S_1). It consists of alternating acid and intermediate volcanics with minor occurrences of meta-sediments near or at the top of the series.

To the east of A_1, the structures on the aeromagnetic maps are somewhat diffuse and the fold axes cannot be drawn with any certainly, with the exception of a small, well-marked and faulted structure interpreted as a dome (A_2). Field observation revealed the presence there of a somewhat migmatitic Lina granite.

Five geological profiles, across the volcanic rocks (NO, SO), are presented in a separate folder together with the geological maps. They present a better idea of the major folds affecting these rocks.

Because of the intense granitization of the volcanic rocks in the map-areas NV and SV, no major structures have been identified there.

It must be mentioned that the schistosity and the gneissification of the volcanic rocks is generally parallel to the banding in these rocks and also to lithological boundaries. Therefore, they probably reflect features of primary origin and have apparently occurred at the same time as the main deformation.

B – STRUCTURES IN THE PLUTONIC ROCKS

Most of the structures which can be observed on the aeromagnetic maps in granitic areas are "relic" structures originating from poorly assimilated supracrustal rocks. There exists, however, a few large structures which are apparently directly related to the emplacement of the plutonic rocks.

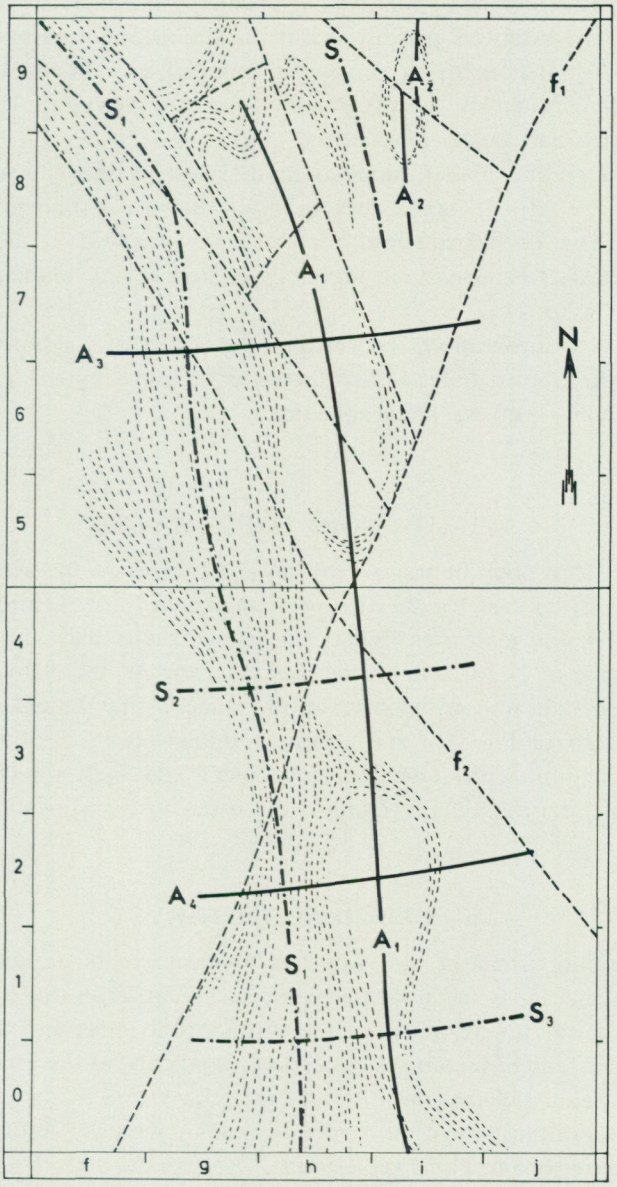

Fig. 9. Schematic structural map over Fjällåsen NO and SO. The volcanic complex is shaded. A = antiform, S = synform, f = fault.
Tektonisk översiktskarta. A = antiform, S = synform, f = förkastning.

The largest structure of this type is visible in the map areas NV and NO, within the extensive perthite granite and monzonite massif described above (p. 26). It consists of somewhat rounded and diffuse patterns of lower magnetic intensity. This is possibly due to a concentric distribution of quartz-rich and quartz-poor types.

The Lina granite massif, situated to the west of the volcanics rocks at Sjaunja-ape (3—4f—g) is rather homogeneous (aeromagnetic interpretation). The strong cataclastic deformation observed in the adjacent volcanic rocks, to the east, is probably related to the emplacement of this massif (See p. 14.).

Structural considerations concerning the Akkavare gabbro and the Nabrenjarka gabbro diabase are discussed to some extent in the text (pp. 23—26, 34—39) and in the appendix.

C – LATE RIGID DEFORMATION

Major faults can often be traced over large distances on the aeromagnetic maps. This is the case for the two very important faults f_1 and f_2 shown on Fig. 9. In the map area, two main sets of faults exist: one with an average strike of N 30° E and one striking from W 33° N to N 20° W. This corresponds well with observations made in the Lainio map-sheet (Witschard 1970, Fig. 41) and confirms the presence of a widespread rigid deformation with rather constant shear and fault directions. The geophysical interpretation of faults is discussed in the appendix.

GEOLOGICAL HISTORY

The time relationships of the various geological events presented below summarizes the ideas and hypotheses expressed earlier in this publication. The lack of way-up structures in the supracrustal rocks and the lack of radiometric age determinations are serious handicaps to the establishment of a stratigraphic succession.

The geological history of the map area is unknown prior to the intrusion and deposition of the Porphyry Group.

The Porphyry Group, also called the Volcanic Series, is a well differentiated series of rocks ranging in composition from rhyolite to basalt. In a general way, basic- to intermediate-composition volcanic rocks pre-

dominate at the base of the series, while acid volcanic rocks are mainly encountered higher in the series. Rocks of sedimentary or volcano- sedimentary origin occur mainly at, or near the summit of the series. This is however an over-simplification and alternating volcanic rocks of various compositions occur throughout the series.

After their deposition, the rocks of the Porphyry Group were intensively folded and are generally steeply dipping in the field. The major direction of folding is north-south, combined with a minor east-west direction (fold-axes direction). Probably at the same time as the deformation, a large part of the volcanic rocks were transformed to schists and gneisses.

Although very little is known about the time of emplacement of the gabbros, by analogy with neighboring map areas, they are thought to have been emplaced after the Porphyry Group, possibly after the main folding phase.

Probably after a considerable lapse in time, the Perthite Granite Series and the Lina Granite Series were emplaced. Both series present migmatitic characteristics and perthite granites and monzonites apparently originated from a slow, isochemical recrystallization of the volcanic rocks.

At a time when the granites had totally crystallized and were rigid, an extensive fracture of more than 100 km in length was injected by basic magma, thereby giving rise to the Nabrenjarka gabbro diabase. It was accompanied by the injection of many minor diabases.

This was followed by important faulting and shearing along two main directions (NNE—SSW and NW—SE) which seem to be rather constant throughout Norrbotten.

ECONOMIC ASPECTS

No deposit of economic interest is presently, or has been mined in the map-sheet area. Ore indications, however, occur at several places and have been investigated on various occasions.

The iron ore Peltovaara (0i, 0j) was discovered some time before 1943. Geophysical (magnetic) measurements and diamond drillings (17 holes) were carried out in the years 1959—1964 by Stora Kopparbergs Bergslags AB. The ore mineral is magnetite, found either as veinlets or as

impregnations in somewhat skarn-altered meta-sediments. The ore is about 3 km long, generally less than 15 m wide and strikes NW—SE. The average iron content is low (20 %).

The iron- and titanium-rich Akkavare gabbro was apparently already known at the begining of this century. A geological description of the gabbro was made by Geijer in 1930. Geophysical (magnetic) measurements and diamond drillings (14 holes) were carried out by Stora Kopparbergs Bergslags AB in the years 1957—1958. Magnetic, gravimetric and slingram measurements were made by SGU in the years 1968—1970. A geological and geophysical interpretation of the Akkavare gabbro, based on this new material, was made by M. Ambros and H. Henkel in 1973. The Akkavare gabbro is described at some length in the present paper (See pp. 23—26 and appendix.).

The intermediate- and acid-composition volcanic rocks occurring in the map areas NO and SO are sometimes copper-bearing. Copper concentrations are apparently mainly localized in the region situated between Allavare (3h) to the south and Risbäck hpl. (5h) to the north. Granitization of the volcanic rocks is often well developed in this region.

FIGS. 10—27
AND
TABLES 1—4

Fig. 10. Intermediate-composition volcanic rocks.

a — Metamorphic porphyrite displaying a weak schistosity resulting from the parallel orientation of plagioclase laths (andesine). *Exposure 1304 (9i).*
b — Irregularly banded, sub-gneissic volcanic rocks of acid and intermediate composition, north of Allavaara. *Exposure 1200 (4h).*

c — Sharp contact between a porphyrite (to the right) and a fine-grained greenstone (to the left). The contact is outlined by a thin, epidote-rich zone. *Exposure 1207 (4h).*

d, e, f — Various aspects of a porphyrite horizon occurring at Nietsakist-jåkkå. Irregular fine-grained bands are visible in d. The plagioclase laths make up flow-like patterns in f. *Exposure 1140 (0h).*

Intermediära vulkaniter.

Fig. 11. Volcanic breccia in greenstone milieu occurring to the SW of Kassakåbbå.

Exposure 1316 (5f, 6f).

a — General aspect of the breccia. The lighter porphyry fragments are often deformed and lens-shaped. They are strongly flattened along the plane of schistosity. They are enclosed in a foliated, dark, intermediate-composition matrix.

b — Bleached margin around a porphyry fragment.

c, d — Porphyry fragments of irregular shapes (volcanic bombs?) are more or less moulded by the matrix.

Vulkanisk breccia i grönstensmiljö SV om Kassakåbbå.

Fig. 10

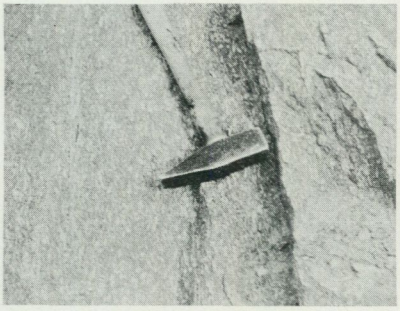

a

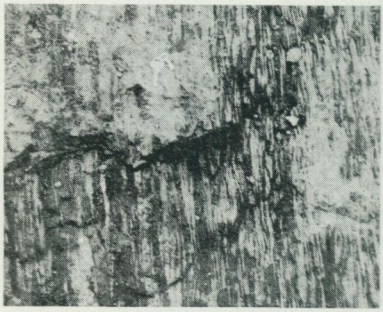

b

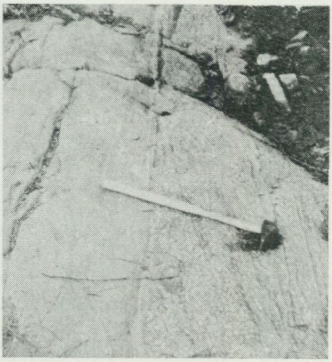

c

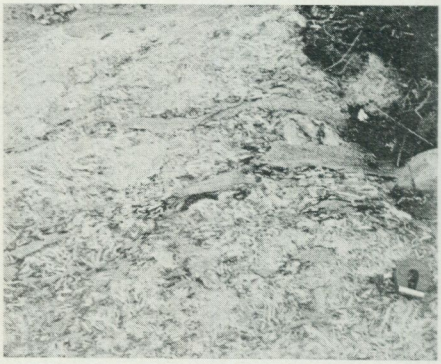

d

e

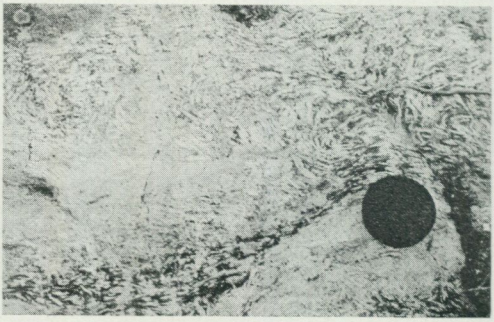

f

Fig. 11

a

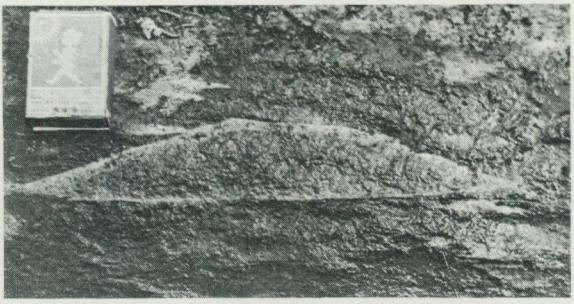

b

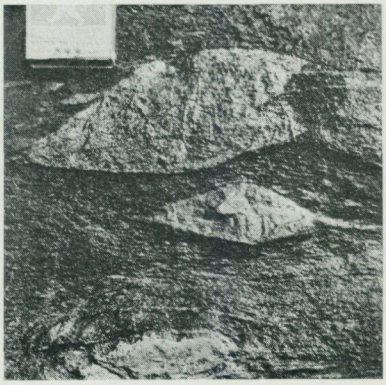

c

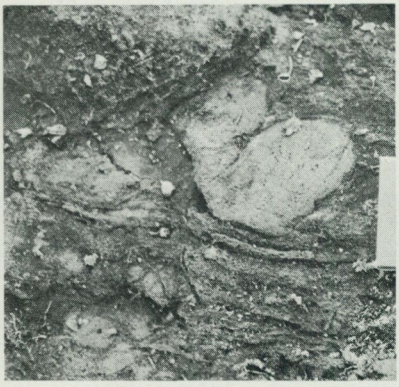

d

Fig. 12. Cataclastic acid volcanics and porphyries N of Allavaara (normal and polarized light × 15).

a, b, c — Progressive mylonitization in porphyries. Chlorite and saussurite (dark) occur along the fracture planes. A very fine-grained saussurite-chlorite matrix, enclosing fractured quartz and plagioclase relics, is visible in c. *Samples 1168, 1163 A and 1163 B (3h, 4h).*

d — Metamorphic porphyry displaying a porphyroclastic texture. Plagioclase porphyroclasts are clear. They are more or less moulded by the fine-grained matrix. *Sample 1171 B (4h).*

e — Metamorphic and foliated porphyry enclosing a few plagioclase phenocryst relics. *Sample 1169 (4h).*

f — Metamorphic and foliated porphyry. In places, the rock has the aspect of a schist, with alternating bands of different grain-size. The porphyritic texture is generally strongly obscured. *Sample 1170 (4h).*

g — Metamorphic porphyry displaying a flow-like texture of cataclastic origin. *Sample 1170 (4h).*

h — Deformed plagioclase in a sub-mylonitic porphyry. *Sample 1166 (3h).*

i — Fine-grained foliated rock of probable volcanic origin. *Sample 1169 (4h).*

Kataklastiska sura vulkaniter och porfyrer N om Allavaara (4h, 3h).

Fig. 13. Perthite Granite Series.

a, b, c — Granitization of a gabbro diabase by the perthite granite. The granitization often proceeds along small fractures in the diabase. *Exposure 1461 (6b).*

d — Sharp contact (×) between a coarse-grained perthite granite and a fine-grained rock of probable volcanic origin. *Exposure 1046 (0d).*

e, f — Angular porphyrite and intermediate-composition volcanic xenoliths in a perthite granite. Some relics are strongly assimilated (f). *Exposure 1046 (0d).*

Pertitgranitserien (6b, 0d).

Fig. 14. Various habits of perthites in cataclastic rocks of the Perthite Granite Series (polarized light × 25).

a, b — Irregular strain-perthites in a perthite monzonite. *Sample 1545 A (9c).*

c — Strain- and patch-perthites in a quartz-monzonite. *Sample 1513 (5c).*

d — Linear deformation of the "strain-slip" type resulting from stress. *Sample 1526 D (5b).*

e — Kinking of a perthite crystal. Note the strain-perthites which are not affected by the kinking (from upper-left to lower-right). *Sample 1545 A (9c).*

f — Irregular kink-boundary. *Sample 1513 (5c).*

Pertittyper i kataklastiska pertitgraniter.

Fig. 12

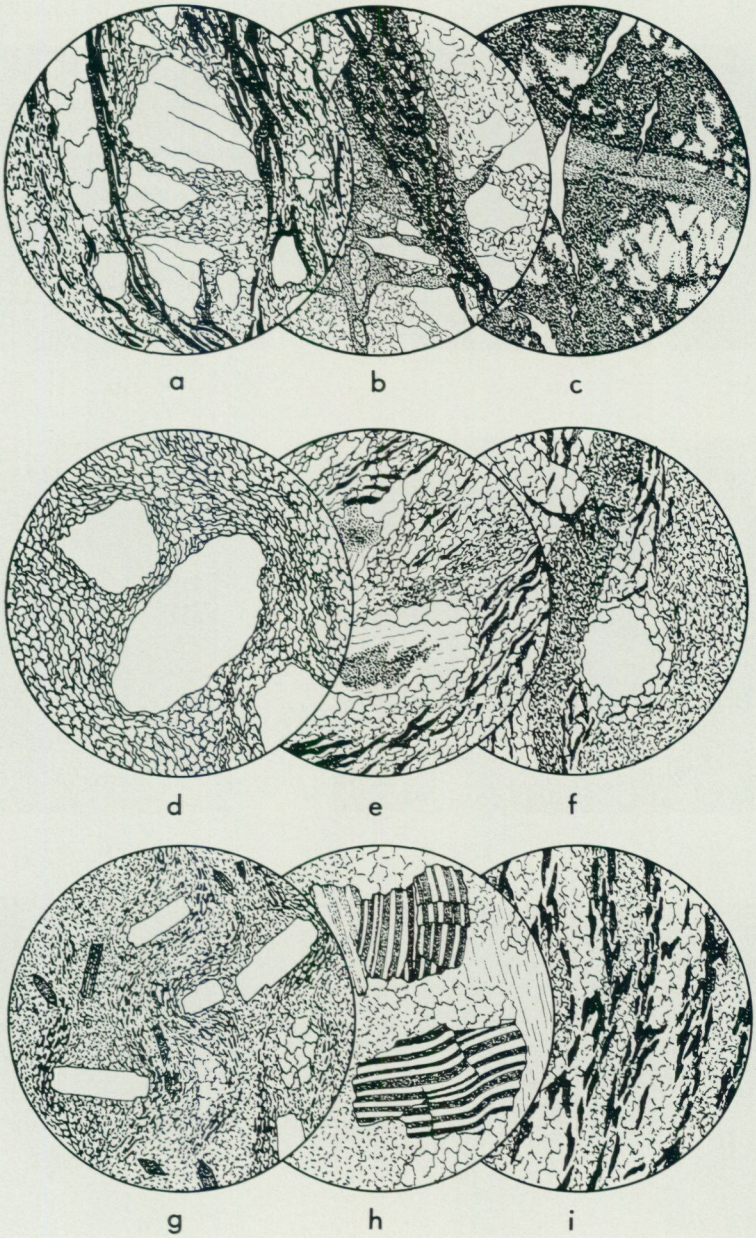

Fig. 13

a

b

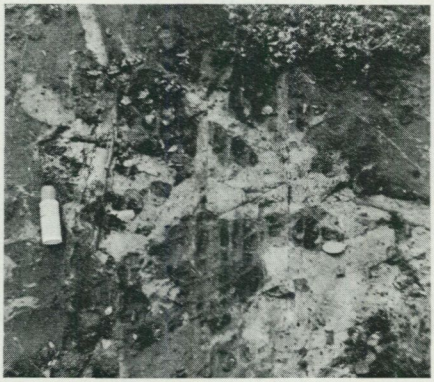

c

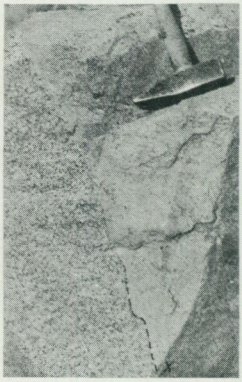

d

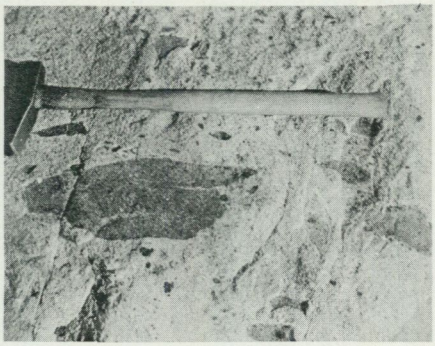

e

f

Fig. 14

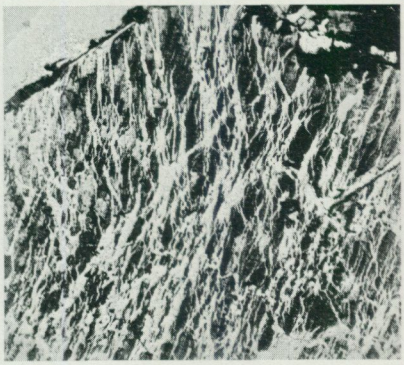

a

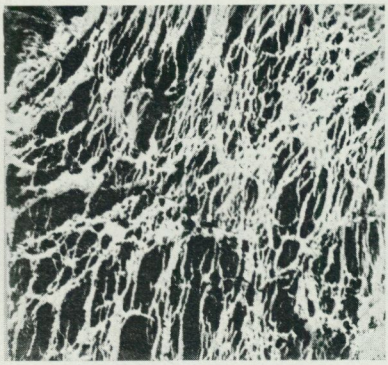

b

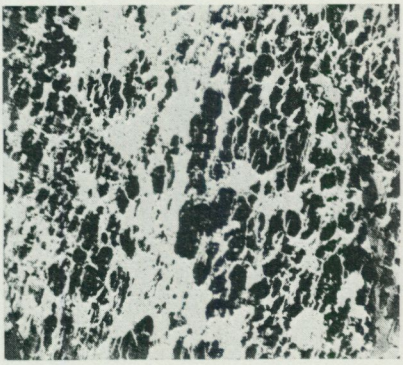

c

d

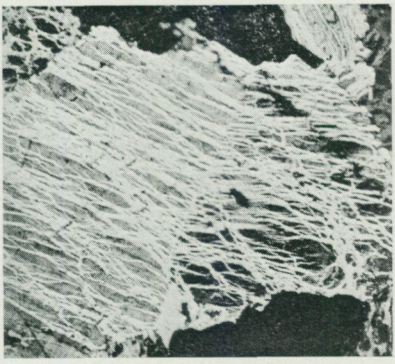

e

f

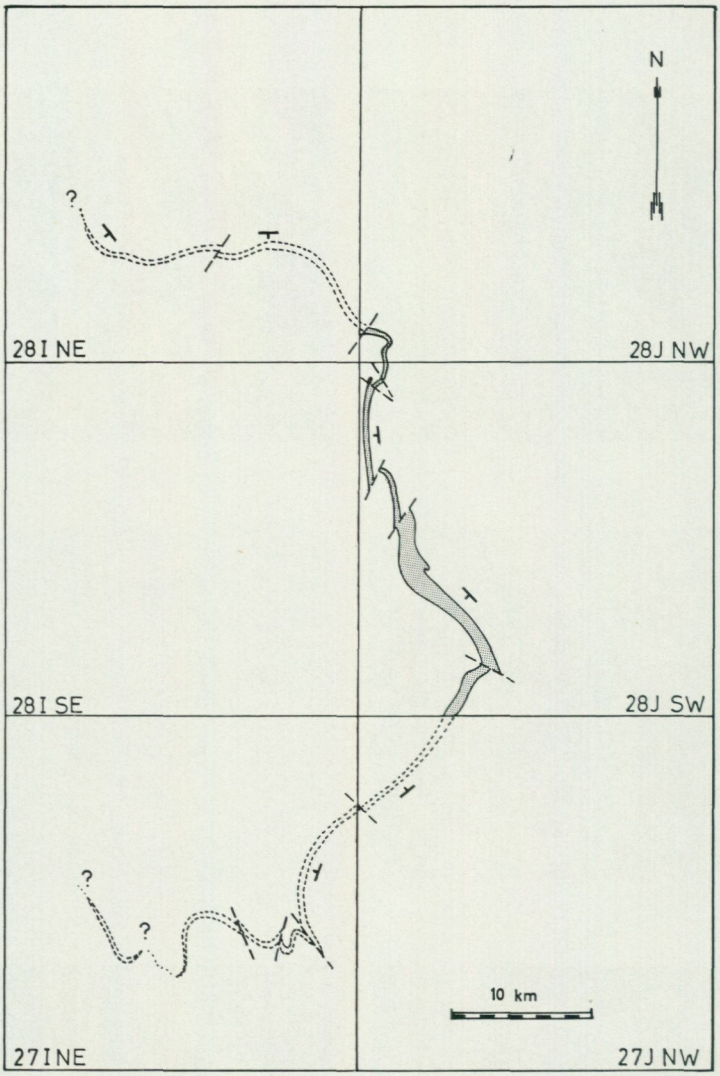

Fig. 15. Extension of the Nabrenjarka gabbro diabase in the map-sheets 28 J Fjällåsen, 27 J Porjus, 27 I Tjåmotis and 28 I Stora Sjöfallet. The map is based on exposures (28 I, 28 J) and on aeromagnetic interpretation (27 I, 27 J).
Nabrenjarka gabbrodiabas.

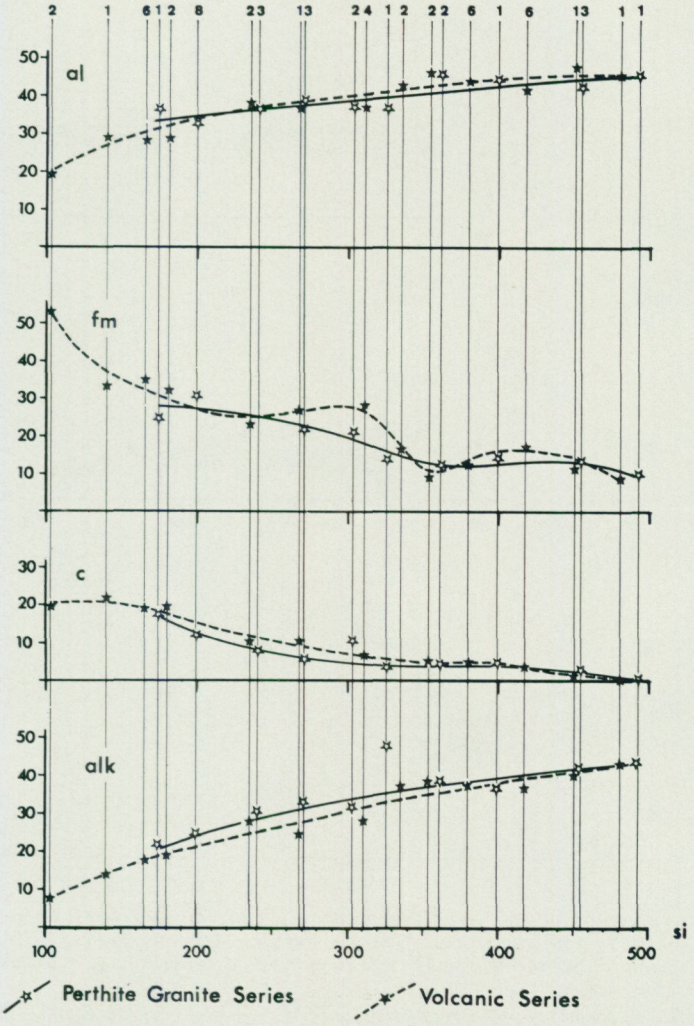

Fig. 16. Variations of the Niggli values *al, fm, c* and *alk* as a function of *si*. The small numbers in the upper-part of the diagram correspond to the number of chemical analyses. Each point on the diagram corresponds to an average calculation.

Variationsdiagram över Nigglivärden.

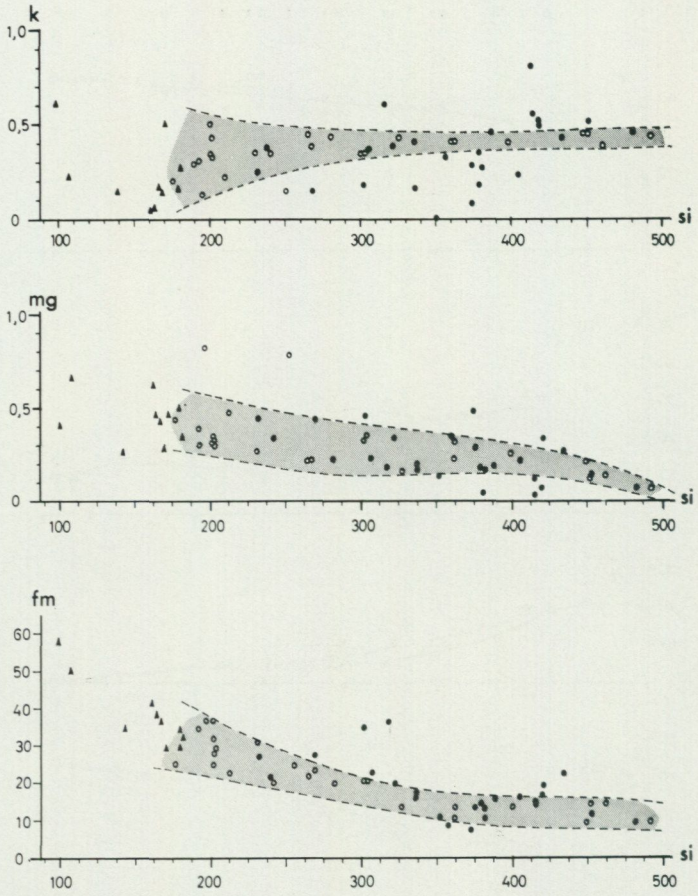

Fig. 17. Variations of the Niggli values *k*, *mg* and *fm* as a function of *si*. The shaded area corresponds to the Perthite Granite Series. ○ = Perthite Granite Series, ● = acid volcanics and porphyries, ▲ = andesites and greenstones.

Variationsdiagram över Nigglivärden. ○ = *pertitgranitserien,* ● = *sura vulkaniter och porfyrer,* ▲ = *andesiter och grönstenar.*

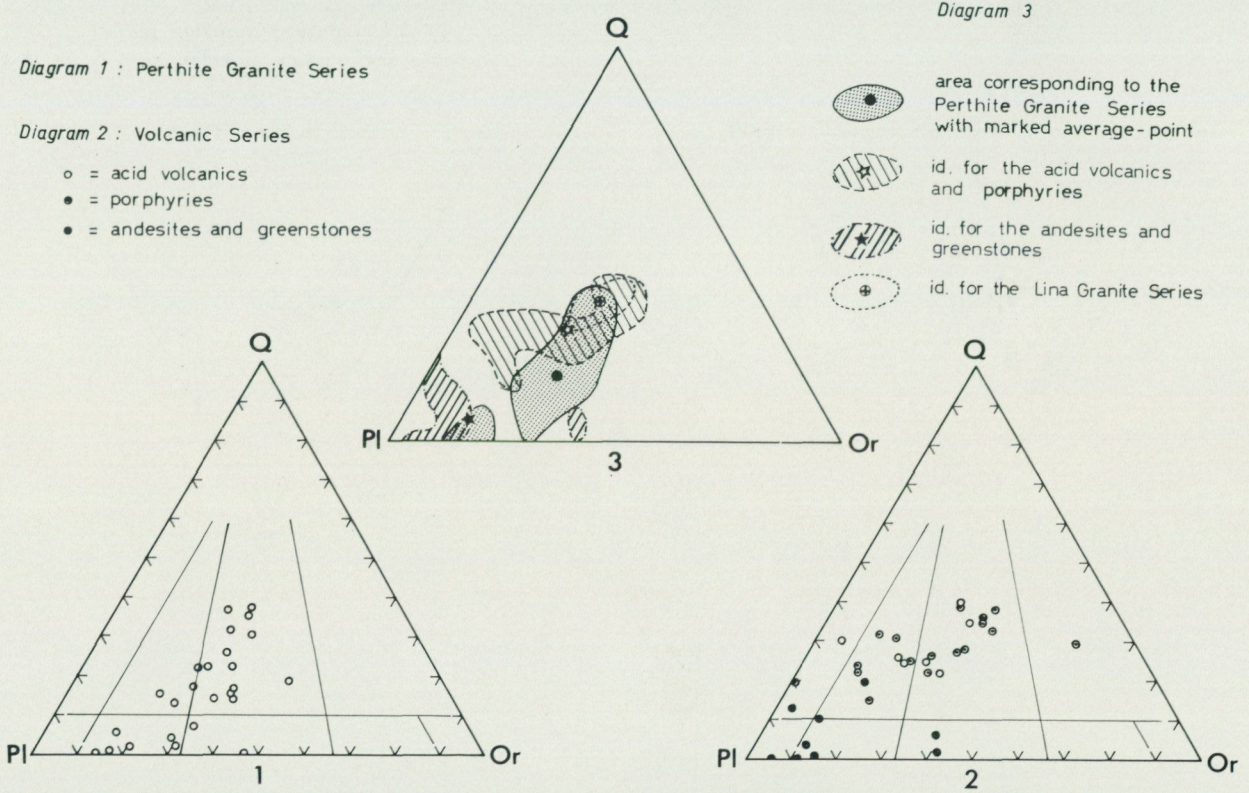

Fig. 18. Q-Pl-Or (quartz-plagioclase-K-feldspar) diagrams based on CIPW norms.
Q-Pl-Or (qvarts-plagioclas-K-fältspat) diagram baserat på CIPW norms.
Diagram 1 = pertitgranitserien, diagram 2 ○ = sura vulkaniter, ⊙ = porfyrer, ● = andesiter och grönstenar.

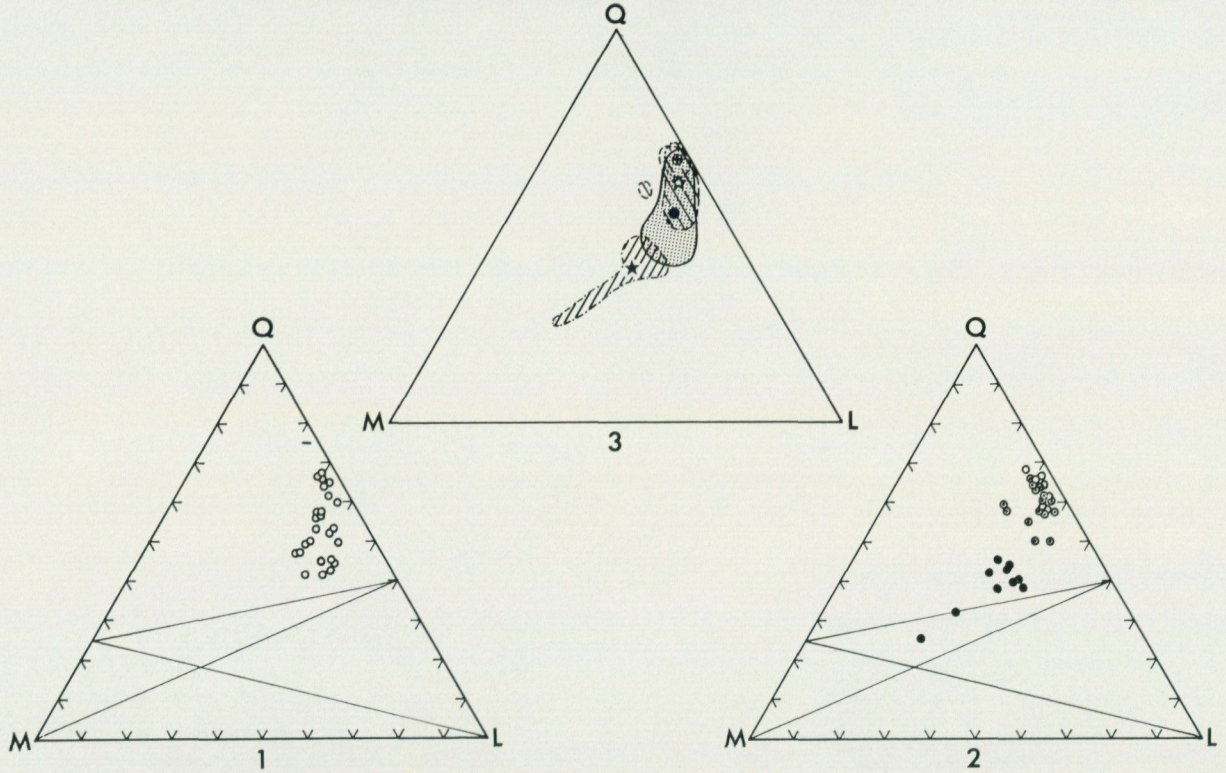

Fig. 19. Q-L-M diagrams. Legend: see Fig. 18.
Q-L-M diagram. Legend se fig. 18.

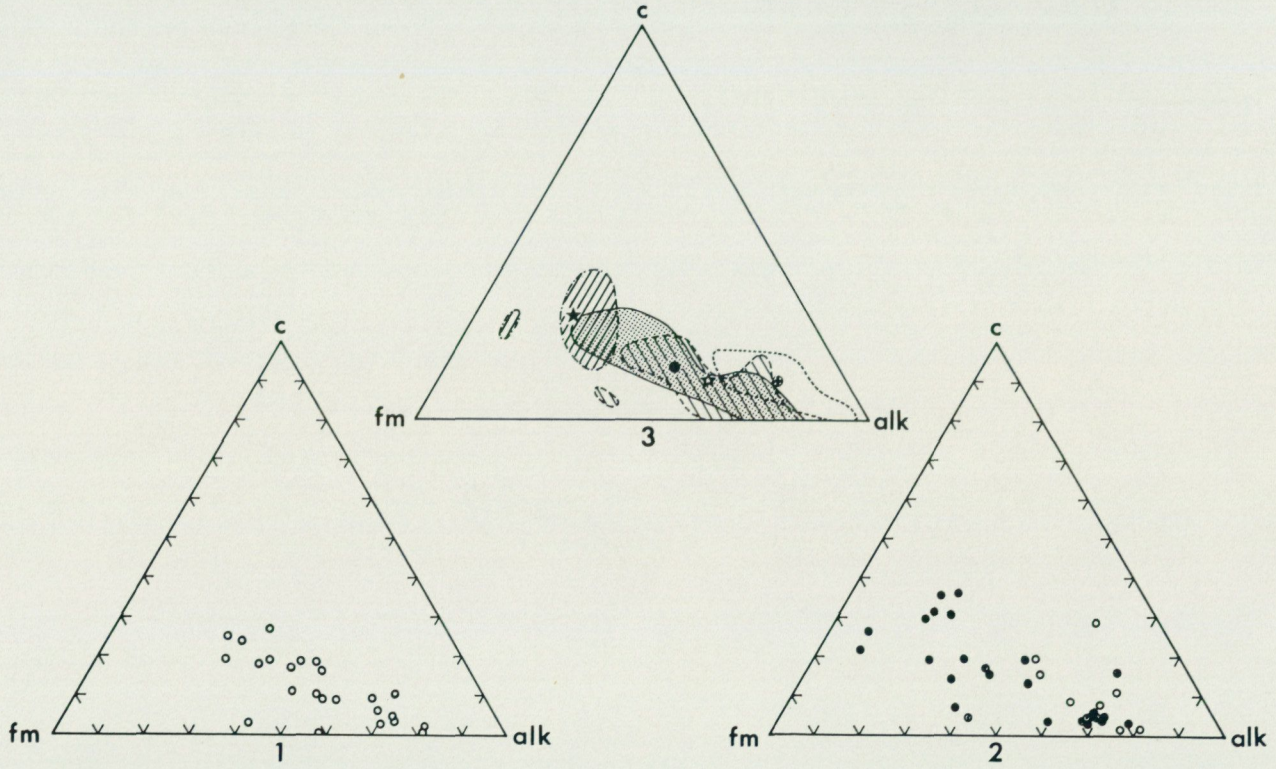

Fig. 20. c-alk-fm (Niggli values) diagrams. Legend: see Fig. 18.
c-alk-fm (Nigglivärden) diagram. Legend: se fig. 18.

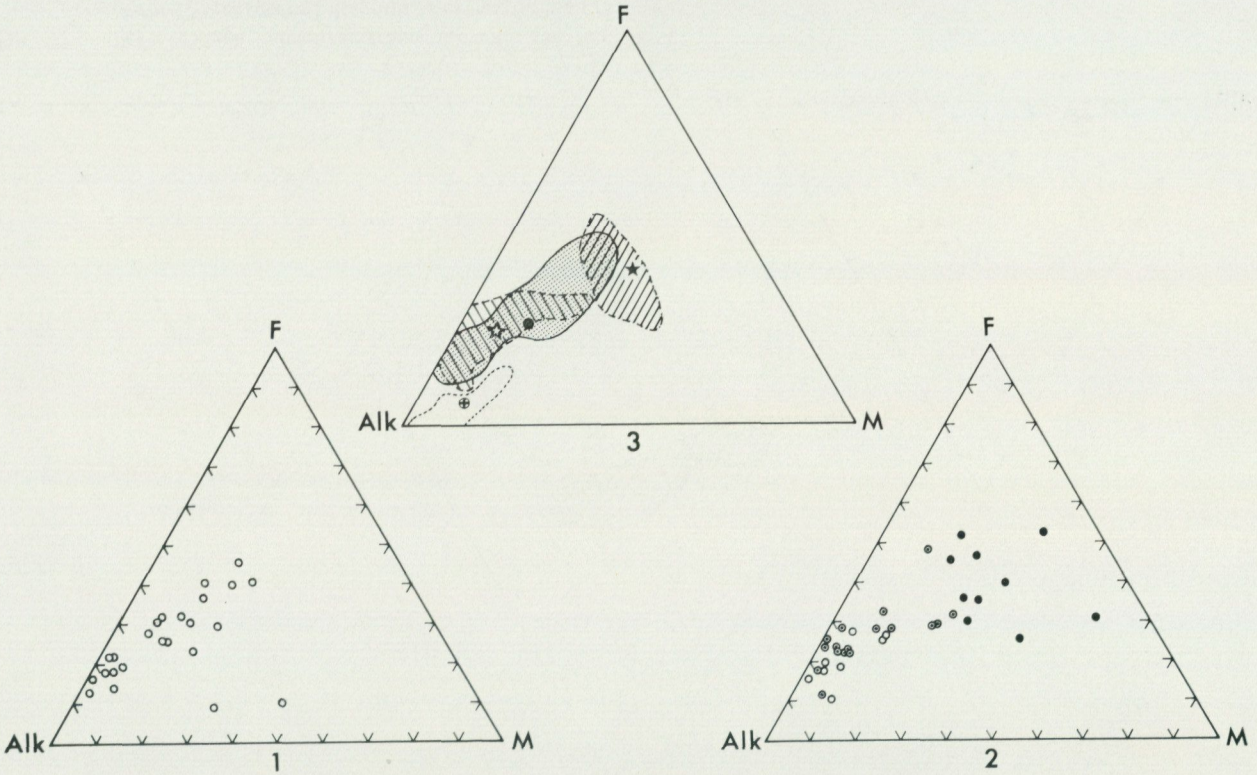

Fig. 21. Alk-F-M (Alk = $K_2O + Na_2O$, F = $FeO + 2Fe_2O_3 + MnO$, M = MgO) diagrams. Legend: see Fig. 18.
Alk-F-M (Alk = $K_2O + Na_2O$, F = $FeO + 2Fe_2O_3 + MnO$, M = MgO) diagram. Legend: se fig. 18.

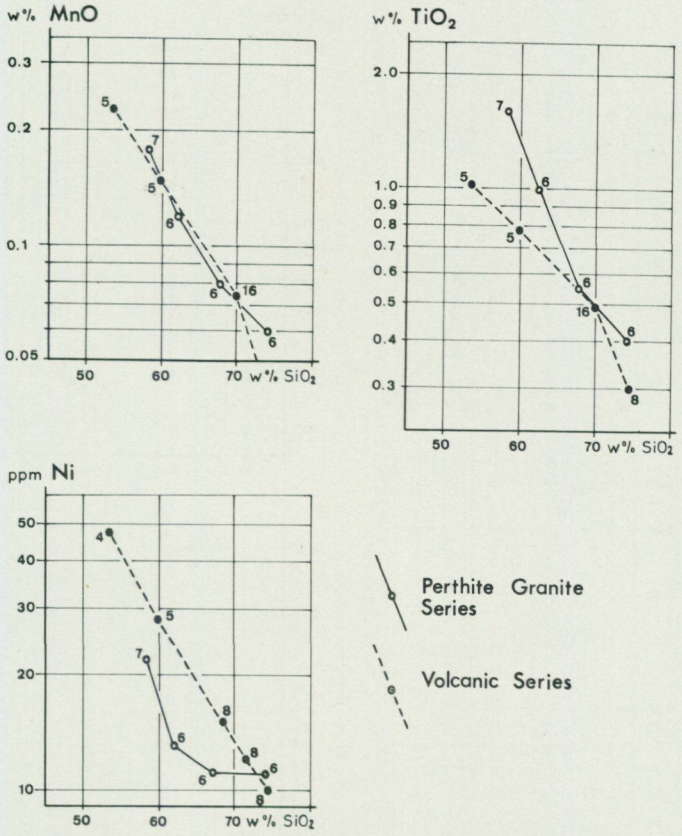

Fig. 22. Variations of MnO, TiO_2 and Ni as a function of SiO_2. The number of chemical analyses for each point is indicated in the diagram.
Variationsdiagram över MnO/SiO_2, TiO_2/SiO_2 och Ni/SiO_2. ○ = *pertitgranitserien,* ● = *porfyrgruppen.*

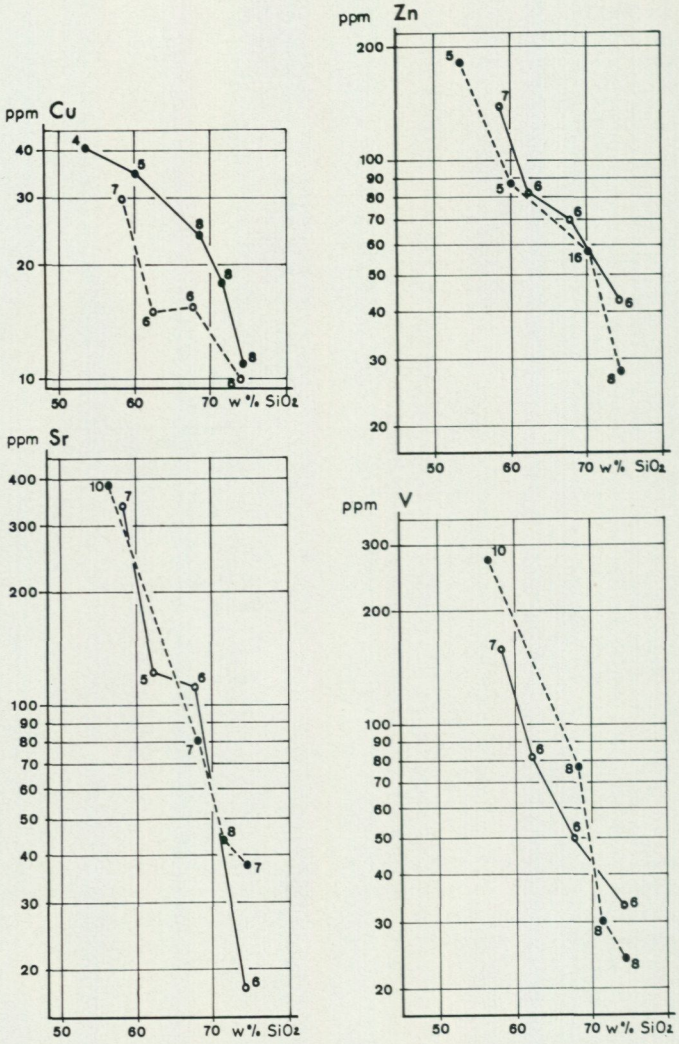

Fig. 23. Variations of Cu, Zn, Sr and V as a function of SiO_2. Legend: see Fig. 22. *Variationsdiagram över Cu/SiO_2, Zn/SiO_2, Sr/SiO_2 och V/SiO_2. Legend: se fig. 22.*

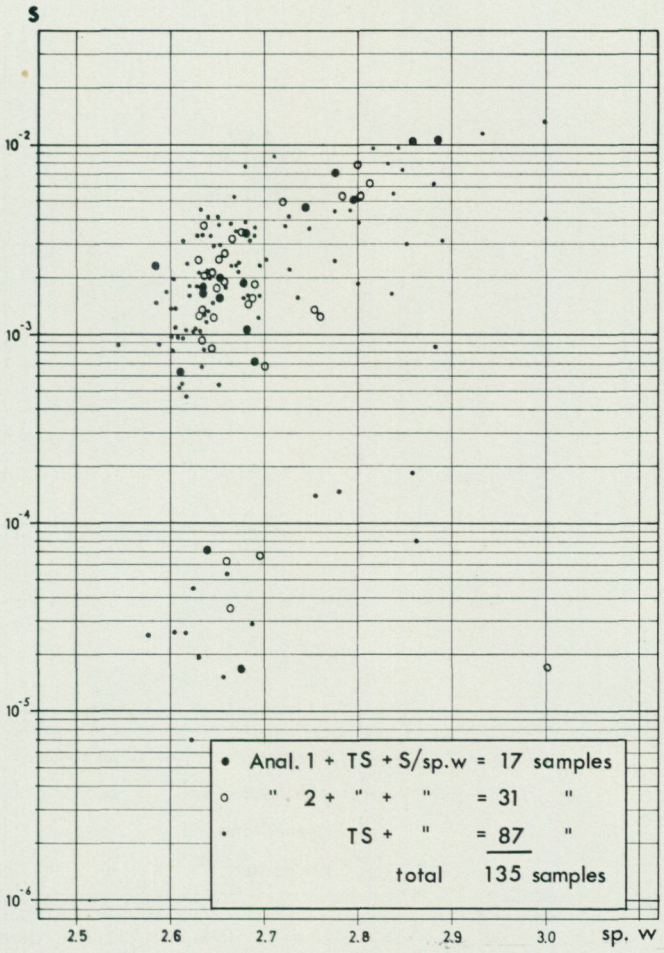

Fig. 24. Variations of the magnetic susceptibility (S) as a function of the specific weight (sp. w) in samples of the Porphyry Group and of the Perthite Granite Series. Anal. 1 = chemical analysis by wet method, Anal. 2 = chemical analysis by spectrographic method, TS = thin section.

Specifik vikt (sp. w) — magnetisk susceptibilitet (S) diagram för pertitgranitseriens och porfyrgruppens bergarter.

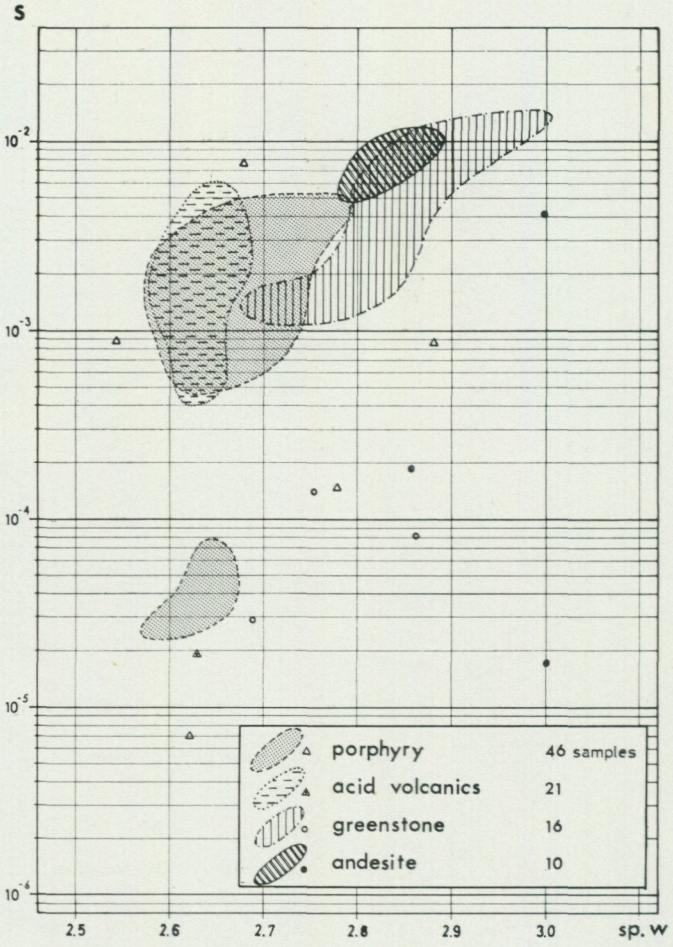

Fig. 25. Specific weight-susceptibility diagram indicating the areas corresponding to various volcanic rocks.
Specifik vikt-susceptibilitet diagram för vulkaniska bergarter.

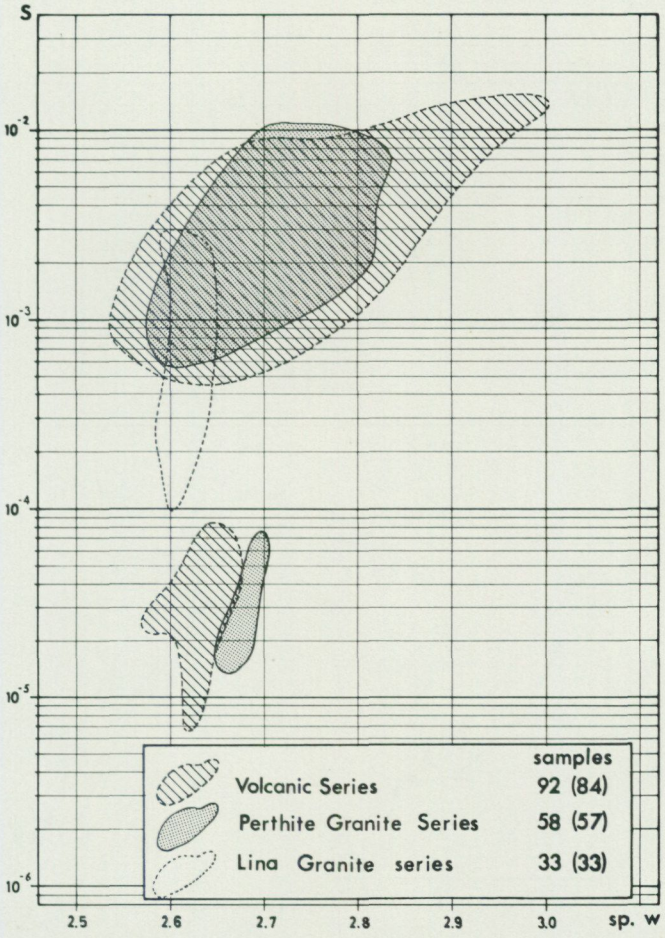

Fig. 26. Specific weight-susceptibility diagram for various rock series. The first number under "samples" corresponds to the total number of samples measured. The second number, in brackets, corresponds to the number of samples falling within the areas delimited on the diagram.

Specifik vikt-susceptibilitet diagram för olika bergsartsserier.

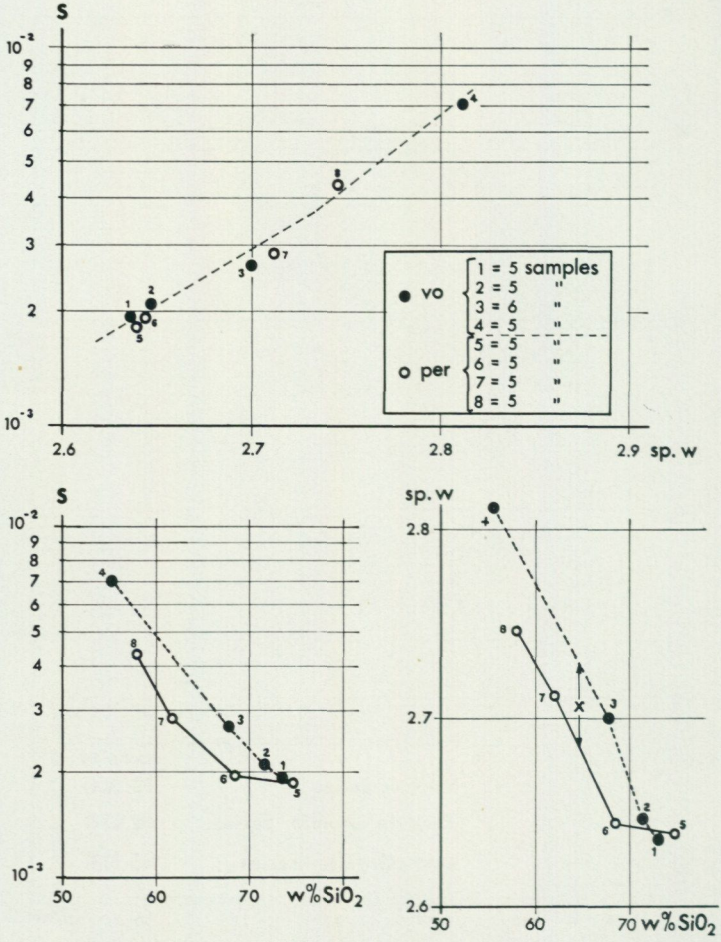

Fig. 27. Specific weight (sp. w), magnetic susceptibility (S) and silica content diagrams for rocks of the Porphyry Group (vo) and of the Perthite Granite Series (per). x, in the sp. w/SiO_2 diagram, represents the average difference in specific weight between the two series of rocks, when $SiO_2 < 68\ \%$.

Specifik vikt, susceptibilitet och SiO_2 diagram. vo = porfyrgruppen, per = pertitgranitserien.

Table 1. Nomenclature, suite-type and suite-index of rocks belonging to the Porphyry Group. Corresponding chemical analyses are given in Table 2.

Nomenklatur, svit-typ och svit-index (enligt Rittmann) för vulkaniska bergarter inom 28 J Fjälläsen.

Analysis Nr	Nomenclature (Rittmann 1952)	Suite-type (Rittmann 1962)	Suite-index σ (Rittmann 1962)
26	alkali-rhyolite	average Pacific	2.4
27	„ „	„ „	1.9
28	rhyolite	strong „	1.5
29	„	average „	2.4
30	soda-rhyolite	„ „	2.2
31	light dacite	strong „	1.4
32	alkali-rhyolite	average „	2.9
33	„ „	weak „	3.8
34	„ „	average „	3.0
35	rhyolite	„ „	2.9
36	alkali-rhyolite	weak „	3.1
37	soda-rhyolite	average „	2.8
38	„ „	„ „	2.6
39	„ „	„ „	3.0
40	„ „	„ „	2.8
41	quartz-latite	„ „	2.7
42	rhyolite	„ „	2.6
43	soda-rhyolite	„ „	3.0
44	rhyolite	weak „	3.4
45	dacite	average „	1.8
46	dark rhyolite	„ „	2.1
47	rhyolite	„ „	2.9
48	dacite	„ „	2.1
49	quartz-latite	—	4.5
50	rhyodacite	weak Pacific	3.3
51	dark rhyodacite	strong „	1.3
52	pigeonite-andesite	weak „	3.6
53	andesite	average „	2.8
54	„	„ „	1.9
55	pigeonite-andesite	weak „	3.6
56	latite	weak Mediterranean	4.6
57	pigeonite-andesite	weak Atlantic	5.7
58	„ „	transitional Atlantic	4.4
59	olivine-basalt	weak Pacific	3.1
60	dark leucite-basanite	strong Mediterranean	∞

Table 2 a. Chemical analyses of rocks from 28 J Fjällåsen. Cation %, O and OH contents (for 100 cations), Niggli values, partial CIPW norms, Q-L-M and Q-Or-Pl proportions, trace elements. Rock-type symbols and sample numbers are given on p. 94.

Kemiska analyser av bergarter från 28 J Fjällåsen.

Analysis Nr		1	2	3	4	5	6	7	8	9	10
rock type square (28 J)		QMz 4a	QMz 4c	QMz 4a	QMz 4a	QMz 4c	QMz 4c	QMz 1b	QMz 2a	QMz 2g	QMz Ob
weight %	SiO_2	75.6	75.6	75.2	74.4	72.6	70.9	70.0	69.3	68.1	67.8
	TiO_2	0.18	0.46	0.52	0.32	0.32	0.61	0.33	0.53	0.55	0.67
	Al_2O_3	12.0	12.2	11.4	12.5	13.9	14.5	15.7	13.0	14.6	13.7
	Fe_2O_3	1.8	1.1	2.7	0.9	2.4	1.1	1.7	3.0	1.6	3.9
	FeO	—	1.5	—	0.6	—	1.2	—	—	2.1	—
	MnO	0.03	0.09	0.06	0.03	0.03	0.14	0.05	0.16	0.09	0.08
	MgO	0.07	0.21	0.22	0.22	0.42	0.39	0.43	0.30	1.0	1.1
	CaO	0.1	0.3	0.6	0.2	0.8	0.5	1.1	0.6	2.3	2.3
	BaO	0.02	<0.01	0.02	0.03	0.07	<0.01	0.09	0.01	0.20	0.08
	Na_2O	3.8	3.8	4.2	4.2	4.0	4.8	4.2	5.9	4.6	4.7
	K_2O	4.7	4.8	3.9	5.3	4.4	5.2	4.6	6.8	3.8	4.0
	H_2O+	—	0.2	—	<0.1	—	0.2	—	—	0.2	—
	H_2O-	—	0.1	—	0.3	—	0.2	—	—	0.3	—
	P_2O_5	—	0.01	—	0.03	—	0.05	—	—	0.11	—
	CO_2	—	0.03	—	<0.01	—	<0.01	—	—	<0.01	—
	F	—	0.02	—	0.03	—	0.06	—	—	0.04	—
	S	—	<0.02	—	<0.02	—	<0.02	—	—	<0.02	—
	total	98.3	100.4	98.8	99.1	98.9	99.9	98.2	99.6	99.6	98.3
cation %	Si	72.10	70.87	71.47	70.13	68.53	65.94	66.07	63.79	63.85	64.08
	Ti	0.12	0.32	0.37	0.22	0.22	0.42	0.23	0.36	0.38	0.47
	Al	13.48	13.48	12.77	13.88	15.46	15.89	17.46	14.10	16.13	15.26
	Fe'''	1.29	0.77	1.93	0.63	1.70	0.76	1.20	2.07	1.12	2.77
	Fe''	—	1.17	—	0.47	—	0.93	—	—	1.64	—
	Mn	0.02	0.07	0.04	0.02	0.02	0.11	0.03	0.12	0.07	0.06
	Mg	0.09	0.29	0.31	0.30	0.59	0.54	0.60	0.41	1.39	1.54
	Ca	0.10	0.30	0.61	0.20	0.80	0.49	1.11	0.59	2.31	2.32
	Ba	0.00	0.00	0.00	0.01	0.02	0.00	0.03	0.00	0.07	0.02
	Na	7.02	6.90	7.74	7.67	7.32	8.65	7.68	10.53	8.36	8.61
	K	5.71	5.74	4.72	6.37	5.29	6.16	5.53	7.98	4.54	4.82
anions	OH	—	1.25	—	0.62	—	1.24	—	—	1.25	—
	O	173.25	171.36	172.96	170.25	171.03	166.61	169.03	163.00	165.86	166.85

Table 2 a (continued)

Analysis Nr		1	2	3	4	5	6	7	8	9	10
Niggli values	*al*	46.06	42.96	41.11	44.43	44.96	43.62	47.60	36.12	38.14	36.17
	fm	9.66	14.77	14.75	9.24	13.48	12.92	10.09	13.39	20.06	20.79
	c	0.74	1.94	3.98	1.36	4.85	2.75	6.24	3.05	11.27	11.18
	alk	43.52	40.31	40.14	44.95	36.69	40.69	36.04	47.42	30.51	31.84
	si	492.43	451.84	460.26	448.82	398.52	362.00	360.19	326.81	301.90	303.78
	si'	274.08	261.26	260.58	278.26	246.76	262.77	244.19	255.81	222.06	227.38
	qz	218.35	190.58	199.68	170.56	151.76	99.23	116.00	71.00	79.84	76.40
	k	0.44	0.45	0.37	0.45	0.41	0.41	0.41	0.43	0.35	0.35
	mg	0.07	0.12	0.13	0.21	0.25	0.22	0.32	0.15	0.32	0.35
	w	—	0.39	—	0.57	—	0.45	—	—	0.40	—
	ti	0.88	2.06	2.39	1.45	1.32	2.34	1.27	1.87	1.83	2.25
	p	—	0.02	—	0.07	—	0.10	—	—	0.20	—
	h	—	3.98	—	2.01	—	3.40	—	—	2.95	—
	T	2.53	2.65	0.97	–0.51	8.27	2.93	11.55	–11.29	7.62	4.32
	t	1.79	0.70	–3.01	–1.88	3.41	0.17	5.31	–14.34	–3.64	–6.85
CIPW norms	Q	35.8	33.7	35.1	29.7	30.4	21.6	25.4	16.5	20.6	20.4
	Or	28.2	28.3	23.3	31.7	26.3	30.8	27.7	40.3	22.6	24.0
	Ab	32.7	32.0	36.0	35.2	34.2	40.7	36.2	29.1	39.2	40.4
	An	0.5	1.1	0.7	—	4.1	1.7	5.7	—	8.0	4.5
	salic	97.8	95.4	95.2	96.6	96.1	95.2	96.7	86.00	90.4	89.4
	femic	2.2	4.4	4.8	3.3	3.8	4.5	3.2	14.0	9.2	10.5
triangular diag.	Q	67.7	66.4	66.6	65.0	63.9	60.0	61.5	56.7	57.7	56.4
	L	29.6	29.9	29.3	32.5	31.4	36.3	34.1	34.4	34.1	34.1
	M	2.7	3.7	4.1	2.5	4.7	3.7	4.4	9.2	7.9	9.5
	Q	36.8	35.4	36.9	30.8	32.0	22.8	26.7	19.2	22.8	22.8
	Or	29.0	29.7	24.5	32.8	27.6	32.5	29.2	46.9	25.0	26.9
	Pl	34.2	34.9	38.6	36.4	40.4	44.7	44.1	33.9	52.2	50.3
trace elements (ppm)	Cu	24	<5	7	9	<5	6	7	7	12	29
	Pb	30	18	16	23	32	26	33	50	18	37
	Zn	38	54	24	20	46	75	51	116	70	112
	Mo	10	<10	<10	<10	<10	<10	<10	<10	<10	<10
	Ni	18	10	<10	<10	12	10	14	<10	13	13
	V	41	17	21	32	57	30	51	34	57	69
	Sr	5	—	3	20	79	1	157	3	245	143
	As	141	<50	<50	<50	89	<50	50	92	<50	<50

Table 2 b.

Analysis Nr		11	12	13	14	15	16	17	18	19	20
rock type square (28 J)		QMz 5c	DMz 4d	QMz 4a	QMz 6a	Mz 7a	GrD 1a	DMz 4a	DMz 9j	GrD 9c	Mz 6a
weight %	SiO_2	65.6	65.0	64.7	63.1	63.0	62.3	61.0	60.1	60.0	58.7
	TiO_2	0.77	0.99	0.42	1.3	1.1	1.3	0.48	0.83	1.5	2.4
	Al_2O_3	15.6	15.9	17.6	16.4	16.8	14.8	17.3	18.0	16.2	15.8
	Fe_2O_3	5.8	4.5	1.8	5.1	1.7	7.9	2.7	4.4	2.7	7.3
	FeO	—	—	—	—	2.6	—	—	—	4.8	—
	MnO	0.07	0.14	0.03	0.15	0.15	0.19	0.05	0.04	0.14	0.33
	MgO	0.82	0.70	3.3	0.74	1.1	1.5	6.3	2.0	2.2	1.6
	CaO	1.5	1.2	0.1	1.3	2.5	3.1	0.6	3.1	4.6	2.1
	BaO	0.08	0.04	0.01	0.06	0.12	0.20	0.02	0.17	0.13	0.03
	Na_2O	5.0	4.5	7.9	4.3	5.5	4.4	7.8	6.5	4.0	5.4
	K_2O	5.0	5.5	2.2	5.5	4.7	3.7	1.8	2.9	3.3	6.6
	H_2O+	—	—	—	—	0.4	—	—	—	0.3	—
	H_2O-	—	—	—	—	0.4	—	—	—	0.3	—
	P_2O_5	—	—	—	—	0.33	—	—	—	0.40	—
	CO_2	—	—	—	—	0.03	—	—	—	<0.01	—
	F	—	—	—	—	0.04	—	—	—	0.10	—
	S	—	—	—	—	<0.02	—	—	—	<0.02	—
	total	100.2	98.5	98.1	98.0	100.5	99.4	98.1	98.0	100.7	100.3
cation %	Si	60.78	61.27	58.66	59.95	58.03	58.93	54.81	55.67	56.09	54.13
	Ti	0.53	0.70	0.28	0.92	0.76	0.92	0.32	0.57	1.05	1.66
	Al	17.03	17.66	18.80	18.36	18.24	16.50	18.32	19.65	17.85	17.17
	Fe'''	4.04	3.19	1.22	3.64	1.17	5.62	1.82	3.06	1.89	5.06
	Fe''	—	—	—	—	2.00	—	—	—	3.75	—
	Mn	0.05	0.11	0.02	0.12	0.11	0.15	0.03	0.03	0.11	0.25
	Mg	1.13	0.98	4.45	1.04	1.51	2.11	8.43	2.76	3.06	2.19
	Ca	1.48	1.21	0.09	1.32	2.46	3.14	0.57	3.07	4.60	2.07
	Ba	0.02	0.01	0.00	0.02	0.04	0.07	0.00	0.06	0.04	0.01
	Na	8.98	8.22	13.88	7.92	9.82	8.07	13.58	11.67	7.25	9.65
	K	5.91	6.61	2.54	6.66	5.52	4.46	2.06	3.42	3.93	7.76
anions	OH	—	—	—	—	2.45	—	—	—	1.87	—
	O	164.41	164.98	160.75	164.59	159.93	164.65	157.38	160.07	160.80	158.20

Table 2 b (continued)

Analysis Nr		11	12	13	14	15	16	17	18	19	20
Niggli values	*al*	37.50	40.13	40.57	40.56	37.82	32.19	32.86	37.25	31.87	31.91
	fm	23.03	24.37	19.69	21.27	19.94	30.79	36.95	22.21	31.52	27.96
	c	6.68	0.42	5.63	5.94	10.41	12.55	2.09	11.89	16.62	7.75
	alk	32.78	35.06	34.08	32.22	31.82	24.45	28.07	28.62	19.97	32.37
	si	267.60	250.35	281.50	264.84	240.68	229.98	196.65	211.08	200.31	201.20
	si'	231.13	240.25	236.34	228.88	227.28	197.83	212.31	214.51	179.89	228.11
	qz	36.47	10.10	45.16	35.96	13.40	32.15	–15.66	–3.43	20.42	–26.91
	k	0.39	0.15	0.44	0.45	0.35	0.35	0.13	0.22	0.35	0.44
	mg	0.21	0.78	0.22	0.21	0.31	0.26	0.81	0.47	0.34	0.29
	w	—	—	—	—	0.37	—	—	—	0.33	—
	ti	2.36	1.22	3.22	4.10	3.16	3.60	1.16	2.19	3.76	6.18
	p	—	—	—	—	0.53	—	—	—	0.56	—
	h	—	—	—	—	5.09	—	—	—	3.34	—
	T	4.71	5.06	6.49	8.34	5.99	7.73	4.78	8.62	11.89	–0.45
	t	–1.96	4.63	0.85	2.39	–4.41	–4.81	2.68	–3.27	–4.72	–8.21
CIPW norms	Q	13.3	5.3	14.4	13.4	6.8	14.9	—	2.4	10.9	—
	Or	29.5	13.3	33.0	33.2	27.7	22.0	10.8	17.5	19.4	38.9
	Ab	42.2	68.2	38.7	37.1	46.5	37.5	67.3	56.1	33.7	44.4
	An	5.3	0.5	6.1	6.7	7.3	9.8	3.1	11.6	16.4	—
	salic	90.4	89.3	92.5	91.4	88.3	84.1	82.7	87.6	80.5	83.3
	femic	9.6	10.7	7.5	8.6	11.2	15.7	17.3	12.3	19.1	16.7
triangular diag.	Q	51.9	48.0	53.5	52.2	49.9	50.1	41.2	45.7	49.4	41.5
	L	38.7	40.3	38.7	38.6	41.5	35.0	39.3	42.9	35.2	43.3
	M	9.4	11.7	7.8	9.2	8.6	14.9	19.5	11.4	15.4	15.2
	Q	14.8	15.6	6.1	14.8	7.7	17.7	—	2.7	13.6	—
	Or	32.6	35.8	15.2	36.7	31.4	26.2	13.4	20.0	24.1	46.7
	Pl	52.6	48.6	78.7	48.5	60.9	56.1	86.6	77.3	62.3	53.3
trace elements (ppm)	Cu	34	8	11	8	9	24	<5	36	37	7
	Pb	32	12	34	65	29	45	14	40	34	62
	Zn	61	10	77	109	102	144	20	45	84	175
	Mo	<10	<10	10	25	<10	10	<10	10	13	16
	Ni	10	<10	<10	16	<10	<10	<10	32	17	16
	V	69	21	50	106	45	97	24	173	192	102
	Sr	124	4	35	59	150	236	9	1018	307	9
	As	<50	<50	<50	298	<50	73	16	100	91	207

Table 2 c.

Analysis Nr		21	22	23	24	25	26	27	28	29	30
rock type square (28 J)		QMz 4a	GrD 6a	DMz 6a	DMz 9a	DMz 2i	Vo 4g	Po 1a	Vo 3d	Vo 5h	mPo 2a
weight %	SiO_2	58.5	58.5	58.5	58.2	56.0	75.7	74.6	73.6	73.0	72.6
	TiO_2	1.8	1.7	1.3	1.3	1.2	0.21	0.33	0.47	0.27	0.44
	Al_2O_3	14.5	16.5	18.6	15.4	20.1	12.1	11.6	11.8	13.0	13.1
	Fe_2O_3	9.9	3.8	6.0	8.4	5.7	1.9	2.2	1.0	2.2	2.9
	FeO	—	3.6	—	—	—	—	0.7	1.6	—	—
	MnO	0.16	0.21	0.16	0.16	0.07	0.01	0.72	0.20	0.01	0.05
	MgO	2.2	1.8	1.6	2.7	2.3	0.08	0.72	0.77	0.17	0.41
	CaO	3.7	3.7	2.9	5.0	5.2	0.1	0.3	1.9	0.1	0.4
	BaO	0.12	0.25	0.29	0.13	0.15	0.02	0.02	0.06	0.04	0.03
	Na_2O	2.9	5.4	5.3	3.9	5.6	3.8	3.5	2.6	3.2	5.4
	K_2O	4.7	3.9	4.4	2.6	2.3	5.1	4.3	4.1	5.3	2.7
	H_2O+	—	0.3	—	—	—	—	0.2	0.6	—	—
	H_2O-	—	0.3	—	—	—	—	0.3	0.2	—	—
	P_2O_5	—	0.66	—	—	—	—	0.02	0.01	—	—
	CO_2	—	0.03	—	—	—	—	<0.01	<0.01	—	—
	F	—	0.05	—	—	—	—	0.01	0.13	—	—
	S	—	<0.02	—	—	—	—	<0.02	<0.02	—	—
	total	98.5	100.7	99.1	97.8	98.6	99.0	99.5	99.0	97.3	98.0
cation %	Si	56.55	54.13	54.39	55.91	51.95	71.64	70.99	71.02	70.51	68.77
	Ti	1.30	1.18	0.90	0.93	0.83	0.14	0.23	0.34	0.19	0.31
	Al	16.52	17.99	20.38	17.43	21.97	13.49	13.01	13.42	14.79	14.62
	Fe'''	7.20	2.64	4.19	6.07	3.97	1.35	1.57	0.72	1.59	2.06
	Fe''	—	2.78	—	—	—	—	0.55	1.29	—	—
	Mn	0.13	0.16	0.12	0.13	0.05	0.00	0.58	0.16	0.00	0.04
	Mg	3.17	2.48	2.21	3.86	3.18	0.11	1.02	1.10	0.24	0.57
	Ca	3.83	3.66	2.88	5.14	5.16	0.10	0.30	1.96	0.10	0.40
	Ba	0.04	0.09	0.10	0.04	0.05	0.00	0.00	0.02	0.01	0.01
	Na	5.43	9.68	9.55	7.26	10.07	6.97	6.45	4.86	5.99	9.91
	K	5.79	4.60	5.21	3.18	2.72	6.15	5.22	5.04	6.53	3.26
anions	OH	—	1.85	—	—	—	—	1.26	3.86	—	—
	O	164.11	158.27	160.20	163.37	159.37	172.65	172.03	171.34	172.64	170.84

Table 2 c (continued)

Analysis Nr		21	22	23	24	25	26	27	28	29	30
Niggli values	*al*	29.23	32.15	37.58	29.84	36.84	45.30	39.68	39.60	47.33	42.99
	fm	37.16	28.87	24.12	34.47	24.19	9.89	22.78	19.41	11.84	15.79
	c	13.72	13.43	11.04	17.78	17.51	0.73	1.91	11.72	0.75	2.45
	alk	19.87	25.53	27.24	17.88	21.45	44.07	35.62	29.25	40.05	38.75
	si	200.13	193.45	200.60	191.42	174.19	480.95	433.10	419.22	451.07	404.39
	si'	179.49	202.15	208.97	171.55	185.80	276.28	242.48	217.00	260.22	255.00
	qz	20.64	–8.70	–8.37	19.87	–11.61	204.67	190.62	202.22	190.85	149.39
	k	0.51	0.32	0.35	0.30	0.21	0.46	0.44	0.50	0.52	0.24
	mg	0.30	0.30	0.33	0.38	0.44	0.07	0.27	0.33	0.13	0.21
	w	—	0.48	—	—	—	—	0.73	0.35	—	—
	ti	4.63	4.22	3.35	3.21	2.80	1.00	1.44	2.01	1.25	1.84
	p	—	0.92	—	—	—	—	0.04	0.02	—	—
	h	—	3.30	—	—	—	—	3.87	11.39	—	—
	T	9.35	6.61	10.34	11.95	15.39	1.23	4.06	10.35	7.27	4.24
	t	–4.36	–6.81	–0.70	–5.82	–2.11	0.49	2.15	–1.37	6.52	1.79
CIPW norms	Q	13.8	3.9	2.2	12.8	0.6	34.1	36.3	37.7	34.5	30.0
	Or	28.2	22.9	26.3	15.7	13.8	30.4	25.6	24.5	32.2	16.3
	Ab	24.9	45.5	45.3	33.7	48.0	32.5	29.8	22.3	27.8	46.6
	An	12.9	9.2	14.1	17.2	23.2	0.5	1.3	8.5	0.6	2.1
	salic	79.8	81.6	87.9	79.5	85.7	97.6	93.8	92.9	97.0	95.5
	femic	20.1	17.9	12.0	20.5	14.2	2.3	6.0	6.4	3.0	4.5
triangular diag.	Q	47.3	44.9	44.7	47.1	43.4	66.8	66.1	68.3	66.2	63.3
	L	33.7	40.3	43.4	33.4	43.2	30.6	27.4	26.7	29.4	31.7
	M	19.0	14.8	11.9	19.5	13.4	2.6	6.5	5.0	4.4	5.0
	Q	17.3	4.8	2.5	16.1	0.8	34.9	39.0	40.5	36.3	31.6
	Or	35.3	28.1	29.9	19.8	16.1	31.2	27.5	26.4	33.8	17.1
	Pl	47.4	67.1	67.6	64.1	83.1	33.9	33.5	33.1	29.9	51.3
trace elements (ppm)	Cu	20	25	25	52	18	7	8	<5	31	20
	Pb	47	39	34	59	26	14	29	21	23	22
	Zn	189	174	126	188	48	<10	48	49	17	49
	Mo	<10	<10	<10	11	<10	<10	<10	<10	10	<10
	Ni	20	12	10	33	30	<10	11	<10	14	<10
	V	265	121	87	247	184	15	32	19	33	27
	Sr	209	305	245	408	699	2	9	23	12	9
	As	61	<50	55	257	52	<50	104	<50	93	83

Table 2 d.

Analysis Nr		31	32	33	34	35	36	37	38	39	40
rock type square (28 J)		Vo 1c	mPo 3d	mPo 1c	Po 3d	mPo 2d	Po 3d	Vo Ob	Vo 4h	mPo 2d	Po 5g
weight %	SiO_2	72.5	72.4	72.4	72.0	71.6	71.6	71.5	71.1	70.4	70.3
	TiO_2	0.14	0.55	0.38	0.61	0.25	0.55	0.51	0.36	0.25	0.68
	Al_2O_3	15.3	13.0	12.4	13.3	12.7	13.9	13.7	14.1	14.1	15.5
	Fe_2O_3	0.2	2.1	2.4	1.3	3.5	2.8	2.4	2.1	3.1	2.5
	FeO	0.7	0.7	0.8	1.4	—	—	—	—	—	—
	MnO	0.03	0.08	0.01	0.24	0.01	0.19	0.04	0.03	0.01	0.01
	MgO	0.48	0.19	0.06	0.38	0.15	0.34	0.50	0.23	0.07	0.19
	CaO	2.7	0.5	0.3	0.5	0.3	0.5	0.8	1.0	0.4	0.3
	BaO	0.08	0.06	0.13	0.04	0.15	0.03	0.05	0.05	0.12	0.02
	Na_2O	5.6	3.3	1.4	4.0	3.1	4.2	5.5	5.4	4.8	8.7
	K_2O	0.9	6.0	9.2	5.3	5.3	5.2	3.5	3.2	4.2	0.0
	H_2O+	0.4	0.2	<0.1	0.2	—	—	—	—	—	—
	H_2O-	0.1	0.2	0.3	0.2	—	—	—	—	—	—
	P_2O_5	0.04	0.05	0.03	0.07	—	—	—	—	—	—
	CO_2	<0.01	<0.01	<0.01	0.02	—	—	—	—	—	—
	F	0.01	0.02	0.01	0.03	—	—	—	—	—	—
	S	<0.02	<0.02	<0.02	<0.02	—	—	—	—	—	—
	total	99.2	99.4	99.8	99.6	97.1	99.3	98.5	97.6	97.5	98.2
cation %	Si	67.69	69.12	69.12	67.79	69.66	67.23	67.06	67.34	67.18	64.82
	Ti	0.09	0.39	0.27	0.43	0.18	0.38	0.35	0.25	0.17	0.47
	Al	16.83	14.62	13.95	14.75	14.56	15.38	15.14	15.73	15.85	16.84
	Fe'''	0.14	1.50	1.72	0.92	2.56	1.97	1.69	1.49	2.22	1.73
	Fe''	0.54	0.55	0.73	1.10	—	—	—	—	—	—
	Mn	0.02	0.06	0.00	0.19	0.00	0.15	0.03	0.02	0.00	0.00
	Mg	0.66	0.27	0.08	0.53	0.21	0.47	0.69	0.32	0.09	0.26
	Ca	2.70	0.51	0.30	0.50	0.31	0.50	0.80	1.01	0.40	0.29
	Ba	0.02	0.02	0.04	0.01	0.05	0.01	0.01	0.01	0.04	0.00
	Na	10.13	5.55	2.59	7.30	5.84	7.64	10.00	9.91	8.88	15.55
	K	1.07	7.30	11.20	6.36	6.57	6.22	4.18	3.86	5.11	0.00
anions	OH	2.49	1.27	0.63	1.25	—	—	—	—	—	—
	O	169.44	170.52	170.02	168.63	172.20	169.36	168.74	169.32	169.40	166.80

Table 2 d (continued)

Analysis Nr		31	32	33	34	35	36	37	38	39	40
Niggli values	*al*	46.42	43.84	41.80	42.21	43.72	43.33	42.26	44.61	44.76	45.51
	fm	7.60	14.40	14.72	15.72	16.74	14.67	13.53	10.46	13.17	10.82
	c	15.05	3.20	2.13	2.96	2.22	2.89	4.59	5.85	2.56	1.64
	alk	30.91	38.54	41.33	39.09	37.30	39.08	39.60	39.06	39.50	42.02
	si	373.32	414.38	414.24	387.80	418.32	378.80	374.35	381.75	379.26	350.26
	si'	223.64	254.19	265.35	256.37	249.23	256.35	258.41	256.26	258.00	268.09
	qz	149.68	160.19	148.89	131.43	169.09	122.45	115.94	125.49	121.26	82.17
	k	0.09	0.56	0.81	0.46	0.52	0.44	0.29	0.28	0.36	0.00
	mg	0.48	0.11	0.03	0.19	0.07	0.18	0.28	0.17	0.04	0.13
	w	0.20	0.72	0.72	0.45	—	—	—	—	—	—
	ti	0.54	2.36	1.73	2.45	1.09	2.18	2.00	1.45	1.01	2.54
	p	0.08	0.12	0.07	0.15	—	—	—	—	—	—
	h	6.86	3.81	1.90	3.59	—	—	—	—	—	—
	T	15.51	5.29	0.46	3.12	6.41	4.24	2.66	5.54	5.26	3.49
	t	0.45	2.09	−1.66	0.15	4.19	1.35	−1.92	−0.31	2.70	1.84
CIPW norms	Q	29.9	31.2	28.7	26.9	33.3	25.8	24.3	25.6	26.0	19.1
	Or	5.4	35.9	54.6	31.5	32.3	30.9	21.0	19.4	25.5	—
	Ab	47.8	25.7	11.9	34.0	27.0	35.8	47.2	46.8	41.7	75.0
	An	13.3	2.1	0.4	1.8	1.8	2.6	2.4	4.9	2.3	1.6
	salic	96.7	95.6	95.5	94.6	95.6	95.6	95.0	96.7	96.3	96.3
	femic	2.8	4.1	4.3	5.2	4.3	4.4	5.0	3.3	3.7	3.7
triangular diag.	Q	65.2	64.8	63.3	62.6	64.7	61.5	60.9	62.0	61.3	57.9
	L	32.4	31.2	32.5	33.1	29.7	33.9	34.8	34.8	34.0	38.1
	M	2.4	4.0	4.2	4.3	5.6	4.6	4.3	3.2	4.7	4.0
	Q	31.0	32.9	30.0	28.5	35.2	27.2	25.6	26.5	27.3	20.0
	Or	5.6	37.8	57.1	33.4	34.2	32.5	22.1	20.0	26.7	—
	Pl	63.4	29.3	12.9	38.1	30.6	40.3	52.3	53.5	46.0	80.0
trace elements (ppm)	Cu	6	9	19	15	13	6	12	75	10	<5
	Pb	13	33	23	50	24	27	24	35	36	29
	Zn	21	48	19	138	27	105	40	44	39	20
	Mo	<10	11	<10	10	<10	<10	<10	11	11	<10
	Ni	<10	<10	<10	<10	15	<10	<10	17	17	11
	V	34	45	20	39	30	23	34	56	44	47
	Sr	475	29	83	6	87	12	41	100	58	16
	As	—	114	53	115	50	60	73	147	201	137

Table 2 e.

Analysis Nr		41	42	43	44	45	46	47	48	49	50
rock type		mPo	Vo	Po	Vo	Po	mPo	Po	Po	Po	Po
square (28 J)		1c	5d	5g	2i	4h	3d	1a	4h	2i	3h
weight %	SiO_2	70.0	70.0	69.0	68.7	68.5	68.1	67.7	65.8	62.5	61.9
	TiO_2	0.22	0.52	0.69	0.48	0.34	0.53	0.78	0.62	1.0	0.68
	Al_2O_3	15.8	14.7	15.5	14.3	13.7	12.6	14.4	15.4	17.3	17.1
	Fe_2O_3	1.3	1.0	3.5	4.0	2.2	8.4	1.8	4.9	4.8	5.2
	FeO	—	2.4	—	—	3.1	—	2.9	—	—	—
	MnO	0.04	0.07	0.02	0.03	0.10	0.13	0.13	0.07	0.07	0.12
	MgO	0.38	1.0	0.42	0.40	2.4	0.98	0.75	2.0	1.2	2.1
	CaO	1.5	1.9	0.3	0.9	0.6	0.9	1.6	2.4	2.7	2.5
	BaO	0.21	0.13	0.05	0.10	0.04	0.08	0.16	0.11	0.14	0.18
	Na_2O	4.8	4.2	6.7	4.5	5.0	2.1	4.4	5.1	4.7	5.1
	K_2O	3.7	4.2	2.1	4.8	1.8	5.1	4.1	1.8	4.7	2.8
	H_2O^+	—	0.2	—	—	1.7	—	0.2	—	—	—
	H_2O^-	—	0.3	—	—	0.3	—	0.3	—	—	—
	P_2O_5	—	0.10	—	—	0.10	—	0.17	—	—	—
	CO_2	—	<0.01	—	—	0.01	—	<0.01	—	—	—
	F	—	0.10	—	—	0.05	—	0.07	—	—	—
	S	—	<0.02	—	—	<0.02	—	<0.02	—	—	—
	total	98.0	100.8	98.3	98.2	99.9	98.9	99.5	98.2	99.1	97.7
cation %	Si	65.98	64.98	64.44	65.18	64.89	66.23	63.89	62.10	58.32	58.44
	Ti	0.15	0.36	0.48	0.34	0.24	0.38	0.55	0.44	0.70	0.48
	Al	17.55	16.08	17.06	15.99	15.29	14.44	16.01	17.13	19.02	19.02
	Fe'''	0.92	0.69	2.45	2.85	1.56	6.14	1.27	3.48	3.37	3.69
	Fe''	—	1.86	—	—	2.45	—	2.28	—	—	—
	Mn	0.03	0.05	0.01	0.02	0.08	0.10	0.10	0.05	0.05	0.09
	Mg	0.53	1.38	0.58	0.56	3.38	1.42	1.05	2.81	1.66	2.95
	Ca	1.51	1.88	0.30	0.91	0.60	0.93	1.61	2.42	2.69	2.52
	Ba	0.07	0.04	0.01	0.03	0.01	0.03	0.05	0.04	0.05	0.06
	Na	8.77	7.56	12.13	8.27	9.18	3.96	8.05	9.33	8.50	9.33
	K	4.44	4.97	2.50	5.80	2.17	6.32	4.93	2.16	5.59	3.37
anions	OH	—	1.23	—	—	10.74	—	1.25	—	—	—
	O	168.76	166.80	167.36	167.90	162.53	171.77	166.04	167.10	163.17	163.93

Table 2 e (continued)

Analysis Nr		41	42	43	44	45	46	47	48	49	50
Niggli values	*al*	47.52	39.71	44.36	41.13	35.66	34.37	38.30	37.02	38.97	37.74
	fm	8.05	19.75	15.91	17.72	34.94	36.53	22.60	27.44	20.87	26.75
	c	8.62	9.56	1.65	4.89	2.90	4.60	8.02	10.66	11.26	10.29
	alk	35.79	30.95	38.05	36.23	26.48	24.48	31.06	24.85	28.88	25.20
	si	357.28	320.96	335.17	335.35	302.60	315.25	305.62	268.46	238.94	231.82
	si'	243.18	223.81	252.22	244.95	205.93	197.93	224.24	199.42	215.42	200.82
	qz	114.10	97.15	82.95	90.40	96.67	117.32	80.38	69.04	23.42	31.00
	k	0.33	0.39	0.17	0.41	0.19	0.61	0.38	0.18	0.39	0.26
	mg	0.35	0.34	0.19	0.16	0.45	0.18	0.22	0.44	0.32	0.43
	w	—	0.27	—	—	0.38	—	0.35	—	—	—
	ti	0.84	1.79	2.52	1.76	1.12	1.84	2.64	1.90	2.87	1.91
	p	—	0.19	—	—	0.18	—	0.32	—	—	—
	h	—	3.05	—	—	25.04	—	3.01	—	—	—
	T	11.72	8.76	6.31	4.89	9.17	9.88	7.24	12.17	10.09	12.53
	t	3.10	–0.80	4.65	0.00	6.27	5.28	–0.77	1.50	–1.17	2.23
CIPW norms	Q	24.5	23.0	21.0	21.9	26.6	33.3	21.3	21.4	9.9	13.2
	Or	22.3	24.7	12.6	28.9	10.7	30.5	24.4	10.8	28.0	16.9
	Ab	41.5	35.3	57.7	38.8	42.4	18.0	37.5	43.9	40.1	44.2
	An	8.0	8.2	1.6	4.7	2.0	4.7	6.7	12.3	12.3	13.0
	salic	97.3	91.5	94.6	94.3	84.5	88.3	90.3	89.1	90.4	88.4
	femic	2.6	8.2	5.4	5.6	13.7	11.6	9.4	10.8	9.5	11.5
triangular diag.	Q	61.6	59.9	57.8	58.4	58.1	59.9	58.2	55.7	50.5	50.8
	L	35.1	33.6	35.7	35.5	27.4	25.8	34.2	32.8	40.3	36.6
	M	3.3	6.5	6.5	6.1	14.5	14.3	7.6	11.5	9.2	12.6
	Q	25.4	25.2	22.6	23.3	32.5	38.5	23.7	24.2	10.9	15.1
	Or	23.2	27.0	13.6	30.6	13.1	35.3	27.1	12.2	31.0	19.4
	Pl	51.4	47.8	63.8	46.1	54.4	26.2	49.2	63.6	58.1	65.5
trace elements (ppm)	Cu	<5	16	15	19	18	<5	21	99	38	107
	Pb	34	31	49	34	8	24	39	16	45	18
	Zn	53	72	39	43	30	80	110	45	95	54
	Mo	<10	<10	16	12	<10	<10	<10	<10	12	<10
	Ni	10	14	20	17	21	<10	<10	21	26	12
	V	51	98	88	74	97	32	49	127	164	165
	Sr	568	152	21	95	36	52	138	252	455	234
	As	45	40	290	108	<50	95	28	<50	160	30

Table 2 f.

Analysis Nr		51	52	53	54	55	56	57	58	59	60
rock type square (28 J)		G 5h	G 3h	G 1c	mA 4h	G 3h	mA 3i	A 3h	A Oh	mA 5g	G 9a
weight %	SiO_2	58.9	57.8	57.2	56.8	56.5	56.0	55.3	51.2	47.0	43.0
	TiO_2	0.60	0.65	0.97	0.70	0.88	1.0	0.91	1.9	0.86	2.3
	Al_2O_3	15.1	16.7	16.8	15.3	15.7	16.0	18.1	18.5	17.3	11.8
	Fe_2O_3	8.9	7.1	5.5	9.2	6.9	3.7	9.1	7.1	9.7	19.4
	FeO	—	—	3.2	—	—	3.3	—	4.4	—	—
	MnO	0.12	0.17	0.27	0.26	0.18	0.26	0.10	0.21	0.38	0.24
	MgO	2.3	3.6	1.8	4.0	6.1	3.2	3.4	2.1	9.6	6.7
	CaO	8.3	4.0	8.1	7.2	4.7	6.4	3.1	7.5	8.4	7.5
	BaO	0.10	0.05	0.07	0.03	0.04	0.24	0.07	0.07	0.03	0.21
	Na_2O	3.3	6.4	4.9	4.8	6.4	2.9	6.4	4.6	2.4	1.3
	K_2O	2.0	1.9	1.4	0.4	0.6	4.8	2.0	1.4	1.1	3.3
	H_2O^+	—	—	0.2	—	—	0.9	—	0.9	3.1	3.6
	H_2O^-	—	—	0.2	—	—	0.3	—	0.2	—	—
	P_2O_5	—	—	0.27	—	—	0.36	—	0.52	—	—
	CO_2	—	—	<0.01	—	—	<0.01	—	0.03	—	—
	F	—	—	0.04	—	—	0.09	—	0.09	—	—
	S	—	—	<0.02	—	—	<0.02	—	<0.02	—	—
	total	99.6	98.4	100.9	98.7	98.0	99.5	98.5	100.7	99.9	99.4
cation %	Si	55.95	53.53	53.11	53.58	52.15	53.25	51.38	48.29	44.74	43.75
	Ti	0.42	0.45	0.67	0.49	0.61	0.71	0.63	1.34	0.61	1.76
	Al	16.90	18.23	18.38	17.01	17.08	17.93	19.82	20.56	19.41	14.15
	Fe'''	6.36	4.94	3.84	6.53	4.79	2.64	6.36	5.03	6.94	14.85
	Fe''	—	—	2.48	—	—	2.62	—	3.47	—	—
	Mn	0.09	0.13	0.21	0.20	0.14	0.20	0.07	0.16	0.30	0.20
	Mg	3.25	4.97	2.49	5.62	8.39	4.53	4.70	2.95	13.62	10.16
	Ca	8.44	3.96	8.05	7.27	4.64	6.52	3.08	7.57	8.56	8.17
	Ba	0.03	0.01	0.02	0.01	0.01	0.08	0.02	0.02	0.01	0.08
	Na	6.07	11.49	8.82	8.77	11.45	5.34	11.52	8.41	4.43	2.56
	K	2.42	2.24	1.65	0.48	0.70	5.82	2.37	1.68	1.33	4.28
anions	OH	—	—	1.23	—	—	5.70	—	5.66	19.68	24.43
	O	163.77	158.71	159.28	161.21	157.62	156.12	158.15	155.05	145.81	144.37

Table 2 f (continued)

Analysis Nr		51	52	53	54	55	56	57	58	59	60
Niggli values	*al*	27.35	30.35	29.13	25.94	26.18	28.75	31.84	29.74	23.08	16.08
	fm	31.43	33.47	28.62	37.70	40.86	32.12	35.82	33.64	49.65	57.34
	c	27.45	13.28	25.62	22.22	14.29	21.20	9.99	22.00	20.40	18.78
	alk	13.75	22.87	16.60	14.12	18.64	17.91	22.33	14.60	6.85	7.78
	si	181.05	178.31	168.35	163.42	159.93	170.80	165.09	139.70	106.41	99.47
	si'	155.01	191.51	166.43	156.49	174.58	171.64	189.32	158.41	127.42	131.14
	qz	26.04	–13.20	1.92	6.93	–14.65	–0.84	–24.23	–18.71	–21.01	–31.67
	k	0.28	0.16	0.15	0.05	0.05	0.52	0.17	0.16	0.23	0.62
	mg	0.33	0.49	0.27	0.45	0.62	0.45	0.42	0.25	0.65	0.40
	w	—	—	0.60	—	—	0.50	—	0.59	—	—
	ti	1.38	1.50	2.14	1.51	1.87	2.29	2.04	3.89	1.46	4.00
	p	—	—	0.33	—	—	0.46	—	0.60	—	—
	h	—	—	1.96	—	—	9.15	—	8.19	23.41	27.77
	T	13.59	7.48	12.62	11.81	7.54	10.84	9.51	15.14	16.22	8.30
	t	–13.85	–5.80	–13.19	–10.41	–6.75	–10.35	–0.48	–6.85	–4.17	–10.47
CIPW norms	Q	15.3	1.2	7.8	9.7	0.2	5.3	—	3.2	—	1.1
	Or	11.9	11.4	8.2	2.4	3.6	28.6	12.0	8.2	6.5	19.6
	Ab	28.0	55.1	41.2	41.2	55.3	24.7	55.0	38.7	20.3	11.1
	An	20.6	11.4	19.6	19.3	12.6	16.6	15.0	25.6	33.2	16.7
	salic	75.8	79.1	76.9	72.5	71.7	75.3	82.0	75.7	60.1	48.5
	femic	24.2	20.9	22.8	27.5	28.3	23.6	18.0	23.3	36.8	47.7
triangular diag.	Q	46.8	40.8	43.8	42.5	38.3	43.4	38.7	40.0	32.2	25.2
	L	29.5	38.6	34.5	30.7	35.0	35.0	41.1	38.0	29.3	24.9
	M	23.7	20.6	21.7	26.8	26.7	21.6	20.2	22.0	38.5	49.9
	Q	20.2	1.6	10.4	13.4	0.2	7.0	—	4.2	—	2.3
	Or	15.7	14.4	10.7	3.3	5.1	38.0	14.6	10.9	10.8	40.4
	Pl	64.1	84.0	78.9	83.3	94.7	55.0	85.4	84.9	89.2	57.3
trace elements (ppm)	Cu	11	6	15	825	<5	10	6	25	169	21
	Pb	27	29	27	24	21	30	22	35	14	26
	Zn	98	85	108	174	90	153	60	214	375	133
	Mo	<10	<10	<10	<10	<10	<10	<10	16	<10	<10
	Ni	59	29	14	77	52	82	28	34	293	43
	V	232	378	372	303	296	244	307	294	227	670
	Sr	598	319	516	426	378	714	355	416	222	199
	As	107	114	<50	89	128	76	<50	<50	66	<50

Table 2 g.

Analysis Nr		61	62	63	64	65	66	67	68	69	70
rock type square (28 J)		VoS 1b	VoS 5g	LGr 7i	LGr 9i	QMz 6b	GrD 1e	DMz 4i	D 2g	D 4i	D 9i
weight %	SiO_2	79.0	73.5	74.8	76.0	69.2	59.6	54.6	48.7	48.6	48.5
	TiO_2	0.13	0.49	0.14	0.09	0.53	0.56	1.6	1.2	2.9	1.2
	Al_2O_3	12.1	13.4	13.0	12.7	15.0	18.6	15.4	20.1	13.9	16.6
	Fe_2O_3	0.3	0.8	0.8	0.7	2.7	5.5	6.8	12.0	10.0	9.5
	FeO	—	—	0.8	0.4	—	—	5.5	—	7.1	—
	MnO	0.01	0.03	0.02	0.01	0.03	0.14	0.15	0.18	0.14	0.12
	MgO	0.12	1.3	0.69	0.08	0.46	2.6	2.5	5.4	3.3	5.9
	CaO	1.0	1.0	0.8	0.5	0.9	5.0	5.4	8.1	7.3	11.0
	BaO	0.02	0.04	0.13	0.08	0.13	0.13	0.01	0.07	0.02	0.04
	Na_2O	5.6	5.9	3.0	3.5	3.7	4.9	5.5	4.3	5.1	3.4
	K_2O	0.4	1.3	4.8	4.9	4.5	1.3	1.6	0.6	0.8	0.4
	H_2O+	—	—	0.3	0.2	—	—	0.3	—	0.4	3.1
	H_2O-	—	—	0.2	0.3	—	—	0.1	—	0.1	—
	P_2O_5	—	—	0.03	0.02	—	—	0.29	—	0.73	—
	CO_2	—	—	<0.01	<0.01	—	—	0.27	—	0.02	—
	F	—	—	0.01	0.01	—	—	0.19	—	0.18	—
	S	—	—	<0.02	<0.02	—	—	<0.02	—	<0.02	—
	total	98.7	97.8	99.5	99.5	97.2	98.3	100.2	100.7	100.6	99.8
cation %	Si	74.37	69.07	70.94	71.92	66.57	55.88	51.20	44.95	46.26	46.67
	Ti	0.09	0.34	0.09	0.06	0.38	0.39	1.12	0.83	2.07	0.86
	Al	13.42	14.84	14.53	14.16	17.00	20.55	17.02	21.86	15.59	18.82
	Fe'''	0.21	0.56	0.57	0.49	1.95	3.88	4.79	8.33	7.16	6.87
	Fe''	—	—	0.63	0.31	—	—	4.31	—	5.65	—
	Mn	0.00	0.02	0.01	0.00	0.02	0.11	0.11	0.14	0.11	0.09
	Mg	0.16	1.82	0.97	0.11	0.65	3.63	4.39	7.42	4.68	8.46
	Ca	1.00	1.00	0.81	0.50	0.92	5.02	5.42	8.01	7.44	11.34
	Ba	0.00	0.01	0.04	0.02	0.04	0.04	0.00	0.02	0.00	0.01
	Na	10.22	10.75	5.51	6.42	6.90	8.90	10.00	7.69	9.41	6.34
	K	0.48	1.55	5.80	5.91	5.52	1.55	1.91	0.70	0.97	0.49
anions	OH	—	—	1.89	1.26	—	—	1.87	—	2.53	—
	O	175.93	170.96	171.98	172.51	170.22	163.26	156.72	156.68	153.86	156.97

Table 2 g (continued)

Analysis Nr		61	62	63	64	65	66	67	68	69	70
Niggli values	*al*	49.83	43.63	45.45	48.10	46.38	36.43	26.08	27.97	20.49	23.75
	fm	2.88	14.17	13.74	6.35	14.39	27.03	39.00	40.70	46.27	38.96
	c	7.54	6.00	5.38	3.64	5.32	17.97	16.64	20.56	19.58	28.65
	alk	39.72	36.18	35.41	41.89	33.88	18.54	18.26	10.75	13.64	8.62
	si	552.18	406.13	443.78	488.48	363.16	198.13	156.95	115.03	121.57	117.77
	si'	258.91	244.74	241.67	267.58	235.55	174.19	173.04	143.00	154.57	134.49
	qz	293.26	161.39	202.11	220.90	127.61	23.94	–16.09	–27.97	–33.00	–16.72
	k	0.04	0.12	0.51	0.47	0.44	0.14	0.16	0.08	0.09	0.07
	mg	0.43	0.75	0.44	0.12	0.24	0.47	0.27	0.46	0.26	0.54
	w	—	—	0.47	0.61	—	—	0.52	—	0.55	—
	ti	0.68	2.03	0.62	0.43	2.09	1.39	3.45	2.13	5.45	2.19
	p	—	—	0.07	0.05	—	—	0.35	—	0.77	—
	h	—	—	5.93	4.28	—	—	2.87	—	3.33	—
	T	10.11	7.44	10.03	6.20	12.50	17.88	7.82	17.22	6.84	15.13
	t	2.56	1.43	4.64	2.56	7.17	–0.08	–8.81	–3.33	–12.73	–13.52
CIPW norms	Q	43.1	30.8	36.2	36.0	28.6	11.7	4.3	—	1.5	0.4
	Or	2.4	7.9	28.6	29.2	27.4	7.8	9.4	3.5	4.7	2.4
	Ab	48.0	51.1	25.6	29.8	32.2	42.2	46.5	36.2	42.9	29.8
	An	5.1	5.2	3.9	2.4	4.8	25.3	12.6	33.6	12.6	29.8
	salic	99.2	95.3	95.7	98.2	95.4	87.0	72.8	73.2	61.7	62.4
	femic	0.7	4.7	3.9	1.5	4.5	12.9	26.8	26.7	37.7	37.5
triangular diag.	Q	72.3	64.6	67.5	68.4	62.2	49.6	39.8	33.5	32.4	34.4
	L	26.7	31.0	28.0	29.6	31.6	37.0	35.4	36.7	32.1	30.3
	M	1.0	4.4	4.5	2.0	6.2	13.4	24.8	29.8	35.5	35.3
	Q	43.7	32.4	38.4	36.8	30.7	13.4	5.8	—	0.6	0.6
	Or	2.4	8.3	30.1	29.9	29.4	9.0	13.0	4.8	7.8	3.9
	Pl	53.9	59.3	31.5	33.3	39.9	77.6	81.2	95.2	91.6	95.5
trace elements (ppm)	Cu	9	6	26	30	9	82	9	81	7	141
	Pb	15	18	33	33	18	25	25	17	36	33
	Zn	23	24	26	11	25	96	100	111	108	78
	Mo	<10	<10	<10	<10	<10	<10	<10	<10	<10	10
	Ni	<10	12	26	14	<10	21	21	37	29	96
	V	12	30	40	28	53	226	240	284	595	385
	Sr	86	91	117	67	96	995	106	444	330	1998
	As	<50	<50	87	51	<50	<50	<50	<50	<50	131

Table 2 h.

Analysis Nr		71	72	73	74	75	76	77	78	79	80
rock type		Sk	Sk	UB	UB	Ga	Ga	AG	ND	NG	NG
square (28 J)		Oj	3i	5f	5f	7b	8d	2e	4a	2a	Ob
weight %	SiO_2	63.9	60.0	46.9	41.3	52.0	48.5	46.7	49.0	48.7	46.9
	TiO_2	0.69	1.25	0.29	0.24	1.4	0.97	2.22	1.31	2.44	2.54
	Al_2O_3	16.4	15.7	7.4	6.0	16.6	18.1	17.5	16.6	14.3	13.3
	Fe_2O_3	1.3	7.5	12.4	4.5	11.6	10.6	17.7	13.1	16.1	17.7
	FeO	1.7	—	—	6.8	—	—	—	—	—	—
	MnO	0.05	0.13	0.45	0.36	0.18	0.15	0.22	0.24	0.28	0.22
	MgO	2.2	3.5	19.7	26.1	6.0	9.8	4.8	7.5	5.7	7.0
	CaO	3.8	5.1	7.4	5.1	7.1	8.4	8.4	7.8	7.5	9.9
	BaO	<0.01	0.14	0.01	<0.01	0.09	0.06	0.10	0.03	0.03	0.04
	Na_2O	8.5	4.1	0.1	0.2	3.4	2.9	3.0	3.0	2.8	2.1
	K_2O	0.3	3.1	<0.1	0.2	1.5	0.8	0.5	0.8	1.2	0.7
	H_2O+	0.4	—	4.7	5.7	—	—	—	—	—	—
	H_2O-	0.2	—	—	0.3	—	—	—	—	—	—
	P_2O_5	0.15	—	—	0.01	—	—	—	—	—	—
	CO_2	0.03	—	—	2.40	—	—	—	—	—	—
	F	0.03	—	—	<0.01	—	—	—	—	—	—
	S	<0.02	—	—	<0.02	—	—	—	—	—	—
	total	99.7	100.5	99.4	99.2	99.9	100.3	101.1	99.4	99.1	100.4
cation %	Si	57.77	55.63	45.45	38.87	48.78	44.52	44.41	46.22	47.16	45.09
	Ti	0.46	0.87	0.21	0.16	0.98	0.66	1.58	0.92	1.77	1.83
	Al	17.47	17.15	8.45	6.65	18.35	19.58	19.61	18.45	16.32	15.07
	Fe'''	0.88	5.23	9.04	3.18	8.18	7.32	12.66	9.30	11.73	12.80
	Fe''	1.28	—	—	5.35	—	—	—	—	—	—
	Mn	0.03	0.10	0.36	0.28	0.14	0.11	0.17	0.19	0.22	0.17
	Mg	2.96	4.83	28.46	36.62	8.39	13.40	6.80	10.54	8.22	10.03
	Ca	3.68	5.06	7.68	5.14	7.13	8.26	8.55	7.88	7.78	10.19
	Ba	0.03	0.05	0.00	0.00	0.03	0.02	0.03	0.01	0.01	0.01
	Na	14.89	7.37	0.18	0.36	6.18	5.16	5.53	5.48	5.25	3.91
	K	0.34	3.66	0.12	0.24	1.79	0.93	0.60	0.96	1.48	0.85
anions	OH	2.41	—	—	35.79	—	—	—	—	—	—
	O	158.72	162.18	139.07	128.81	159.05	155.59	159.07	157.81	159.60	158.47

Table 2 h (continued)

Analysis Nr		71	72	73	74	75	76	77	78	79	80
Niggli values	*al*	34.60	29.19	8.46	6.13	24.76	23.32	23.87	22.85	20.65	17.46
	fm	20.48	34.61	75.83	83.81	45.12	49.67	47.78	49.61	51.09	53.33
	c	14.71	17.41	15.39	9.49	19.34	19.73	20.90	19.54	19.72	23.66
	alk	30.19	18.77	0.31	0.55	10.76	7.26	7.46	7.98	8.52	5.53
	si	228.80	189.31	91.01	71.69	131.63	106.67	108.00	114.46	119.35	104.49
	si'	220.76	175.11	101.24	102.23	143.06	129.05	129.85	131.94	134.11	122.12
	qz	8.04	14.20	–10.23	–30.54	–11.43	–22.38	–21.85	–17.48	–14.75	–17.63
	k	0.02	0.33	0.39	0.39	0.22	0.15	0.09	0.14	0.21	0.17
	mg	0.57	0.47	0.75	0.80	0.50	0.64	0.34	0.52	0.40	0.43
	w	0.40	—	—	0.37	—	—	—	—	—	—
	ti	1.85	2.96	0.42	0.31	2.66	1.59	3.86	2.30	4.49	4.25
	p	0.22	—	—	0.00	—	—	—	—	—	—
	h	4.77	—	30.42	33.00	—	—	—	—	—	—
	T	4.41	10.41	8.15	5.57	13.99	16.06	16.38	14.86	12.12	11.93
	t	–10.30	–7.00	–7.24	–3.91	–5.34	–3.67	–4.51	–4.68	–7.59	–11.73
CIPW norms	Q	4.5	10.2	4.5	—	4.4	—	4.0	2.6	6.4	5.6
	Or	1.8	18.2	0.6	1.2	8.9	4.7	2.9	4.8	7.2	4.1
	Ab	72.2	34.5	0.9	1.7	28.8	24.5	25.1	25.5	23.9	17.7
	An	5.7	15.2	19.6	10.1	25.6	33.9	32.4	29.6	23.1	24.7
	salic	84.3	78.1	25.5	14.3	67.7	63.1	64.5	62.5	60.6	52.1
	femic	15.2	21.7	69.8	79.4	32.2	36.9	35.5	37.4	39.4	47.9
triangular diag.	Q	47.4	45.8	25.7	17.4	37.0	31.7	32.6	33.6	33.8	30.1
	L	39.8	33.8	9.2	5.9	31.4	30.1	31.2	29.3	27.7	23.4
	M	12.8	20.4	65.1	76.7	31.6	38.2	36.2	37.1	38.5	46.5
	Q	5.4	13.1	17.5	—	6.5	—	6.2	4.1	10.5	10.7
	Or	2.1	23.3	2.3	9.2	13.1	7.5	4.5	7.6	11.8	7.9
	Pl	92.5	63.6	80.2	90.8	80.4	92.5	89.3	88.3	77.7	81.4
trace elements (ppm)	Cu	7	—	28	53	69	66	150	44	78	136
	Pb	20	—	10	0	33	17	39	20	115	44
	Zn	27	—	123	80	140	99	154	111	248	168
	Mo	<10	—	<10	<10	<10	<10	—	—	—	—
	Ni	14	—	1924	1521	100	364	124	170	77	133
	V	73	—	373	73	331	199	600	514	1126	1074
	Sr	87	—	5	0	469	446	—	—	—	—
	As	<50	—	70	<50	62	<50	—	—	—	—

Table 3. Modal estimates of rocks for which chemical analyses exist. The following signs have been used: ● = predominant mineral (> 40 %), ++++ = main mineral (20—40 %), +++ = essential mineral (10—20 %), ++ = subordinate mineral (1—10 %), + = accessory mineral (< 1 %), • = trace mineral. The analyses Nr correspond to those of Table 2.

Mineralfördelning i analyserade prover. ● = > 40 %, ++++ = 20—40 %, +++ = 10—20 %, ++ = 1—10 %, + = < 1 %, • = spår.

Analysis Nr	1	2	3	4	5	6	7	8	9	10
Quartz	++++	++++	++++	++++	++++	++++	++++	+++	++++	++++
Plagioclase	++++	++++	++++	++++	++++	●	++++	++++	++++	++++
% Anorthite [1]	0	0/30	0/35	0/33	0/25	0/30	0/20	0/20	0/25	0/35
K-feldspar (perthitic)	++++	++++	++++	++++	++++	++++	++++	●	++++	++++
Muscovite (sericite)										
Biotite	+	+	++	++	+++	++	+++		+++	+++
Chlorite					+		•	•		+
Epidote group					+					
Common hornblende		++	++			++		++	+++	
Orthorhombic pyroxene										
Monoclinic pyroxene									+++	
Olivine										
Opaque minerals	+	++	++	+	++		+	+	+	•
Apatite					+		+	+	+	•
Zircon		•					•			•
Sphene + leucoxene	+	++	++	+	++	+	++	+	+	+
Rutile	•		+	•			•	+		

[1] Statistical optical determination

Table 3 (continued)

Analysis Nr	11	12	13	14	15	16	17	18	19	20
Quartz	+++	++	+++	+++	++	+++		++	+++	
Plagioclase	●	●	++++	++++	++++	++++	●	●	++++	●
% Anorthite	0/30	0/25		0/30	0/25	0/20		0/28	0/40	0/28
K-feldspar (perthitic)	++++	+++	++++	++++	++++	++++	+++	+++	+++	++++
Muscovite (sericite)						+				++
Biotite	°	++	+++	++	+	+++	++++	+	++	+
Chlorite			•	•			+			+
Epidote group								+		
Common hornblende	+++	++		+++	++	++++	++	+++	++++	+
Orthorhombic pyroxene									++	
Monoclinic pyroxene				+	++			++	++++	
Olivine										
Opaque minerals	++	++		+++	+	++	+	+	+++	+
Apatite		+	+	++	+	++			++	+
Zircon			•							
Sphene + leucoxene	•	++	+	++	+		+	++		+
Rutile				+	•	•		•	+	•

Table 3 (continued)

Analysis Nr	21	22	23	24	25	26	27	28	29	30
Quartz	+++	++	++	+++	+	++++	++++	++++	++++	++++
Plagioclase	++++	●	●	++++	●	++++	++++	++++	++++	●
% Anorthite		0/20	0/20	0/30	0/40		20	25	33	
K-feldspar (perthitic)	++++	++++	++++	+++	+++	++++	++++	++++	++++	+++
Muscovite (sericite)	+++	+		++	+++					+
Biotite	+++	++	+	+++						++
Chlorite	+	+			++		+++		+	++
Epidote group										
Common hornblende	+++		+++	++++	+++			++		
Orthorhombic pyroxene										
Monoclinic pyroxene	+++	+++	++	+++						
Olivine										
Opaque minerals	++	+++	+	•	+	+	+	++	++	++
Apatite	++	++	+	•	+					
Zircon										
Sphene + leucoxene					+	+	•	+		+
Rutile	+	+	+				+	•		

Table 3 (continued)

Analysis Nr	31	32	33	34	35	36	37	38	39	40
Quartz	++++	++++	++++	++++	++++	++++	++++	++++	++++	+++
Plagioclase	●	++++	+++	++++	++++	++++	●	●	●	●
% Anorthite		0/25	30	30	30	28	35		30	0
K-feldspar (perthitic)	++	++++	●	++++	++++	++++	++++	+++	++++	
Muscovite (sericite)			+		++			+	++	
Biotite	+++	+++	+	+		++	+++	+	+	+
Chlorite		+	+		+		+	+	+	+
Epidote group										
Common hornblende	++++	•		+++		++	+			
Orthorhombic pyroxene										
Monoclinic pyroxene										
Olivine										
Opaque minerals	+	+++		+	+	+	+	++	++	+
Apatite	++			+	•		•	+		+
Zircon				+			•			
Sphene + leucoxene	++	++	+	+	+	+	+	+	+	+
Rutile				•	+	+	•		•	

Table 3 (continued)

Analysis Nr	41	42	43	44	45	46	47	48	49	50
Quartz	++++	++++	++++	++++	++++	++++	++++	++++	++	+++
Plagioclase	●	●	●	●	●	+++	●	●	●	●
% Anorthite	25	25	30	30	0/35		20		40	35
K-feldspar (perthitic)	++++	++++	+++	++++	++++	++++	++++	+++	++++	+++
Muscovite (sericite)	++				+		+		+++	++
Biotite	+++	+++	+++				+++	++++	+++	
Chlorite	+		+	+	+++	++			+	++++
Epidote group	+				+		•	+		+
Common hornblende		+++					++++		+++	
Orthorhombic pyroxene										
Monoclinic pyroxene										
Olivine										
Opaque minerals	+	+	+	•	•	○	++	+	+	+
Apatite	+	•	+			+		+	+	+
Zircon						•	•	•	+	•
Sphene + leucoxene	+	+	+	+	+	++	++	+	++	+
Rutile								+		

Table 3 (continued)

Analysis Nr	51	52	53	54	55	56	57	58	59	60
Quartz	+++	++	++							+
Plagioclase	●	●	●	●	●	●	●	●	●	++++
% Anorthite	30	35	35	15	0/15	50	35	45	30	
K-feldspar (perthitic)	+++	+++	++		++	++++		++	++	+++
Muscovite (sericite)		+			+++	+++			+++	
Biotite				+++		++	++++	+		
Chlorite		++	•	+				+		++
Epidote group	++++	+	++++	+	+++		+	+++	+++	
Common hornblende	++++		+++	●	++++	+++		●	●	●
Orthorhombic pyroxene										
Monoclinic pyroxene						+++				
Olivine										
Opaque minerals	•	+	+	+++	+++	•	+++	+	+	+++
Apatite	+	+				+	+	+		
Zircon	++	•			•					
Sphene + leucoxene	++	+		•	++	++	+	++		+
Rutile					+		•		+	

Table 3 (continued)

Analysis Nr	61	62	63	64	65	66	67	68	69	70
Quartz	●	++++	++++	++++	++++	+++	++			
Plagioclase [1]	●	●	++++	++++	++++	●	●	●	●	●
% Anorthite [2]	0/25	0/30		25	33	28	15	40	15	28
K-feldspar (perthitic)		++	++++	++++	++++	++	++			
Muscovite (sericite)	+	+	+	++		+			+	
Biotite		+++	++	+	+++	+++	+++	+	+	
Chlorite	++		+	+	+				+	++++
Epidote group						+				++++
Common hornblende						+++	++++	++++	++++	++++
Orthorhombic pyroxene										
Monoclinic pyroxene								++++		
Olivine										
Opaque minerals	•		+	•	+	+	+	•	+++	+
Apatite		•			+	+	+	+	+	
Zircon	•	+		•		•	•		•	
Sphene + leucoxene	+	+			++	+	++		++	
Rutile					•				•	

Table 3 (continued)

Analysis Nr	71	72	73	74	75	76	77	78	79	80
Quartz					+					
Plagioclase [1]	●				●	●	●	●	●	●
% Anorthite [2]	35				73	73	75	65	40	75
K-feldspar (perthitic)										
Muscovite (sericite)		+++	+++*					+	+	
Biotite					+++	+++	++	++++	+++	+++
Chlorite	•			++++°		+°			+	
Epidote group	•	+++								•
Common hornblende	+++	++++	●	●	++++		++	++++	●	+++
Orthorhombic pyroxene					+++	++++	+++			++
Monoclinic pyroxene	●	●			+++	+++	++++			●
Olivine						+++				
Opaque minerals	•	+++	+	+++	+++	++	+++	++	++	+++
Apatite	+				++	+	++	•	+	•
Zircon										
Sphene + leucoxene	++									•
Rutile					+					

* = talc
° = serpentine

Definition of the rock-type symbols used in Table 2.

QMz = quartz monzonite
GrD = granodiorite
Vo = acid volcanic rocks
mPo = meta-porphyry
mA = meta-andesite
VoS = sediment (Volcanic Series)
D = diorite
UB = ultrabasic rock
Ag = Akkavare gabbro
ND = minor diabase (NG type)
DMz = dioritic monzonite
Mz = monzonite
Po = porphyry
G = greenstone
A = andesite
LGr = Lina granite
Sk = skarn
Ga = gabbro
NG = Nabrenjarka gabbro diabase

Corresponding analysis Nr and sample Nr (Table 2).

Anal. Nr	Sample Nr	Anal. Nr	Sample Nr	Anal. Nr	Sample Nr	Anal. Nr	Sample Nr
1	1474A	21	1484A	41	1282B	61	1033
2	1263	22	1457B	42	1503B	62	1300A
3	1486B	23	1457A	43	1287B	63	1331
4	1476A	24	1617B	44	1365B	64	1333
5	1266	25	1361	45	1168	65	1461C
6	1262	26	1284	46	1256	66	1312B
7	1053	27	1026A	47	1065	67	1192
8	1471	28	1254A	48	1169	68	1398
9	1395	29	1426E	49	1364	69	1194
10	1118	30	1101	50	1163C	70	1335
11	1513	31	1113A	51	1283	71	1155A
12	1251	32	1252	52	1213B	72	1356
13	1478E	33	1081A	53	1080	73	1314B
14	1463B	34	1253	54	1179	74	1314A
15	1563	35	1222C	55	1213C	75	1564B
16	1029	36	1258	56	1355	76	1555
17	1478F	37	1003	57	1175	77	1277
18	1307	38	1206B	58	1139	78	1478C
19	1541	39	1222D	59	1367	79	1051
20	1463A	40	1287A	60	1621B	80	1001

Table 4. Chemical analyses of various gabbros of Norrbotten. The results are given in weight %.

Kemiska analyser av olika gabbrotyper i Norrbotten (vikt %).

	Nabrenjarka gabbro diabase (present paper) 37 analyses		28J Fjällåsen (present paper) 2 analyses	29L Lainio (Witschard 1970) 14 analyses	28L Tärendö (Padget 1970) 1 analysis	29J Kiruna (Offerberg 1967) 1 analysis
	variations	average				
SiO_2	49.8—42.0	44.9	50.2	49.8	51.6	49.0
TiO_2	3.9—1.8	2.7	1.2	0.8	1.3	0.8
Al_2O_3	17.6—12.9	14.8	17.3	16.8	17.8	18.7
Fe_2O_3	20.9—14.2	17.6	11.1	8.8	10.1	8.6
MnO	0.28—0.17	0.21	0.16	0.14	0.15	0.14
MgO	7.8—3.0	6.1	7.9	10.0	6.7	8.3
CaO	10.4—6.4	8.8	7.7	7.0	8.3	9.5
Na_2O	3.2—2.1	2.5	3.1	3.0	2.0	2.9
K_2O	1.8—0.6	1.0	1.1	0.9	0.9	0.8
BaO	0.08—0.03	0.04	0.07	0.07	0.01	0.03

REFERENCES

GFF = Geologiska Föreningens i Stockholm Förhandlingar
SGU = Sveriges geologiska undersökning

AMBROS, M., and HENKEL, H., 1973: Titanjärnmalmsfyndigheten Akkavare (Melko), Kartbladet 28J Fjällåsen. — SGU Malmbyrån.

BURRI, C., 1959: Petrochemische berechnungsmethoden auf äquivalenter grundlage. — Birkhäuser Verl., Basel-Stuttgart.

CORNWELL, J. D., 1964: Notes on some aeromagnetic anomalies from northern Sweden. — Geoexploration 2, pp. 150—158.

ERIKSSON, T., 1954: Pre-Cambrian geology of the Pajala district, northern Sweden. — SGU C 522.

FRIETSCH, R., 1963: Järnmalmsförekomster inom Norrbottens län. — SGU C 592.

— 1966: Berggrund och malmer i Svappavaarafältet, norra Sverige. — SGU C 604.

GEIJER, P., 1913: On poikilitic intergrowths of quartz and alkali feldspar in volcanic rocks. GFF 35, pp. 51—80.

— 1930: On the iron-rich norite of Akkavare (Sjaunja). — GFF 52, pp. 391—397.

— 1931: Berggrunden inom malmtrakten Kiruna—Gällivare—Pajala. — SGU C 366.

— 1966: Cykeltänkandet och granitproblem. — GFF 87, pp. 455—483.

GULSON, B. L., 1972: The precambrian geochronology of granitic rocks from northern Sweden. — GFF 94, pp. 229—244.

HJELMQVIST, S., 1956: On the occurrence of ignimbrite in the Pre-Cambrian. — SGU C 542.

— 1966: Beskrivning till berggrundskarta över Kopparbergs län. — SGU Ca 40.

JUNG, J., and ROQUES, M., 1952: Introduction à l'étude zonéographique des formations crystallophylliennes. — Bull. Serv. Carte geol. France Nr 235, pp. 1—62.

LUNDQVIST, G., 1943: Norrlands jordarter. — SGU C 457.

MARMO, V., 1956: On the granites. — Amer. Jour. Sc. Nr 254—8, pp. 479—492.

— 1958: The problem of latekinematic granites. Schweiz. — Min. Pet. Mitt. Zurich Nr 38—1, pp. 19—42.

— 1966: On the petrological classification of granites. — C. R. Soc. Geol. Finlande Nr 38, pp. 69—73.
— 1968: The origin of granite, a hydrothermal model. — Lithos, Vol. 1, Universitetsförlaget, Oslo.
OFFERBERG, J., 1967: Beskrivning till berggrundskartbladen Kiruna NV, NO, SV, SO. — SGU Af 1—4.
PADGET, P., 1970: Beskrivning till berggrundskartbladen Tärendö NV, NO, SV, SO. — SGU Af 5—8.
RAGUIN, E., 1957: Géologie du granite. — Paris, Masson et Cie.
READ, H. H., 1957: The granite controversy. — London, Thomas Murby and Co.
RITTMANN, A., 1952: Nomenclature of volcanic rocks. — Bull. Volcanologique 12, pp. 75—102.
— 1962: Volcanoes and their activity. — New York, John Wiley & Sons.
SCHROCK, R. R., 1948: Sequence in layered rocks. — New York, McGraw-Hill Book Company.
TRAVIS, R. B., 1955: Classification of rocks. — Quart. Bull. Colorado School of Mines, Vol 50, Nr 1, pp. 1—32.
TURNER, F. J., and VERHOOGEN, F., 1960: Igneous and metamorphic petrology. — New York, McGraw-Hill Book Company.
TUTTLE, O. F., and BOWEN, N. L., 1958: Origin of granite in the light of experimental studies. — Geol. Coc. Am. Mem. 74.
WAHL, W., 1936: Om granitgrupperna och bergkedjeveckningarna i Sverige och Finland. — GFF 58, pp. 90—101.
WELIN, E., 1966: The absolute time scale and the classification of Precambrian rocks in Sweden. — GFF 86, pp. 29—33.
— 1970: Den svekofenniska orogena zonen i norra Sverige — en preliminär diskussion. — GFF 92, pp. 433—451.
WELIN, E., and BLOMQVIST, G., 1964: Age measurements on radioactive minerals from Sweden. — GFF 86, pp. 33—50.
— 1966: Further age measurements on radioactive minerals from Sweden. — GFF 88, pp. 3—18.
WELIN, E., BLOMQVIST, G., and PARWEL, A., 1966: Rb/Sr whole rock age data on some swedish Pre-Cambrian rocks. — GFF 88, pp. 19—28.
WELIN, E., CHRISTIANSSON, K., and NILSSON, Ö., 1971: Rb/Sr radiometric ages of extrusive and intrusive rocks in northern Sweden. I. — SGU C 666.
WERNER, S., 1963: Aeromagnetic mapping by the Geological Survey of Sweden. Methods and general considerations. — Geoexploration 1, pp. 21—31.
WHITFIELD, J. M., and ROGERS, J. J. W., 1959: Relationships among textural properties and modal compositions of some granitic rocks. — Geochimica et Cosmochimica Acta 17, pp. 272—285.
WINKLER, H. G. F., 1967: Die genese der metamorphen gesteine. — 2. Auflage. Berlin-Heidelberg.
WITSCHARD, F., 1965: Contribution à l'étude géologique, pétrographique et métallogénique des massifs granitiques du Sénégal oriental. — Paris, Mémoire BRGM 44.
— 1970: Description of the geological maps Lainio NV, NO, SV, SO. — SGU Af 9—12.
ÖDMAN, O., 1939: Urbergsgeologiska undersökningar inom Norrbottens län. — SGU C 426.
— 1957: Beskrivning till berggrundskarta över Norrbottens län. — SGU Ca 41.

APPENDIX: GEOPHYSICAL INVESTIGATIONS ON THE MAP-SHEET 28 J FJÄLLÅSEN

by

HERBERT HENKEL

CONTENTS

SAMMANFATTNING

1967 utfördes flygmagnetiska mätningar inom kartområdet och 1974 avslutades de regionala tyngdkraftsmätningarna. (Tyngdkraftskartan som återges i pl. 2C bygger på totalt 819 stationer.) De bergartsprover som samlats in under den geologiska karteringen har undersökts med avseende på sina fysikaliska egenskaper täthet, magnetisk susceptibilitet och remanent magnetisering, s. k. parametermätning.

Tolkningen av de flygmagnetiska kartorna har gjorts med avseende dels på anomalistruktur och -mönster och dels anomalinivå. Bandat anomalimönster tillskrivs områden med parallella och kontinuerliga anomalier. I områden med oregelbundet anomalimönster är dessa drag mindre tydliga eller saknas helt. Ett gånglikt anomalimönster tillskrivs enstaka mycket uthålliga anomalier med diskordant uppträdande.

Förutom dessa egenskaper i anomalibilden har vid tolkningen tagits fram magnetiska kontakter, dislokationer samt konnektioner mellan likartade anomalier. I pl. 2A anges de områden som har olika anomalimönster, vidare visas anomalistrukturen av linjerna för olika grad av bandning. I fig. 29 har mindre domlika strukturer indikerats i områden med oregelbundet anomalimönster. Lokalt förekommer anomalier som indikerar gångsystem. Speciellt framträdande är den stora Nabrenjarka gången (ruta 5a—0b).

Pl. 2B visar *magnetiska dislokationer* och möjliga laterala förskjutningsbelopp. Dessa har tagits fram genom analys av störningar i vissa lätt identifierbara anomalier (gångar, kontakter och band), s. k. referensstrukturer. Man noterar att 2 nära ortogonala riktningar dominerar — se även fig. 30. De båda dislokationssystemen i östra delen av kartområdet sträcker sig över 100 km utanför kartbladsgränserna.

Tyngdkraftsanomalierna är i allmänhet väl korrelerade med ytgeologin. Undantag utgör den stora positiva anomalin på SV-bladet. I fig. 31 visas en möjlig tolkning av denna anomali såsom orsakad av en på litet djup liggande tung, skivliknande kropp. En annan tolkning vore en kulmination (på något större djup) av en täthetsgräns mot ett tyngre underlag. Regionala tyngdkraftsdata tillsammans med täthetsbestämningar för bergarter lämpar sig väl för uppskattningar av bergarternas volymsfördelning, denna återges i några profiler i fig. 31.

De *geofysiska markmätningarna* har redovisats i pl. 2D och i tabellen i fig. 32.

Bergarternas fysikaliska egenskaper är sammanfattade i tabell i figur 33 samt för enskilda, kemiskt analyserade prov i tabell 5.

Figurerna 34—44 visar de olika bergarternas fysikaliska egenskaper. Generellt kan sägas att ökad magnetisering även medför ökad täthet samt att de flesta suprakrustalbergarterna har en hög eller mycket hög magnetisering. Inom detta kartblad representerar därför de högsta magnetiska anomalierna suprakrustalbergarter eller basiska bergarter. Remanensen är i allmänhet helt underordnad den inducerade magnetiseringen med undantag av Akkavare och Nabrenjarka gabbron, där förhållandet mellan dessa magnetiseringar (q-värdet) är uppemot 0.8. Fig. 40 visar den remanenta magnetiseringens riktning för dessa gabbror.

Sammanfattningsvis ges en översikt av bergarternas relativa magnetisering i fig. 45. Vidare kan det fastslås att den övervägande delen av bergarterna huvudsakligen är inducerat magnetiserade. Det är således fördelningen av magnetithalten i bergarterna som ger upphov till de flygmagnetiska anomalierna och det finns starka indicier på att magnetithaltens fördelning är kopplad till bergarternas primära strukturer. Genom en kombination av magnetisk, gravimetrisk och parameterinformation är det möjligt att tämligen väl avgränsa områden med suprakrustal respektive djupbergarter.

INTRODUCTION

The aeromagnetic measurements on the map area 28 J Fjällåsen were carried out in 1967. For technical information concerning these measurements, the reader is referred to S. Werner (1963). In 1973, a regional gravity survey was made in the map area.

Measurements of the magnetic remanence, the magnetic susceptibility and of the specific weight have been made on all rock specimens collected during the geological mapping. They have permitted the investigation of the three-dimensional distribution of rocks as well as structures occurring at, or near the surface.

The interpretation of aeromagnetic maps consists mainly of pattern analyses and of the delineation of magnetic contacts and dislocations. The results of this investigation, together with magnetic dip estimations, figure on maps on the scale of 1:50 000 and 1:100 000 which are deposited in the archives of the Geological Survey of Sweden.

In Plate 2, a simplified geophysical interpretation of the area and a gravity map are presented (separate folder, together with the aero- and geological maps).

AEROMAGNETIC INTERPRETATION

In the first phase, a regional interpretation is carried out. This permits the identification of different patterns and magnetization levels. Three types of pattern have been observed: *banded patterns* consisting of parallel and continuous anomalies, *irregular patterns* in which these features are lacking or less pronounced, and *dyke type patterns* where anomalies are super-continuous and generally discordant to banded or irregular patterns. The results obtained depend on the general geometrical configuration of the anomalies. For example it is impossible to identify dykes which are parallel to the banding in rocks or to investigate flat-lying banded structures.

In the second phase of the interpretation, magnetic contacts, connections and dislocations of anomalies are worked out. On well defined anomalies, dip computations are performed for contacts and for sheet-like magnetic bodies. In these computations, characteristic anomaly-parametres are compared with those from model computations. It is assumed that all magnetization is essentially parallel to the geomagnetic field. The magnetization is almost exclusively caused by the distribution of magnetite in the rocks (S. Werner 1945). The correlation between anomaly pattern and the geology becomes possible when the magnetic properties of rocks have been determined. This problem is discussed in a following chapter.

Some phases of the interpretation are evidently somewhat subjective, but the majority of the work can be made in physically and mathematically defined steps. There sometimes exist several solutions to an interpretation problem which all satisfy the measurements. In these cases alternative solutions are given. Additional information, as for example: gravity, petrophysical properties, in-situ suceptibility measurements and geological information, sometimes makes it possible to choose a unique solution.

REGIONAL ANOMALY PATTERNS

High alitude (3 000 m) aeromagnetic measurements, by the Canadian Dominion Observatories (1965) over Scandinavia, indicate that the map area lies in a regional magnetic high striking NW—SE, with an amplitude of more than 700 gammas (Fig. 28). This anomaly extends into the adjacent map areas 28 K and 29 J and does not seem to be correlated with the anomaly distribution obtained from near-surface measurements.

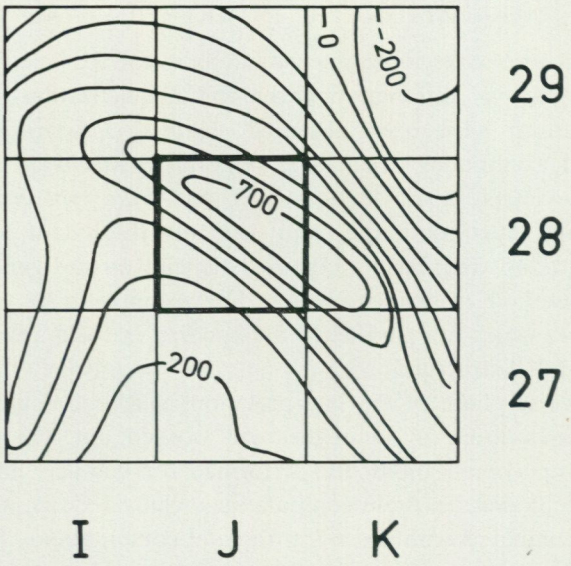

Fig. 28. Regional magnetic anomalies, vertical component measured at 3 000 m altitude. Measurements by Can. Dom. Obs. 1965.
Magnetisk vertikalkomponent mätt på 3 000 m höjd.

On the aeromagnetic maps, the anomaly pattern is dominated by the properties and distribution of rocks lying near the surface. The three types of anomaly patterns described above correspond respectively to three main rock groups. Transitions between the banded and the irregular patterns are common and give rise to quite a number of alternative interpretations. They will be discussed in the next paragraphs where the areal distribution of each pattern group is described.

AREAS WITH BANDED PATTERN

On the simplified interpretation map (Plate 2 A) presented in the same folder as the aeromagnetic and geological maps, banded patterns are denoted by heavy black lines. These lines represent connections of anomalies of limited extent, and take into account similar magnetization and parallelism. When the magnetization of adjacent irregular patterns is similar to that of the matrix of banded patterns, the boundaries between these patterns are undefined. In consequence, the outer limit of banded

areas is usually drawn along the outmost positive anomaly band. In the case of steeply dipping bodies, the maxima are situated over the intersections of sheet-like bodies with the surface.

These banded patterns are widespread in the eastern part of the map area and strike N—S to NNW—SSE. They extend into the map areas 29 J Kiruna to the north and 27 J Porjus to the south. A strongly magnetized matrix dominates parts of the banded area (0i—j, 3h, 4g, 5—6f, 8g, 8—9h, 9d—f, 9a—b and 9i—j). This banded pattern corresponds to rocks with high susceptibility and a limited range of variation. Generally the dip is steep. Folding is observed in many places especially where banded patterns are distorted around small dome-like structures. These will be discussed in more detail below.

To the east, the banded pattern grades into irregular patterns where the continuity of anomalies is less pronounced and finally vanishes. Their strike is nevertheless still parallel to the regional banded anomaly complex. To the west, the boundaries of the banded pattern area are sharp, particularly with areas of low magnetization. A similar situation arises in the SE-corner of the map area (0—2 i—j). Some of the isolated areas figured on the map (Pl. 2 A) as banded patterns (1b—c, 2j, 4e, 7—8j, 8d—e) can also be interpreted as irregular patterns with intermediate magnetization. Banded anomalies at the northern edge of the map area are continuations from larger banded anomaly complexes on the adjacent map area 29 J. In the region 8—9 g—h the interpretation is based on the ground magnetic measurements of the Fjällåsen area.

AREAS WITH IRREGULAR PATTERN

Anomaly regions with diffuse, or no banding occupy the largest part of the map area. On Plate 2 A they are denoted by increasingly dense screens for increasing magnetization levels. Diffuse banding is marked with broken lines. As already mentioned in the previous paragraph, areas east of the main sequence of banded anomalies show a near-parallel, diffuse orientation and they could therefore be interpreted as relic banded patterns.

In the eastern part of the banded pattern area, a series of elongated dome-like structures occur along a nearly N—S direction (2i, 4h—i, 8h, 9i). Dome-like patterns in the irregular anomaly systems are also present to the west of the banded complex, although their aspects are much

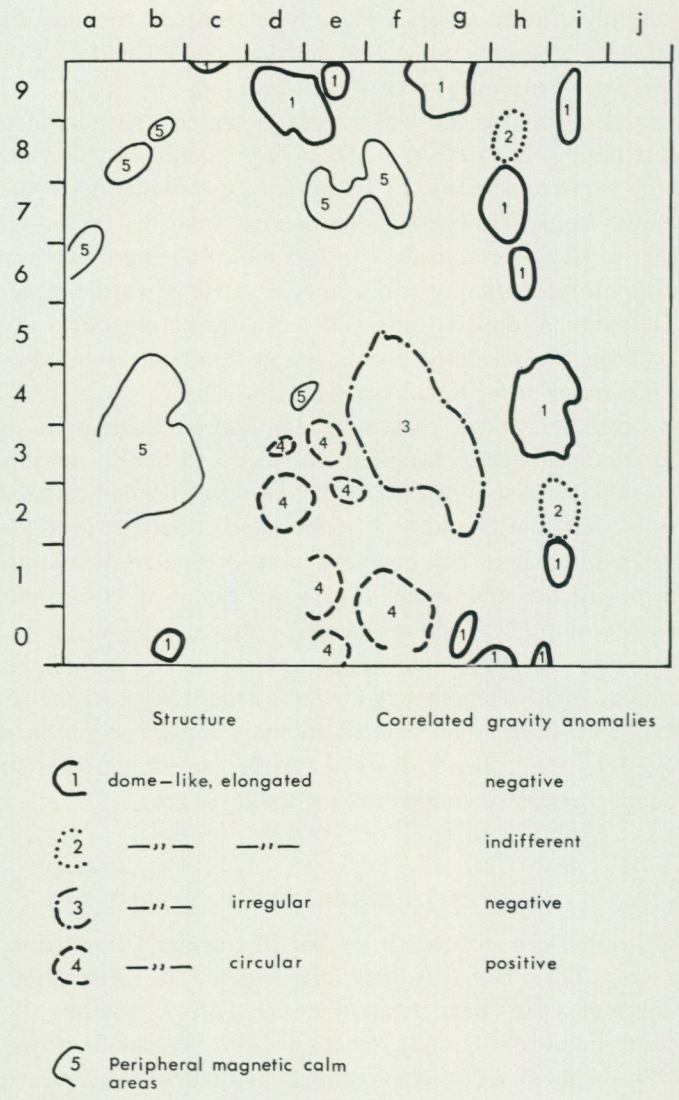

Fig. 29. Irregular Anomaly patterns.
Strukturer i oregelbundna anomalimönster.

more diffuse (0b, 0—1f, 1d—e, 2d, 3e, 9d—e). Their shapes are more circular with diameters of 3—6 km. Figure 29 shows the distribution of these features in the map area.

In the western quadrangles the magnetization of the irregular anomaly complexes have distinct levels, generally with well defined boundaries. Within these levels, the amount of diffuse banding is rather variable, giving rise to completely calm areas and areas with higher amplitude.

Areas of very high mean magnetization (0b, 1j, 2d—e, 6—7f, 9c) usually have a high variability.

Areas of high mean magnetization occupy most of the NW quadrangle and a large area in the south-central part of the map area. Within these areas magnetization is rather variable. A diffuse pattern can be discerned and is parallel to neighbouring banded structures. In the centre of these anomalies, small structures have a concentric configuration, especially in the NW quadrangle. Along the periphery of this anomaly several smaller areas occur with lower magnetization and low variability (4d, 4—5 a—b, 6a, 7e). They can be interpreted as rather flat-lying small, low magnetic sheets (Fig. 29).

The remaining areas are occupied by rock formations with low magnetization displaying rather diffuse internal structures. The large area at (3—4f) has a very "smooth" pattern with sharp boundaries. It thus differs in appearance from the other areas and may possibly represent a dome-like structure. This rock body gives rise to a pronounced gravity minimum indicating a large volume of light matter.

DYKE SYSTEMS

Several systems of dyke-like anomalies can be observed on the aeromagnetic maps. They are denoted with a dotted line on Plate 2 A. It must be mentioned that a dyke gives rise to a magnetic anomaly only if it has rather large dimensions (width exceeding 20 m) and contrasting magnetic properties. On the western margin of the area (0—1a, 5—8a), a dyke swarm with an average N—S strike can be inferred from a series of anomalies intersecting the general anomaly trend. Some of these indications are rather diffuse.

In the central part of the map area a NNE—SSW striking dyke system occurs. It is particularly well marked in the smooth dome-like anomaly area (3—4f).

Although dykes which are parallel to banded structures are usually not discernable, some of the more continuous and slightly discordant anomalies in the large highly magnetized area in the NW quadrangle have been interpreted as dykes.

In the SW part of the map area, a rather high and continuous anomaly can be traced. Locally, it widens and is then figured on the map with the screen used for very highly magnetized irregular patterns. This anomaly extends at least another 50 km outside the map area. It is one of the longest continuous anomalies so far encountered. It corresponds to a rather flat, westward-dipping and highly magnetized sheet. A discussion of its geometry and physical properties is made in a separate paragraph (see the Nabrenjarka gabbro diabase, pp. 34—39).

MAGNETIC DISLOCATIONS

Magnetic dislocations can be deduced from displacements of reference structures such as banding, characteristic contacts or dykes. The frequent occurrence of reference structures in the map area makes possible a rather detailed investigation. Usually, dislocations parallel to prominent bands and dykes or parallel to the flight lines can not be discerned. As distortions along the flight direction are sometimes attributed to lack of

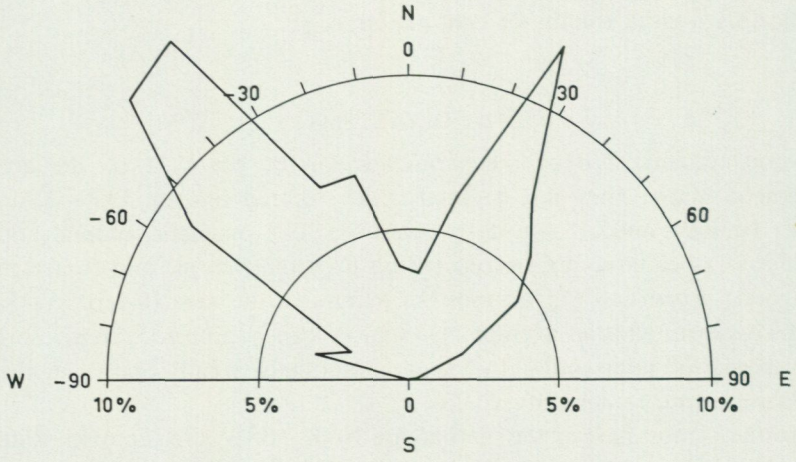

Fig. 30. Direction frequencies for 10 degree intervals of magnetic dislocations. *Riktningar för magnetiskt bestämda dislokationer.*

control in the measurements, they are usually not taken into consideration. Therefore, the tendency of under-representation in these directions is obvious (mainly N—S and E—W respectively).

The dislocations and their lateral displacements are shown on Plate 2 B. Two large super-regional dislocation systems intersect in the central eastern part of the map area. Both systems, one striking NNE—SSW, the other NW—SE, extend over 100 km outside the map area. The apparent lateral displacements along these dislocations are generally within 3 km. The vertical component seems to be significantly smaller. The width of these zones of large displacement is within 0.5 km. In-between major zones of this kind, parallel, less continuous dislocations occur with a mean spacing of about 10 km. Along them, displacements are much smaller (average = 0.4 km). Still smaller dislocations occur with spacings of about 1.5 km. This system of dislocations forms a near orthogonal pattern and can be observed throughout Norrbotten county. Locally N—S striking dislocations can be observed with a maximal apparent displacement of 0.8 km. Figure 30 shows dislocation trend frequencies for 10 degree intervals.

REGIONAL GRAVITY ANOMALIES

In the map area, a regional gravity survey has been carried out on a network of selected profiles. The Bouguer anomaly map (Pl. 2 C) is based on a total of 819 observations, some of which are selected from the ground measurements in the Fjällåsen and Akkavare areas. The anomalies are terrain-corrected and the Bouguer density used is 2.67 g cm^{-3}.

The gravity anomalies give a good picture of the volume distribution of rocks. As a rule, there is a good coincidence between aeromagnetic and gravity anomalies indicating that steep-dipping structures predominate. The anomalies also reveal the major zones of dislocations.

In the SW quadrangle, however, no correlation between gravity and surface geology exists. The light rocks at the surface are obviously underlain by heavy rocks at rather shallow depth. A week correlation with magnetic near-surface structures has been observed. Thus the largest gravity maximum lies on one of the diffuse dome-like patterns (2d) mentioned in a previous chapter. The Akkavare gabbro is situated on its eastern margin.

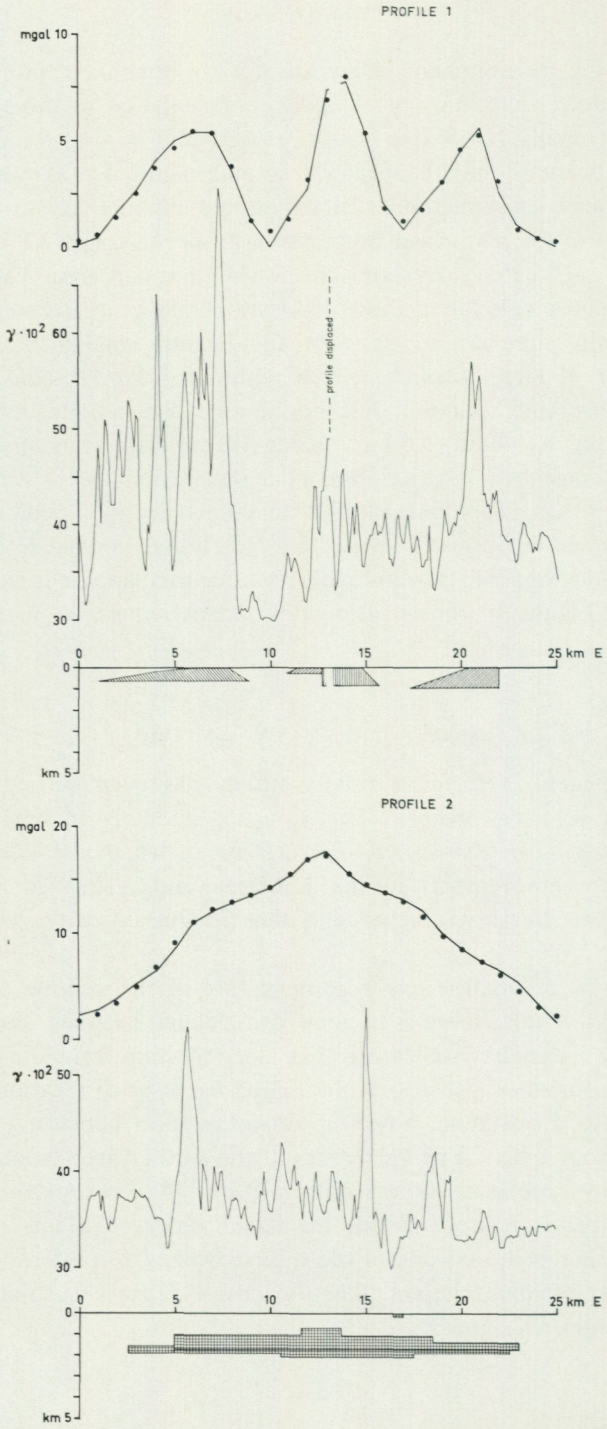

Fig. 31. Text p. 109.

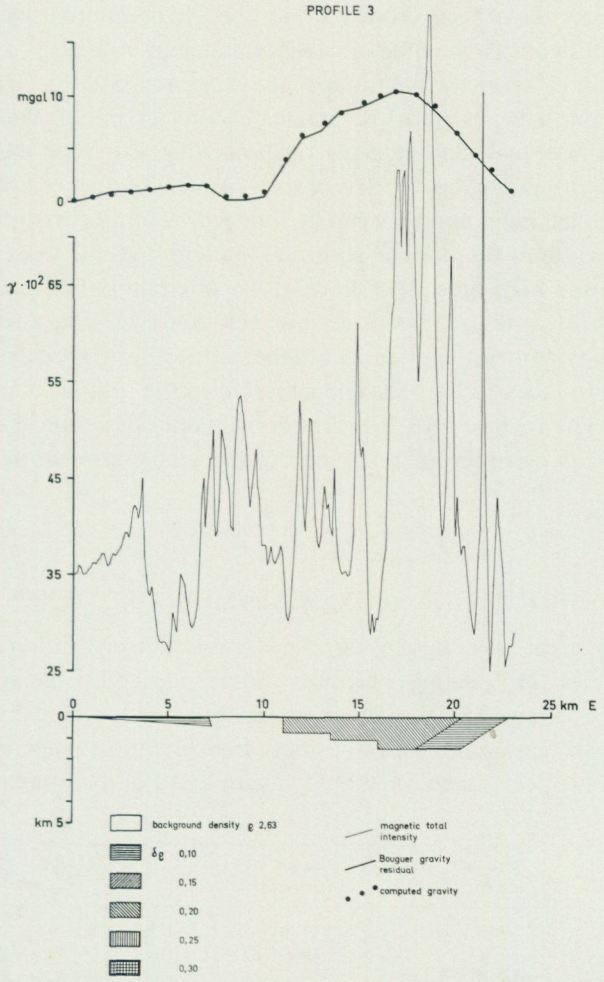

Fig. 31. Gravity profiles, for position of profiles see Pl. 2 D. In profile 2 (p. 108) the position of the surface-reaching Akkavare gabbro is indicated for comparison. *Tyngdkraftsprofiler.*

A series of depth estimates, using the maximal anomaly and the mean density contrasts (Fig. 33), have been made for the supracrustal rocks. These computations show that the surface-reaching supracrustal rocks have a maximum depth of 2 km, the average being 1.4 km, which is significantly smaller than depths for similar complexes in adjacent map areas. A possible explanation is that the Fjällåsen region was uplifted

and the rocks have been eroded more deeply, or alternatively, that the supracrustal deposits were significantly smaller in volume.

The positive anomaly mentioned above in the SW quadrangle must emanate from a heavy and low magnetic body at rather shallow depth. An approximate calculation gives the following values if the density is assumed to be 3.0 g cm^{-3}. The upper-surface of the central part lies 750 m deep, the main anomaly can be induced by an upper-surface 1.1 km deep. The width of the body is about 20 km and it seems to extend southwards into the map area 28 J Porjus. An alternative interpretation is a culmination of a density interface, the amplitude of which is dependent on the density contrast applied. A number of profiles have been computed and are reproduced in Fig. 31. The situation of the profiles is indicated on Plate 2 D. The surface rock distribution is mainly based on the geological map and mean densities are computed from parameter measurements.

GROUND GEOPHYSICAL MEASUREMENTS

In the map area, two major ground geophysical investigations have been performed for prospecting purposes. Some specifications are given in Fig. 32. On Plate 2 D the situation of the measurements is indicated together with map-scales and divisions. Interpretation maps on the scale 1:20 000 have been made for the Akkavare and Fjällåsen areas.

Area	year of measurment	type of measurement	area in km^2	map square
Peltovare	1943	M	1.2	0 i
Akkavara	1957	M (by ABEM)	6	2 e
	1968—70	M	3	
		G	8	
		E	3	
Fjällåsen	1967—70	M	53	8—9 g—h
		G	53	

M Magnetic vertical intensity
G gravity
E electromagnetic slingram

Note: The measurements of Peltovare are made after older standards and do not follow the norms for map scales and divisions otherwise used.

Fig. 32. Specifications of ground geophysical surveys.
Geofysiska markmätningar.

PHYSICAL PROPERTIES OF ROCKS

Rock samples which have been collected during geological mapping in the region, have been measured with respect to the following physical properties: density, magnetic susceptibility and remanent magnetization. In-situ susceptibility measurements and orientated samples have been collected on the Nabrenjarka gabbro diabase and on the Akkavare gabbro.

The density is determined as wet bulk density with an accuracy of 0.01 g cm^{-3}. The magnetic properties are determined in three directions with a relative error of 2 % and a resolution of about $3 \cdot 10^{-6}$ cgs. The

Rock type	Number of samples	Density cgs		Susceptibility 10^3 cgs		q-value	
		mean	st.dev.	mean	st.dev.	mean	st.dev.
1 granite, a	39	2.63	0.02	0.71	0.47	0.20	0.59
b				0.01		1.3	
c				1.2		0.22	
2 granodiorite	11	2.65	0.03	1.02	0.26	0.16	0.64
1+2		2.63	0.02	0.78	0.42	0.19	0.60
3 diorite	7	2.86	0.11	6.5	0.26	0.37	0.75
4 gabbro	19	2.99	0.12	6.9	0.39	0.96	0.74
3+4		2.96	0.13	7.5	0.35	0.71	0.76
5 perthite granite	22	2.63	0.02	1.7	0.16	0.18	0.73
6 „ monzonite	25	2.68	0.04	2.2	0.31	0.27	0.65
7 pyroxene perthite monzonite	6	2.74	0.06	4.0	0.17	0.96	0.80
5+6+7		2.67	0.05	2.1	0.24	0.27	0.73
8 acid gneisses	7	2.69	0.05	0.51	1.21	0.24	0.61
9 intermediate gneisses, a	14	2.88	0.10	0.72	0.98	0.29	0.68
b				0.1		0.45	
c				7.5		0.15	
10 mica schist	4	2.84	0.06	2.9	0.25	0.42	0.71
11 quartzite, a	5	2.70	0.05	0.18	0.79	0.56	0.78
b				0.04		0.9	
c				1.7		0.2	
8+9+10+11		2.80	0.12	0.63	1.17	0.33	0.70
12 acid volcanics, a	86	2.65	0.06	0.60	1.03	0.54	0.85
b				0.03		2	
c				2.2		0.25	
13 intermediate volcanics	14	2.84	0.08	4.4	0.34	0.86	0.73
14 porphyrite, a	11	2.86	0.09	2.1	0.83	0.63	0.75
b				0.18		0.9	
c				9.5		0.3	
13+14		2.85	0.08	3.2	0.53	0.61	0.75
15 dolerite	8	2.94	0.04	1.8	0.55	0.27	0.68
12+13+14+15		2.72	0.12	0.89	0.97	0.53	0.82

Fig. 33. Physical properties of rock groups. a, b, c denotes total group, low magnetic fraction and high magnetic fraction respectively.
Fysikaliska egenskaper för bergartsgrupper.

in-situ susceptibility measurements have the same accuracy and a resolution of about $2 \cdot 10^{-5}$ cgs. The general results of these measurements are given in Fig. 33 and, for the specimens which have been chemically analysed, parameter measurements are given in Table 5.

A plot of susceptibility versus density, showing the covariation of these parameters, has been proved to give valuable information. On such a plot, the effect of the magnetite content (which is logarithmic proportional to the magnetic susceptibility) on the density can be reduced, thereby obtaining a density corresponding more closely to the silicate mineral composition (or silicate-density). Statistically this density directly reflects the chemical composition which corresponds to an acid-basic variation. Any geological process which affects either of these parameters

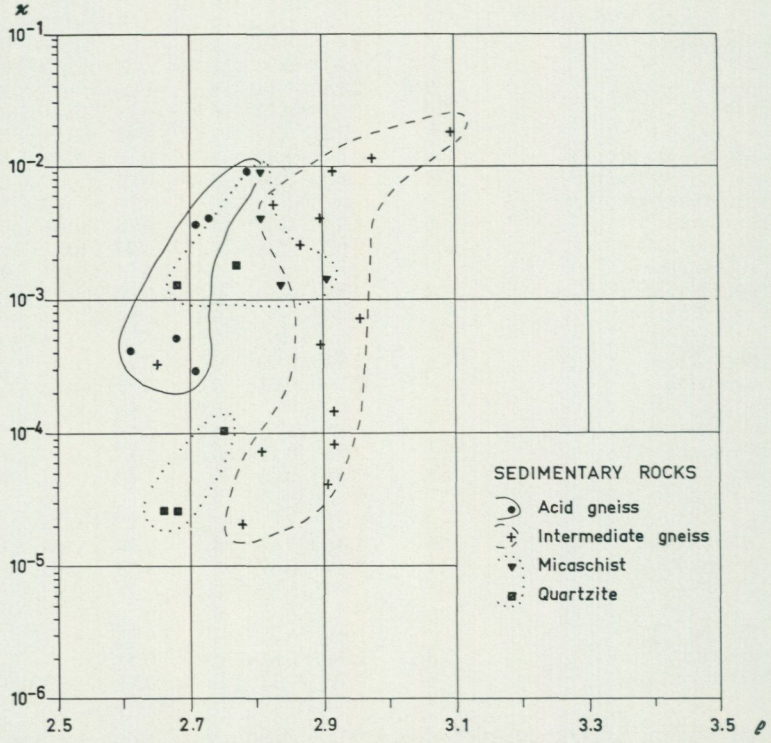

Fig. 34. Susceptibility versus density for major rock groups.
Susceptibilitets-täthetsdiagram för större bergartsgrupper.

will show up as a trend in the covariation diagrams (Henkel 1975). For the study of magnetic contrasts, susceptibility frequency distributions are given for certain rock groups (Figs. 34, 35, 37, 38).

In the following paragraphs a discussion is made of each main group of rocks with reference to diagrams on the covariation of density and susceptibilty. In a final chapter conclusions are drawn regarding the magnetic contrasts expected between rock groups and their expressions on the aeromagnetic map.

SEDIMENTARY ROCKS, FIG. 34

Few samples only of these rocks exist from the map area. They follow a normal trend in their density distribution and display a large variation

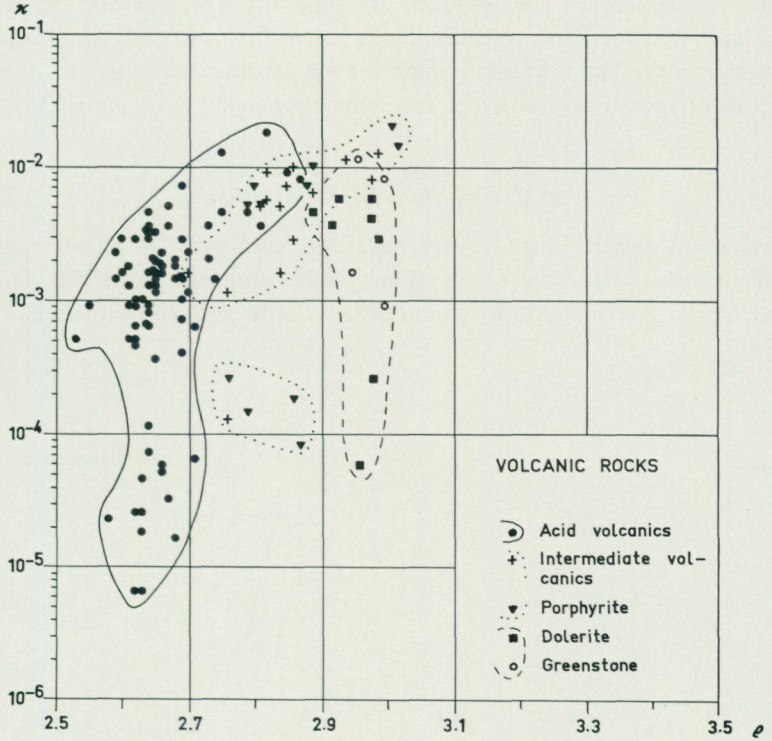

Fig. 35. Legend: see Fig. 34.
Legend: se fig. 34.

in susceptibility with a tendency towards high values. Some specimens of quartzite show high q-values (ratio of remanent to induced magnetization), which commonly are caused by hematite contents. The average q-value is 0.4.

VOLCANIC ROCKS, FIG. 35

Part of the acid volcanic rocks tend towards very low densities and susceptibilities. They also overlap considerably the area of intermediate volcanic rocks. The majority of samples lie in a high susceptibility region (about $3 \cdot 10^{-4}$ cgs). However, all the rock types, except for the greenstones, are also present in a lower susceptibility region. The reason for this tendency is unclear but may, in the case of intermediate volcanic rocks, depend on the destruction of magnetite during metamorphism. In general, the average susceptibility tends to decrease with increasing acidity of the rocks. The q-values are generally low, but are higher for acid and intermediate volcanic rocks than for acid and intermediate plutonic rocks. The average q-value for all volcanic rocks is 0.5. A comparison of the susceptibility of the main rock types is made in Fig. 36.

PLUTONIC ROCKS, FIGS. 37—38

These rocks usually display very restricted variations in silicate density (density reduced for the effect of magnetite contents in rocks). This is particularly true for granite, grandiorite, diorite and perthite rocks. The

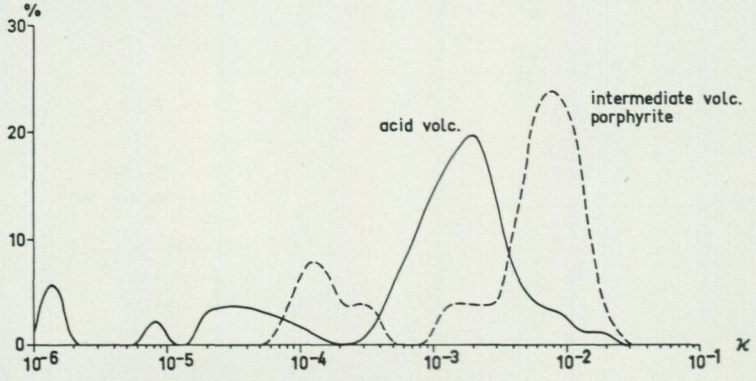

Fig. 36. Susceptibility frequencies for volcanic rocks.
Susceptibilitetsfrekvenser för vulkaniter.

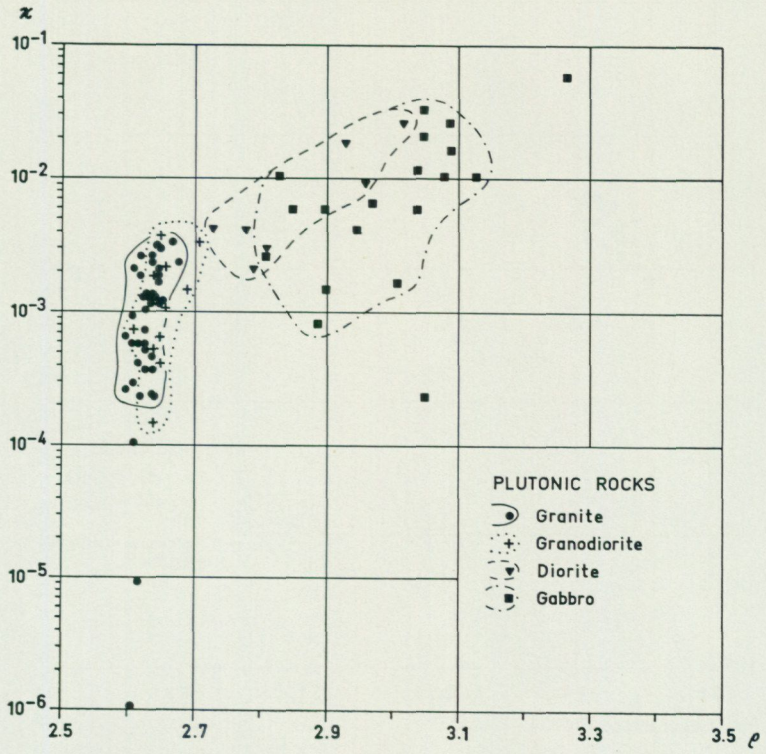

Fig. 37. Legend: see Fig. 34.
Legend: se fig. 34.

plot of gabbro samples partly overlaps the region corresponding to dioritic rocks. The susceptibility of plutonic rocks varies with a factor of 50 which is less than that observed in other map areas of Norrbotten. A comparison of the susceptibilities of three main groups of rocks is made in Fig. 39. Statistically, the most basic rocks have the highest susceptibilities. Granites and granodiorites have the lowest susceptibility. Within the perthite group, perthite monzonites have, on average, a higher susceptibility than perthite granites. The remanent magnetization in the plutonic rocks is generally low. Only a few specimens of gabbros have q-values larger than 1. The mean q-value for all plutonic rocks is 0.3.

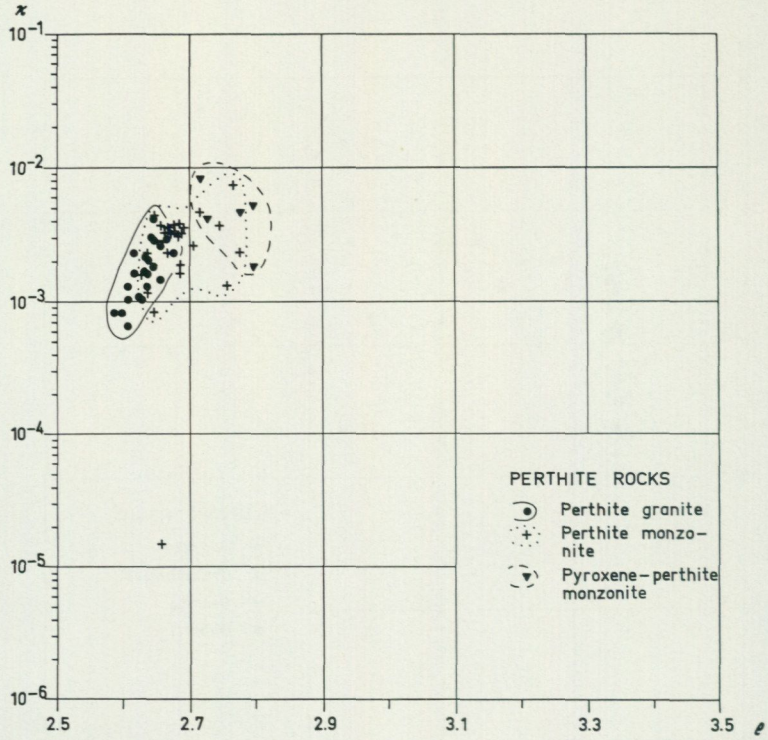

Fig. 38. Legend: see Fig. 34.
Legend: se fig. 34.

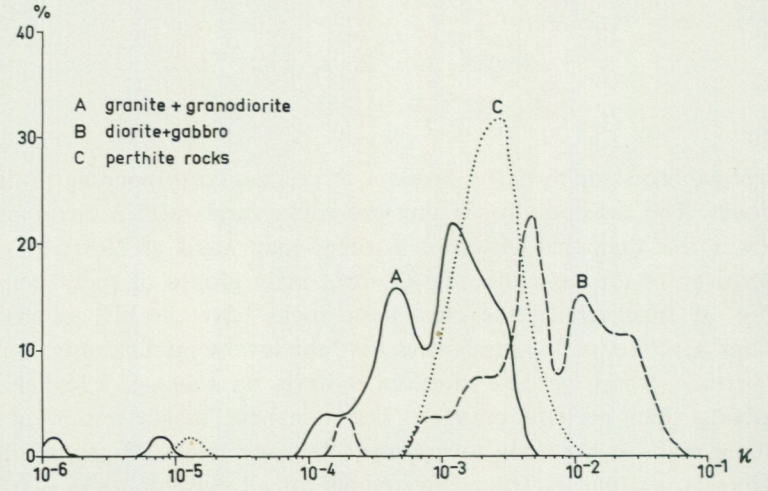

Fig. 39. Susceptibility frequencies for plutonic rocks.
Susceptibilitetsfrekvenser för djupbergarter.

Akkavare and Nabrenjarka gabbros, Figs. 40—43

These gabbros are sufficiently exposed for a detailed study of their physical properties. For both gabbros, orientated samples have been collected and a great number of in-situ susceptibility measurements have been made. They belong to the extreme high susceptibility group with magnetite contents exceeding 3 %. Figs. 40—43 show the physical properties of the Akkavare and Nabrenjarka gabbros.

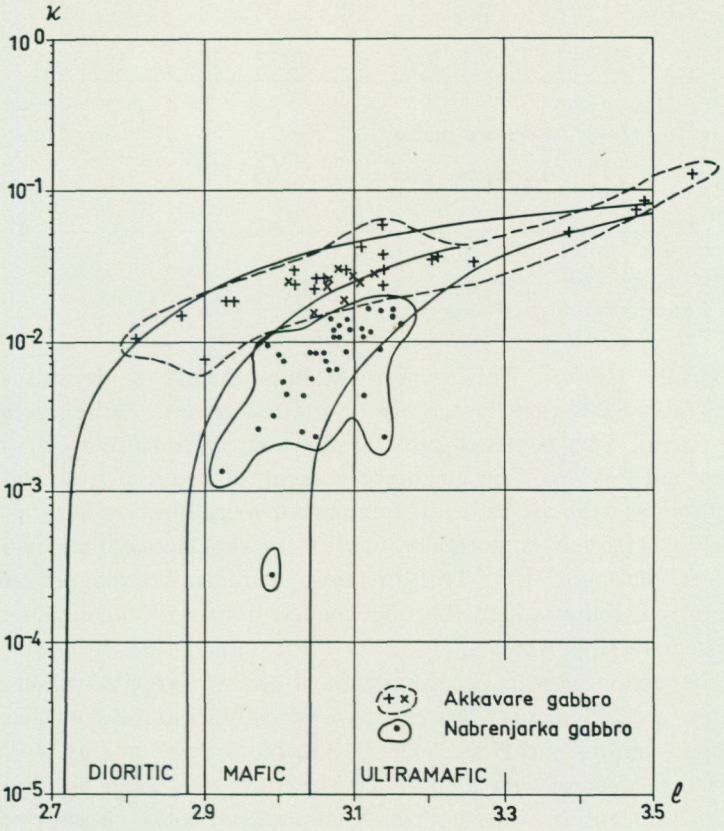

Fig. 40. Susceptibility — density.
Susceptibilitet — täthet.

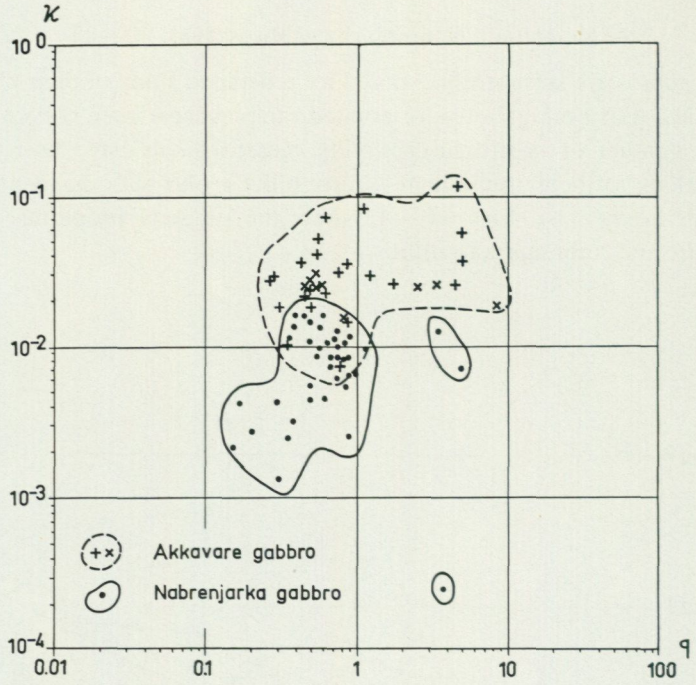

Fig. 41. Susceptibility — q-value.
Susceptibilitet — q-värde.

Akkavare gabbro. This gabbro exhibits mainly a dioritic silicate density (about 2.8 g cm^{-3}) and has only a few samples falling within the gabbro field. This is rather peculiar for a strongly basic rock (see pp. 23—26 and Fig. 40). The magnetite content, as deduced from the mean susceptibility, is about 15 %. The remanent magnetization is rather variable (Fig. 41), but is normally inferior to the induced magnetization (q-values of about 0.7). The direction of remanent magnetization is dispersed but shows a faint ENE declination trend with inclinations down to 40 degrees (Fig. 42).

In connection with the interpretation of ground geophysical surveys in this area, a detailed study was made of this gabbro in order to determine its shape (Ambros and Henkel 1973). The block diagram (Fig. 44) shows that we are dealing with a flat-lying structure with steep dipping sides. Certain dislocations, some with high amplitudes, could be inferred from the ground geophysical measurements. These measurements also indicate some rather flat-lying horizons differing in magnetization.

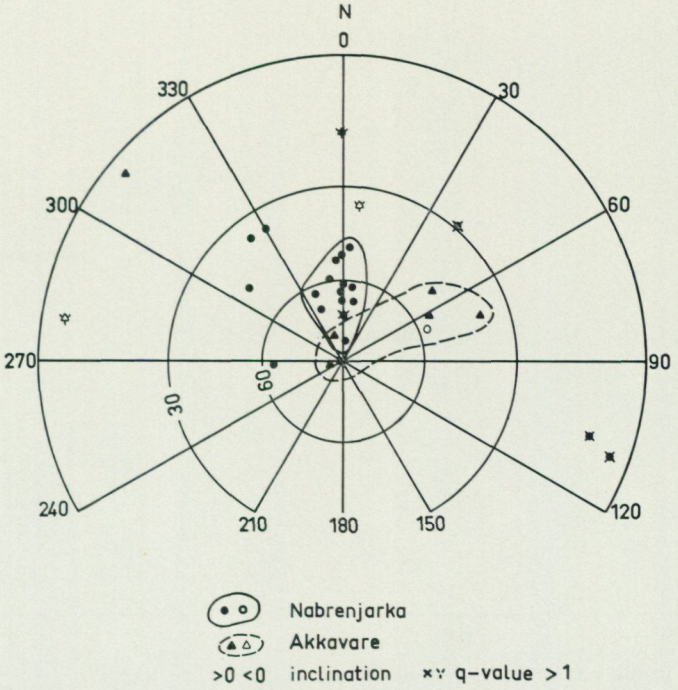

Fig. 42. Directions of natural remanent magnetization (NRM).
Remanensriktningar (NRM).

Nabrenjarka gabbro. This rock has a gabbroic silicate density of 3.0 g cm^{-3} and a few samples show ultrabasic densities (Fig. 40). The average magnetite content, as inferred from susceptibility, is about 4 %, with few samples having considerably lesser amounts. Remanent magnetization is subordinate with a mean q-value of 0.8. A distinct correlation trend between remanence and susceptibility exists in the high susceptibility region of the diagram in Fig. 41. Specimens with high q-values on this trend must be considered as favourable for paleomagnetic determinations. The direction of remanence is North with inclinations reaching 45 degrees. The inclination of the total magnetization is thus somewhat smaller than that of the geomagnetic field. This implies a slightly larger assymmetry of the total field anomalies which is not therefore a function of the dip alone.

A detailed susceptibility profile on the almost continuous outcrops at Råvvevare (0b) shows interruptions in a systematic variation. This could be due to a complex emplacement of the dyke by repeated injections.

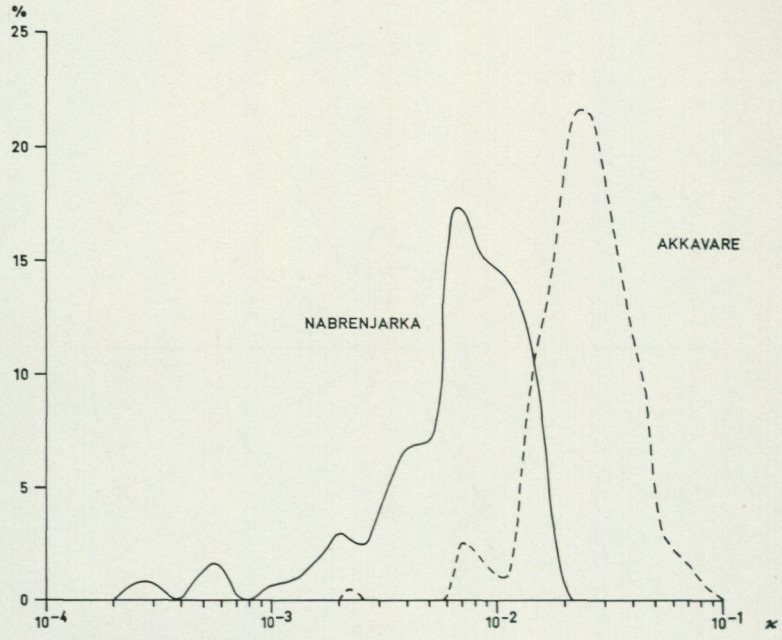

Fig. 43. In-situ susceptibility frequencies.
Hällsusceptibilitet.

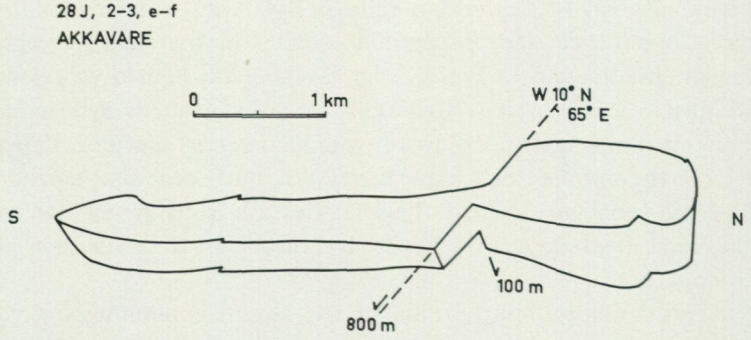

Fig. 44. Block diagram of the Akkavare gabbro.
Blockdiagram över Akkavaregabbron.

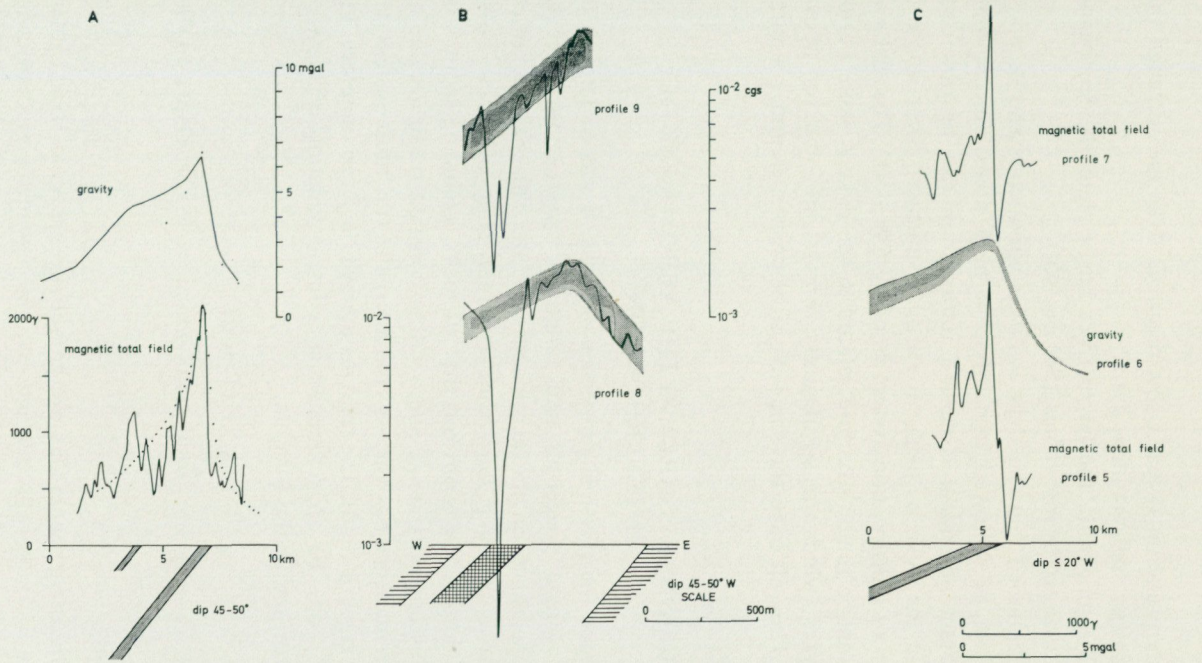

Fig. 45. Geophysical measurements on the Nabrenjarka gabbro-diabase. The situation of the profiles is indicated on Plate 2 D.
A. Computed gravity and magnetic total field anomaly for profile 4.
B. In-situ susceptibility and inferred structure of dyke.
C. Measured gravity and magnetic total field anomalies of northern part of dyke (showing significantly lower dip than along profile 4).

Geofysiska undersökningar på Nabrenjarka gabbro-diabas.

One possible interpretation is that a low magnetic dyke has intruded the central part of a larger, high magnetic dyke.

Towards the hanging wall, the larger dyke has a regularly decreasing susceptibility interrupted by low values. (See Fig. 45.)

It has been mentioned that this dyke is rather continuous and its magnetic anomaly can be followed into adjacent map areas. In the map area 28 I important additional structural information can be obtained. There, the dip of the dyke is steeper towards its northern limit where it becomes parallel to a dislocation system trending SW—NE. The dislocation zone represents a major structure related to the dyke system. Parallel, flat-lying dykes (which are significantly shorter) are observed above the main dyke. They all have the same physical properties and a similar geometry.

CONCLUSIONS REGARDING THE AEROMAGNETIC INTERPRETATION

Having investigated the physical properties of rocks, it was of interest to compare their average properties and range of variation in order to predict their appearance on the aeromagnetic map. This has permitted correlation of an anomaly pattern with a limited suite of rocks. From what has been said above it is obvious that all rocks, excluding sediments, have a limited susceptibility range and a rather constant mean q-value of about 0.4. This remanence has viscous characteristics (i.e. more or less parallel to the geomagnetic field). The total magnetization T can therefore, for the majority of rocks, be approximated as a linear function of the susceptibility k according to the formula:

$$T = k\ H\ (1 + q)$$

where H is the geomagnetic total field which is 0.521 Gauss in the map area.

$$T = 0.73\ k$$

The highest magnetic anomalies are caused by gabbroic rocks, intermediate volcanic rocks, porphyrites and, to some extent, by acid volcanic rocks and sedimentary rocks. Within these groups, a variation of the susceptibility by a factor of 10 is normal. This gives rise to similar variations in the anomaly pattern on a high background level. If present in larger volumes, these rocks should also give rise to positive gravity

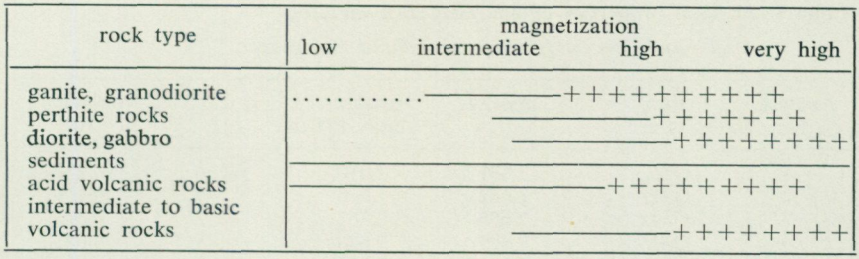

Fig. 46. Schematic outline of the variation of magnetization of different rock groups.
Variationer i magnetiseringen, schematiskt angiven för olika bergartsgrupper.

anomalies (exceptions being made for the acid volcanic rocks). Thus, in the map area, a combination of high gravity and high magnetic anomalies indicates the presence of basic- to intermediate-composition volcanic or plutonic rocks and sediments.

Intermediate and high magnetic anomalies are caused by all rocks with the exclusion of some sedimentary rocks and a large proportion of the acid volcanic rocks. In the lower-range, granite and granodiorite are predominant. These rocks show lows in the gravity, as do rocks of the perthite type. Thus a combination of moderate magnetic anomalies and low gravity is indicative of acid volcanic and plutonic rocks.

Low magnetic anomalies are caused by the low susceptibility portion of acid volcanic rocks and about half of the sedimentary rocks. The presence of large areas with low magnetic, irregular pattern anomalies combined with gravity lows (apparently produced by granitic rocks) indicates that low magnetic rocks are under-represented in the parameter measurements.

Fig. 46 gives a schematic outline of the bulk magnetic properties of rocks from this map area. It can be concluded that banded anomaly patterns can be caused by different magnetic layers within the same rock type, such as sediments or acid volcanic rocks, or by the alternating layering of different types of rocks. As previously mentioned, irregular anomaly patterns may well arise from banded rock complexes. Therefore, a prediction from aeromagnetic anomalies alone is often uncertain and, when possible, better results can be obtained from the combination of magnetic and gravity information.

Table 5. Physical properties of analysed rock samples.

Analyserade bergartsprovers fysikaliska egenskaper.

Analysis Nr	rock type	density	susceptibility·10^3	q-value	remanence 10^3
1	QMz	2.631	2.018	0.236	0.239
2	QMz	2.652	1.578	0.140	0.109
3	QMz	2.658	2.761	0.032	0.043
4	QMz	2.609	0.648	0.128	0.041
5	KMz	2.644	2.166	0.092	0.098
6	QMz	2.633	1.670	0.092	0.077
7	QMz	2.634	1.339	0.240	0.162
8	QMz	2.657	0.015	0.800	0.006
9	QMz	2.679	3.431	0.396	0.680
10	QMz	2.644	0.852	0.092	0.039
12	DMz	2.631	2.463	0.220	0.271
13	QMz	2.674	0.017	0.352	0.013
14	QMz	2.663	3.216	0.128	0.208
15	Mz	2.656	2.656	0.184	0.245
16	GrD	2.754	1.378	0.244	0.169
18	DMz	2.689	1.833	0.196	0.181
19	GrD	2.796	5.178	4.192	10.849
20	Mz	2.676	3.476	0.416	0.721
21	QMz	3.035	11.731	3.916	22.979
22	GrD	2.767	7.091	0.320	1.146
23	DMz	2.719	4.989	0.188	0.467
24	DMz	2.798	1.880	0.348	0.328
25	DMz	2.770	4.383	0.264	0.579
26	Vo	2.630	1.278	0.260	0.167
27	Po	2.639	0.071	0.056	0.002
28	Vo	2.679	1.852	0.140	0.130
30	mPo	2.645	1.440	0.244	0.176
32	mPo	2.633	1.757	0.200	0.176
33	mPo	2.585	2.341	0.244	0.285
34	Po	2.651	1.953	0.180	0.177
35	mPo	2.634	3.762	0.152	0.287
36	Po	2.647	1.715	0.072	0.063
37	Vo	2.656	1.872	0.224	0.208
39	mPo	2.646	1.215	0.340	0.206
40	Po	2.664	0.035	3.600	0.063
41	mPo	2.635	0.926	0.032	0.015
42	Vo	2.744	4.667	0.916	2.140
43	Po	2.660	0.063	1,716	0.054
44	Vo	2.642	2.064	0.216	0.223
45	Po	2.690	0.712	1.412	0.503
47	Po	2.692	1.063	0.276	0.147
48	Po	2.705	0.671	0.672	0.226
49	Po	2.684	1.455	0.336	0.245
50	Po	2.696	1.518	3.600	2.237
51	G	2.812	6.225	0.204	0.638
52	G	2.759	1.216	0.628	0.383
53	G	2.858	10.164	0.224	1.130
54	mA	2.802	5.468	0.408	1.115
56	mA	2.783	5.426	0.496	1.347

Table 5 (continued)

Analysis Nr	rock type	density	susceptibility·10^3	q-value	remanence 10^3
57	A	2.799	7.850	0.120	0.470
58	A	2.884	10.525	0.284	1.502
61	VoS	2.639	0	0	0
62	VoS	2.654	0	0	0
65	QMz	2.639	1.895	0.144	0.136
67	DMz	2.929	18.179	0.152	1.374
68	D	2.952	9.400	7.876	37.118
69	D	3.019	25.802	0.336	4.360
72	Sk	3.243	5.067	0.140	0.350
75	Ga	2.893	5.777	2.228	6.434
76	Ga	2.950	4.458	0.520	1.161
77	AG	3.041	22.003	0.896	9.861
78	ND	2.965	6.669	0.232	0.776
79	NG	3.044	0.242	0.304	0.037
80	NG	3.123	10.726	0.168	0.904

Note: Rock-type symbols and sample Nr are given on p. 94.

REFERENCES

SGU = Sveriges geologiska undersökning

AMBROS, M., and HENKEL, H., 1973: Titanjärnmalmsfyndigheten Akkavare (Melko). — SGU. Malmbyrån. Report.

ELEMAN, F., BORG, K., and ÖQUIST, U., 1969: The aeromagnetic survey of Denmark, Finland, Norway, Sweden 1965. — Swedish Board of Shipping and Navigation. Report.

HENKEL, H., 1975: Studies of density and magnetic properties of rocks from northern Sweden. (In press.)

WERNER, S., 1945: Determinations of the magnetic susceptibility of ores and rocks from Swedish iron ore deposits. — SGU C 472.

— 1963: Aeromagnetic mapping by the Geological Survey of Sweden. Methods and general considerations. — Geoexploration 1, pp. 21—31.

PRISKLASS B

Distribueras genom
LiberTryck
162 89 VÄLLINGBY

Växjö 1975, C. Davidsons Boktryckeri AB
Printed in Sweden

ISBN 91-7158-073-5